Dear Editor,

Please find below the detailed responses to the comments of Referee 1 (anonymous) and Referee 2 (Jonas Kley).

The responses are accomplished by the PDF version of the Word document with track changes in two colours in respect to the two responses.

Content

This page

_____

The submitted revised manuscript is based on the accepted track changes document with some minor edits, which are as follow:

- We resorted and renumbered the figures according to occurrence in the text
- Added "Kirthar Escarpment" to Fig. 3
- Added "frontal anticline" to Fig. 6
- Section 1 some sharpening in the description of our approach:" We use seismic interpretation, section analysis techniques, kinematical forward modelling as well as regional constraints to narrow structural solutions and develop a most likely structural model. Based on the resulting balanced cross sections through the area we conclude that the central Kirthar Fold Belt is driven by thick-skinned inversion which is linked with thin-skinned deformation further toward the foreland"
- Section 5.4. Changing first sentence of second paragraph to better explain purpose of the kinematic model.
- Section 5.5. Shifting a paragraph about the balancing results after the description of the kinematic section to be consistent with the text structure in section 5.4 (intro to the section – kinematic model – balancing results – uncertainty)
- Section 6.5 sharpened the text by adding to the discussion: "On the other hand we think it will be difficult to find a solution much different from our presented model that will honour all the constraints."
- Section 7. Conclusions: minor rewording for clarity
- Smaller edits are in respect to language use consistency throughout the text and typos.

Reply to RC1 by Anonymous Referee #1

We thank the anonymous Referee for reviewing the manuscript. Most of the comments ask for clarifications of interpretations and assumptions. These comments give us the opportunity to substantially improve the readability of the manuscript. Some comments we do not fully agree or we think they are not relevant. All points raised will be discussed below.

1a) RC1:

"As a general point, I struggle to see, and judge the robustness, of some of the interpretations of the seismic data (e.g. the images in figure 8). I think that it would be helpful if the authors: (a) provided un-interpreted, as well as interpreted, images of the sections;"

Response:

a) Figure 8 was composed in a way that as little of the seismic is covered by interpretation and labelling so the reader can get an impression on the (often poor) quality of the seismic image. We followed the example given by other papers in Solid Earth using nearly un-interpreted seismic with some labelling to highlight features discussed in the text (e.g. Malehmir et al. 2018, Tavani et al., 2018, Gallastegui et al. 2016). The interpreted version of the seismic is given in Figures 12a and 14a where one can see the complete interpretation (the semi-transparent seismic in the background). We added cross-references between the figures to clarify this, thus enabling the reader to compare the final structural interpretation and original seismic. Because of the different length of the sections (Seismic in Fig 8 and the final, extended sections in Figs 12a, 14a), it seems unreasonable to combine the figures. Instead, in order to provide an unbiased documentation on the database, we added a supplementary figure that shows the seismic of Figure 8 in high resolution without any annotations at all.

Changes to the MS

Supplementary high resolution figure with blank seismic (Supplementary Figure 2).

Improved cross-references between figure captions (Figs. 12a and 14a to Fig. 8) and text (see track changes MS).

1b) RC1:

"b) provided zooms of the key features discussed in the text;"

Response:

We do not agree that one would be able to see more details in zooms of the seismic. The size of Fig. 8 is limited by the column width of the journal but it already resolves all the features visible in the seismic which are referred to in the text (as they are indicated by small letters). The PDF version of the MS for review might be lacking the quality of the figure expected. We think by providing a large scale high resolution version of the blank seismic (Supplementary Figure 2) we sufficiently provide documentation of the data our interpretation is based on. The seismic won't get better in zoom figures. We will make also sure, that the final submitted version of Fig. 8 will have as high quality as reasonably possible.

Changes to the MS

Providing a high resolution blank seismic of Figure 8 in the supplementary material (Supplementary Figure 2).

A high resolution blank seismic of Figure 9 (Supplementary Figure 3) will be provided as well.

1c) RC1:

"c) marked on the locations of the wells that seem to be key to the correct identification of some horizons"

Response:
This comment likely asks for the exact location of the wells on the seismic?
For confidentiality reasons we cannot give exact well locations. But we edited the text and figures to improve the MS accordingly.

Changes to the MS
We improved the description of the stratigraphic control and well locations in the text (Section 4). We added seismic horizon labelling to Figure 8 with indications in the stratigraphic column (Fig. 3). Better explanation of well control location in Figure 8. Please see track changes MS.

1d) RC1:
"(d) provide in the text a discussion of the reasoning behind interpreting the structures, and the horizon identifications. For example, at the eastern ends of the seismic sections, and in places where it is buried, where the pick of the top of the Kirthar formation is key to the subsequent discussion of regional level, a detailed discussion about the reasoning of the pick would be useful. On some seismic sections I can't tell what the basis is for interpretations (e.g. faults 1 and 2 on fig 9). In general, I think a much more thorough analysis and justification of the seismic data is necessary.

Response:
The horizon interpretation is done based on the well control and seismic facies. As mentioned above seismic horizons as depicted from the well control have been added to Fig. 8 and are explained in Fig. 3. Additionally the seismic characteristics of the Kirthar limestone pick is now given in Section 4.
For the fault interpretation in Figure 9 we added also the non-interpreted seismic as supplementary figure. In addition, a new figure with a kinematic scheme is provided and explained, highlighting the rationale behind the interpretation (this is also part of the answer to RC2).
We think that an interpretation like Fault 1 does not require a detailed justification. Tilting and uplifting strata from a horizontal position the way it is imaged requires a fault. Such basic interpretations follow well known structural concepts, cf. AAPG Atlas of Shaw et al., 2005). The fault 2 (roof thrust) is a geometrical necessity if no further deformation occurs to the east. This rationale is now better explained by the new figure and the description of the missing deformation towards the east in the revised MS.

Changes to the MS
Additions to section 4: Stratigraphic control by wells, seismic grids and seismic characteristics of Kirthar pick.
Additions of the picked horizons to stratigraphic column (Fig. 3) and the eastern part of the seismic lines (Fig 8).
Improved Figure 9 with a kinematic scheme and rewording of the regarding text in Section 4.1.
Supplement Fig. 3: Seismic of Fig. 9 without interpretation

2) RC1:
"I think the authors would benefit from a clearer consideration of the seismicity. Focal mechanisms are provided in Figure 2, but they are wrongly attributed (the ISC only estimates locations, not mechanisms, so these mechanisms must be sourced from elsewhere)."

Response
Focal mechanisms were downloaded from ISC database (http://www.isc.ac.uk/iscbulletin/search/fmechanisms/). We followed the citation scheme proposed on the ISC webpage. The contributing agencies to the ISC database that we used

were actually listed in Table 1 in the author column. See also Lentas et al. (2018, "The ISC Bulletin as a comprehensive source of earthquake source mechanisms")

Changes to the MS
We clarified the contribution of other agencies to the ISC database and added the reference "Lentas et al. (2018)" to the caption of Table 1

2 contd.) RC1:
"The depth of these events is not discussed (i.e. are they within the deformed sedimentary sequence, or the underlying basement?)".

Response:
This is a good point that is missing in the manuscript. We were aware of the depth and considered the depth of the events when interpreting the data (as "Z" is listed in Table 1).

Changes to the MS
We added a consideration of the depth of the events to Section 5.2 (former 5.1). See track changes document.
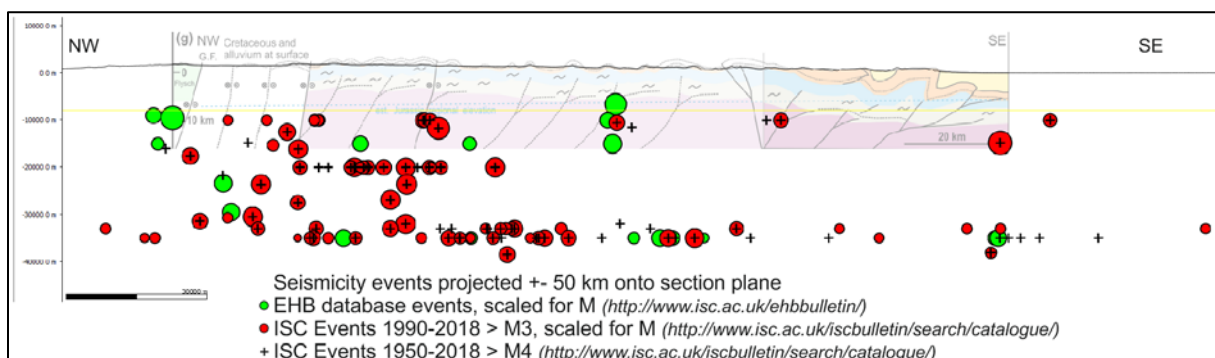
2 contd.) RC1:
"I think the authors would benefit from searching the literature for well-constrained locations, mechanisms, and depths for earthquakes in this region, and discussing the relationship between the geometry of the active faulting and the structural models they propose. In addition, Ambraseys and Bilham (Bulletin of the Seismological Society of America, Vol. 93,p. 1573–1605, 2003) contains much useful information on the historical seismicity, including the 1931 event close to the Krithar range-front, which will have important implications for the kinematics of the shortening"

Response
We struggle to find significant other sources of focal mechanisms relevant to our study area. We consider the ISC Bulletin database with approx. 150 contributing agencies to be the most relevant data source for this study. A dedicated seismological study for the study area would certainly help, but is beyond the scope of this study.

We are of the opinion, that the distribution of seismic events (i.e. the depth distribution) does not add value to the discussion about fault geometries and kinematics. The figure below shows recorded seismic events projected (+- 50 km perpendicular to the section plane) on the extended section of the new regional section (Fig. 16g). Data from the ISC bulletin partly line up in certain depth which could be related to poor depth location/artefacts. Improved locations of the EHB database (using algorithms after Engdahl et al. 1998) do not improve the picture, but actually show that the data in general has a large scatter.

Seismicity events projected +- 50 km onto section plane
● EHB database events, scaled for M (http://www.isc.ac.uk/ehbbulletin/)
● ISC Events 1990-2018 > M3, scaled for M (http://www.isc.ac.uk/iscbulletin/search/catalogue/)
+ ISC Events 1950-2018 > M4 (http://www.isc.ac.uk/iscbulletin/search/catalogue/)

The paper by Ambraseys and Bilham (2003) does not provide focal mechanisms but, as suggested by the reviewer, a discussion on fault kinematics on the 1931 Mach Event (based mainly on levelling data). Using the same levelling data the potential fault shape and

kinematic is evaluated also in Szeliga et al. (2009). Those authors show focal mechanisms on their Fig. 1 after Harvard MCT, a source that is included in the ISC Bulletin database that we used for our Fig. 2.

We follow the suggestion by the referee and introduce the work done on the Mach 1931 Earthquake in Section 5.2. The geological section of Szeliga et al. (2009) with the approx. fault shape of the Mach 1931 event has been added as Figure (Fig. 16d). The fault shape considered by Szeliga et al. 2009 is similar to the frontal fault system in our study area. The consequences are also now discussed in Section 6.2.

Changes to the MS

We added the citations and a description of the results of Ambraseys and Bilham (2003) and Szeliga et al. (2009) to Section 5.2 (former 5.1). The geological section given in Szeliga et al. 2009 has been added to a new Figure 16 (Figure numbers will be resorted in final revision), which shows a compilation of sections (in response to RC2). The fault responsible for the 1931 Mach Event as suggested by Szeliga et al. 2009 is also shown in Figure 16d. The consequences /relationship of the deformation is additionally discussed in Section 6.2. See track changes document.

2 contd.) RC1:

"Some of the arguments based upon the dip of the faulting (e.g. that thrust faults can't form at dips of 45 degrees; section 5.1) are incorrect, based on observations of faults this steep being newly-formed in oceanic outer rises (e.g. Craig et al, EPSL, 392, 94-99, 2014),".

Response

It has not been stated in the reviewed MS that thrusts cannot form at dips of 45°. We say, we consider the steeper faults (i.e. 45° and more) too steep to represent newly initiated faults. That is not exactly the same. The reason, why we think they are not newly initiated faults is based on a line of arguments, which includes fault and fold orientation in respect to the plate kinematic direction. Section 5 and sub-sections 5.1-5.3 have been extended to clarify the reason for our interpretation of inversion (also in respect to RC2)

We consider that the paper by Craig et al. (2014), suggested by the Referee 1, is not relevant in the discussion whether thrust faults can form at higher angles or not. In the paper Craig et al. argue that they observe normal faults forming not at an ideal angle of 60° but cluster around 45° (in oceanic crust). In order for that to happen, they imply that the rocks must have a lower than usual coefficient of friction. They speculate that the suspected low coefficient of friction is a result of hydrothermal alteration of the oceanic crust after it formed at the MOR. Craig et al. also plot histograms of nodal planes from thrust faults which show clusters above and below 45°. However, the histogram shows both nodal planes, so the cluster on the higher angles could represent the auxiliary plane – or reactivated faults. Craig et al. do not suggest that thrust faults form above a certain angle and they explicitly do not analyse the thrust faults (Craig et al. (2014): *"The population of thrust-faulting earthquakes (Fig.3C) is too small for any clear trends to emerge, and is not the subject of further analysis in this study"*). Consequently, their results are only valid for normal faults. Furthermore, the line of arguments that is used for normal faults forming a lower angles seem not to fit for thrust faults forming at steeper angles than usual. If the coefficient of friction is lower than for standard Andersonian faults (i.e. lowered by a hydrothermal processes), thrust faults would form at lower angles, not higher. For thrust/reverse faults to form at higher angles the coefficient of friction would need to be higher than the normally considered used value (i.e. 0.6 for 30° thrust fault, all needed references are given in Craig et al., 2014). Consequently, we interpret reverse faults with dips at 45° or above indicate rather frictionally reactivated faults than newly initiated faults.

Changes to the MS:
Section 5.2 (former section 5.1): "We interpret these steep faults therefore as parts of pre-existing faults that are in a suitable angle for reactivation".
A suggestion on partial fault reactivation and other inversion related deformation in Section 5.3. (marked as reply to RC2). See track changes document.

3) RC1:
"Little detail is given of the structural reconstructions (Figs 12-15). For example, what is the justification behind each step in the reconstruction, and how many other interpretations are possible which match the observations? The authors acknowledge that the solution is not unique, but I have little feel for how many different configurations are possible, why these models were chosen, and how alternative models would affect their conclusions. I think these issues need to be discussed in detail (particularly the final one), and I think that for each stage in the reconstructions a reason should be given for why that deformation has been chosen (e.g. in order to match feature X, we now need to undertake deformation Y)".

Response
Strictly speaking Figures 13 and 15 do not show reconstructions but simplified kinematical forward models. Reconstructions are the restored sections (Fig. 12b and 14b). The techniques how Figs. 12b and 14b are restored are defined in the text (Section 5.4, last paragraph) and follow established procedures (e.g. Woodward et al., 1989). The simplified kinematical forward models in Figs. 13 and 15 are suggestions that show that the restored section also is meaningful in a kinematical sense. The necessity to link restored and present day stages are the main constraints. We clarified this relation in the revision. Some additional reasoning for the individual steps have been added as well.
The question on "how many different configurations are possible, why these models were chosen, and how alternative models would affect their conclusions" is not simple to answer. We follow in the MS the approach of using as many constraints as possible (surface geology, seismic, well data, regional setting, the nodal plane geometries, balancing constraints and regional elevation considerations etc.) and combining them in a logical way in order to shrink the amount of admissible solutions. How much change on our solution is a new solution or just an adaption in the frame of the given solution is a matter of definition and also scale dependent. We consider that the involvement of basement deformation can be considered as certain. That these are likely inverting normal faults (or part of it) is considered as very likely, based on a thread of arguments (which is now elaborated more clearly in Section 5.1. -also in respect to the comments by Referee 2). If these faults are of original Triassic or Jurassic age remains relatively uncertain. The same applies for the amount and exact shape of faults in the subsurface. Our main conclusion is based on the solution which we consider almost certain. It would require some very good ideas to combine all the constraints and come up with a solution that is different from being just a modification of our model. However, learning about potential other solutions has not only a scientific but also a business impact, so we encourage substantial alternative explanations that contradicts our main conclusions. By documenting the database as good as confidentiality allows, we hope to serve this purpose.

Changes to the MS:
The mentioning of the balanced sections and restorations (Figs. 12 and 14) moved up in the text (now in Section 5. Second paragraph). By this we can refer to the restored and balanced section as start and finite stage respectively when explaining the kinematic models (Fig. 13 and 15), improving the context/readability. Additionally some improved reasoning for the chosen steps, as suggested by the Referee1, have been added (see track changes MS). To section 6.5 we added: "How much change on our model is a new solution or just a modification is a matter of definition and also scale dependent."

"Although I can see why the authors have suggested a combination of thick- and thin- skinned deformation in this region, it's not clear to me why this definitely needs to be the case, rather than just one of a range of possibilities. The pattern of folding is described as being analogous to an array of normal faults, but I don't see why this necessarily needs to be the case – the folding looks fairly similar to that in the Zagros Mountains, where it is thought that the folds are decoupled from the underlying basement by the Hormuz salt. The second paragraph of section 5 simply states their view, without justifying it. For example, how have they ruled out the possibility of more thickening in the deeper parts of the sedimentary layer in the western parts of the section giving the change in structural level? Given the thickness of the sediments, this seems equally plausible? If the authors are going to pick a preferred viewpoint, I think they need to give a detailed justification."

Response:

"The second paragraph of section 5 simply states their view, without justifying it."
Manuscript: "We suggest that the order of structural uplift (larger than 5500 m) is linked to a deeper structural level in the basement." The order of uplift is used as an temporary justification. The sentence is part of a paragraph that is a header for the complete Section 5 (including subsections) in which the reasoning for thick-skinned contribution is elaborated and more reasoning/justification is given. We improved the wording to make this clear. Subsection 5.1 in combination with a new Figure 17 now addresses the question why a thin-skinned solution (thickening in deeper parts) is unlikely. This builds up on a newly added regional section (Fig. 16g) plus an overview geological map (new background in Fig. 2) which has been added as part of the response to RC2. The main reason is that a duplexes would cause severe balancing issues and are also not likely in the transpressional setting that does not seem to work like a classical accretionary wedge (details in the Track changes MS).

"the folding looks fairly similar to that in the Zagros mountains, where it is thought that the folds are decoupled from the underlying basement by the Hormuz salt"-
When comparing these regions we probably need to limit the similarity of the complex fold pattern and double plunging folds to the southern/southeastern Fars Arch of the Zagros, where Hormuz salt is present as detachment (cf. Bahroudi and Koyi, 2003). The deformation style in the Simply Folded Belt along strike the Zagros is not everywhere the same (cf. Allen and Talebian 2011). Nevertheless, the main differences are: in the southern Fars area most of the folds return to regional elevation (or close to it) in the trailing synclines (as evident on sections and geological maps, e.g. Jahani et al., 2009). The folds are large scale detachment folds influenced by the halokinetic evolution (requiring diapirs) since the Paleozoic (e.g. Jahani et al. 2009, Callot et al. 2012). The double plunging fold shapes in the SE Fars are a result of complex interaction of halokinetic induced stratigraphic thickness variations and shortening on a salt detachment with a likely not planar detachment plane. The role of basement involvement in the deformation in the Fars has been proposed (e.g. Jackson 1980) and is debated since. For the SE Fars region a strong gain of structural elevation is evident only towards the hinterland in the imbricate zone (behind the High Zagros Fault cf. Fig. 2 of Mouthereau et al, 2007, or Fig. 2 of Bahroudi and Koyi, 2003). This faults thus likely marks a stepping down of the detachment into the basement.
In the Kirthar Fold belt there is no evidence of salt presence in the stratigraphy and no evidence for salt tectonics. The second most important difference is that all rocks west of the Kirthar Escarpment are significantly elevated above their regional elevation of the undeformed foreland (more than 6000 m).
Although the comparison to the Fars Arch might be interesting, we do not think that it would improve the MS.

Changes to the MS:
Added Figure 16g (regional section), Figure 16h (average topographic profile along 16g) and new background in Fig. 2 (overview geological map) also as reply to RC2.
Added Figure 17 schematic scheme for discussion of structural elevation uplift
Section 5.1 now addresses the question why a thin-skinned solution is less likely to explain the structural elevation gain towards the west.
Section 5.1 also includes a discussion why we consider a thick-skinned (not inversion related) deformation less likely also (in response to RC2). See track changes document.

5) RC1:
"In general, I think the manuscript would benefit from many of the statements being backed up with observations and/or reasoning. For example, in section 4 the lateral thickness change in the Ghazij Shales is stated. However, we are not told what information this was based on (i.e. where are the well or surface observations, or how is the top and bottom of this unit recognised in the seismic data). This thickness change is key to their suggestion of the reactivation of normal faults. There are many statements like this in the text, which leave the reader wondering what the conclusion is based upon. I think it would be very helpful to the reader if the authors provided supporting logic or observations of all statements they make."

Response:
We do not agree that we are using un-backed up statements in the MS. Unfortunately, there is only one example given in RC1, which we think is not fully adequate: RC1: "For example, in section 4 the lateral thickness change in the Ghazij Shales is stated. However, we are not told what information this was based on (i.e. where are the well or surface observations, or how is the top and bottom of this unit recognised in the seismic data)". The manuscript reads in Section 4.1, page 8 Line 3-5: *"The low-reflectivity seismic facies below the Kirthar limestones are Eocene Ghazij Shales (Fig. 8a, point g). These shales thicken dramatically from wells in the East (several tens of meters) towards the West (several hundreds of meters, constrained by outcrop and seismic velocity data)"*. We actually would consider this as an explanation and not an un-backed up statement. The location of the gas condensate fields on the frontal anticline has been described in Section 4. The relative reference where the location is on the section was given). The outcrop situation of the Ghazij can be checked on Figure 5 and has been described in Section 3.1. However, we admit, that this might not be easy for the reader to follow. So, for convenience we improved the description of this thickness increase and the observations where it is based on. Well control and seismic interpretation description has been improved (as described in points 1c and 1d of this reply)
RC1:" This thickness change is key to their suggestion of the reactivation of normal faults."
This is actually not the case. The thickness variations in the Ghazij Formation is nowhere used in the MS as argument for normal fault reactivation.
A thick Ghazij Formation, however, is considered as suitable roof thrust. The suitability as weak layer has been already demonstrated in Section 3.1/Fig. 6.
The changes in respect to the other comments from RC1 (above) and also in respect to RC2 should have significantly improved the MS and allow the reader to follow our interpretations and conclusions (without "*non-back-upped statements*").

Changes to the MS:
Section 2 Thickness trend description of Ghazij shales in Tectonostraigraphic evolution
Section 3.1.: These shales reach several hundred meters of thickness east of the Kirthar Escarpment.
Section 4: improved description on well control and stratigraphic interpretation (including annotations of stratigraphy in Fig. 8)

Section 4.1 Changed the description of the thickening shales to: "These shales thicken dramatically from the wells on the frontal anticline in the East (several tens of meters) towards the West (several hundreds of meters, constrained by seismic velocities and outcrop information just west of the Kirthar Escarpment, cf. Fig. 5 and Ahmad et al. 2012)".

References used in this reply not present in the reference list of the revised manuscript:

Allen, M.B. and Talebian, M., Structural variation along the Zagros and the nature of the Dezful Embayment., Geol. Mag., 148 (5-6). pp. 911-924, 2011

Bahroudi, A., Koyi, H.A., Effect of spatial distribution of Hormuz salt on deformation style in the Zagros fold and thrust belt: an analogue modelling approach. J. Geol. Soc. Lond. 160 (5), 719-733, 2003

Callot, J.-P., Trocme, V., Letouzey, J., Albouy, E., Jahani, S., Sherkati, S., Preexisting salt structures and the folding of the Zagros Mountains. In: Alsop, G.I.,Archer, S.G., Hartley, A.J., Grant, N.T., Hodgkinson, R. (Eds.), Salt Tectonics, Sediments and Prospectivity, vol. 363. Geol. Soc. London Spec. Pub., pp. 545-561. 2012

Craig, T. J., Copley, A and Middleton, T.A., Constraining fault friction in oceanic lithosphere using the dip angles of newly-formed faults at outer rises. Earth Planet Sc Lett, 392:94–99, 2014b. doi: 10. 698 1016/j.epsl2014.02.024, 2014

Engdahl, E.R., R. van der Hilst, and R. Buland. Global teleseismic earthquake relocation with improved travel times and procedures for depth determination, Bull. Seism. Soc. Am. 88, 722-743. 1998

Gallastegui, J., Pulgar, J. A., and Gallart, J.: Alpine tectonic wedging and crustal delamination in the Cantabrian Mountains (NW Spain), Solid Earth, 7, 1043-1057, https://doi.org/10.5194/se-7-1043-2016, 2016

Jahani, S., Callot, J.P., Letouzey, J., Frizon de Lamotte, D. The eastern termination of the Zagros Fold-and-Thrust Belt, Iran: structures, evolution, and relationships between salt plugs, folding, and faulting. Tectonics 28 (6), TC6004, 2009

Malehmir, A., Bergman, B., Andersson, B., Sturk, R., and Johansson, M.: Seismic imaging of dyke swarms within the Sorgenfrei–Tornquist Zone (Sweden) and implications for thermal energy storage, Solid Earth, 9, 1469-1485, https://doi.org/10.5194/se-9-1469-2018, 2018.

Mouthereau, F., J. Tensi, N. Bellahsen, O. Lacombe, T. De Boisgrollier, and S. Kargar, Tertiary sequence of deformation in a thin-skinned/ thick-skinned collision belt: The Zagros Folded Belt (Fars, Iran), Tectonics, 26, 2007

Shaw, J.H., C.D. Connors and J. Suppe Seismic interpretation of contractional fault-related folds. An American Association of Petroleum Geologists seismic atlas. American Association of Petroleum Geologists, Studies in Geology, v. 53, 2005

Tavani, S., Parente, M., Puzone, F., Corradetti, A., Gharabeigli, G., Valinejad, M., Morsalnejad, D., and Mazzoli, S.: The seismogenic fault system of the 2017 Mw 7.3 Iran–Iraq earthquake: constraints from surface and subsurface data, cross-section balancing, and restoration, Solid Earth, 9, 821-831, https://doi.org/10.5194/se-9-821-2018, 2018.

Woodward, Boyer and Suppe, Balanced Geological Cross-Sections: An Essential Technique in Geological Research and Exploration, Short Courses in Geology, Volume 6, American Geophysical Union, DOI:10.1029/SC006, 1989

Reply to RC2 by Referee #2 Jonas Kley

We thank the reviewer for the effort of the thorough review of the manuscript. We think that our revisions based on the comments significantly improved the revised manuscript.

Our responses to the specific comments of RC2:

1) RC2
Page C2 Paragraph 1): "In the way of data, the weakest part of the paper is definitely the claim that reactivated normal faults are involved in the deep structure. The seismic profiles do not reach deep enough to show anything conclusive. The earthquake nodal planes except one at 57° dip too gently to satisfy the Coulomb-Mohr prediction for normal faults. In fact, the average (arithmetic mean) dip angle of the west-dipping nodal planes is only 38°, much closer to an ideal Mohr-Coulomb thrust fault than normal fault. The normal faults of the structural model dip around 50°. Judging from the stratigraphic description and the authors' comments, the timing of active rifting isn't very well constrained, either. The same seems to hold true for the depth to and nature of the basement. I therefore recommend to tone down the inversion-related part of the interpretation while maintaining that the basement must be involved in thrusting".

Response:
The interpretation that the required basement involvement in the deformation is related to inversion is not only based on the fact that some of the nodal planes are too steep to represent newly initiated faults but on a combined series of observations. We will elaborated this below and have changed Section 5 accordingly.

Jonas Kley suggest that the average of the west-dipping nodal planes (38°) is close to the ideal angle for Mohr-Coulomb faults. We consider that taking an average is not suitable for this discussion. In our manuscript and in our structural model we suggest that only the steeper events are considered to represent inverting normal faults. In our model there are also newly initiated thrust faults (flats and ramps) in the sedimentary succession, which would also contribute to the events recorded. An average value thus is not indicative.

On page 9 line 25 of RC2 supplement it is commented that steeper faults are also "too gently dipping to represent normal faults".

We do not fully agree to this point. The angles are below the 60° usually assumed for the formation of normal faults. The listric nature of extensional faults in rift systems can lead to rotation of faults in the hanging wall, making them more suitable for reactivation (as proposed for example by Jackson 1980). Direct fault inversion indeed is a complex matter. Fault angles, partly rotated through the extensional history, as wells fluid pressures on inversion may play a role (Sibson, 1995). It is beyond the scope of this manuscript to discuss all the potential parameters - instead, we changed the text to clarify, that we consider the presence of inversion as a most likely scenario based on a line of constraints (reworked Section 5). We clarify that we do not only consider (partly) fault inversion, but also other deformation structures often associated with inversion, where faults are not suitable for direct inversion (e.g. hanging wall shortcuts, buttressing effects, back-thrusts, cf. Cooper et al., 1989; Hayward and Graham, 1989).

We expanded Section 5.1 to explain the regional constraints which we interpret as being indicative of inversion rather than non-inversion basement thrusting. The main argument is the orientation of the fold axes west of the Kirthar Escarpment (NNW-SSE to N-S) which does not fit well with shortening one would expect from transpression with the main left lateral strike-slip faults striking N-S to NNE to SSW.

With all the clarifications given above (and implemented in the MS) we think it is justified to keep our interpretation that the deformation in the study area is related to inversion. Nevertheless, we clearly state that this model remains an indirect conclusion on several observations and interpretations, rather than a direct observation (6.5 Uncertainty).

Changes on the MS:
Section 5 and subsection have been re-ordered and extended to improve the line of argumentation based on all constraints. This includes addressing the following main questions: a) could a pure thin-skinned (duplex) solution explain the same (regional) pattern? (requested by RC1) b) Which are the indications for inversion in contrast to a (non-inversion) basement involved model?

All constraints from geological maps (Fig. 5 and reworked Fig. 2) and the new regional section (new Fig. 16g) are elaborated in subsection 5.1 "Constraints from regional structures". The former sub-section "Deformation pattern west of the Kirthar Escarpment is included here). After this, the constraints from the focal mechanisms are elaborated (Section 5.2.). To the sub-section 5.3 "A simplified thick-skinned - thin-skinned inversion model" we added that we consider also other inversion features and a higher complexity (Cooper et al., 1989; Hayward and Graham, 1989). See text as in the track-changes manuscript file.

Section 6.5 Uncertainty, added: "The inversion model is very likely, but remains a conclusion, rather than a direct observation".

2) RC2
Page C2 Paragraph 2): "When the authors compare their new structural models to Banks and Warburtons passive-roof duplex interpretation they should at least briefly discuss what happens in the more internal parts of the belt, away from the deformation front. The passive roof model was motivated by the need to explain gently folded strata raised well above the regional level for a considerable across-strike distance. I assume that this problem also applies to the central Kirthar Range. If the Kirthar Range is held up by a series of reactivated normal faults, where is the reverse displacement of the more internal faults accommodated that cannot be transferred to the thin-skinned front? Or, in other words, is there enough shortening in the internal Kirthar Range to support its topographic and structural elevation assuming that the basal detachment is in the basement?"

Response:
The question raised is interesting, but difficult to answer. We do not have enough geological data to confidently constrain the amount of shortening all across the lateral mountain belt towards the strike slip faults at the plate boundary. West of our core study area we do not have a high resolution geological map, no bedding dip information and no thickness control on the stratigraphy etc. However we address this question as best as possible in Section 5.1, making use of the new regional sketch section Fig. 16 g (as recommended by the referee, see Point 5 below) as well as a small sketch to explain the consequences of thick-skinned/thin-skinned shortening (Fig. 17).

The regional sketch section indicates a deformation style with some inversion and distributed ductile deformation (including wedging/LPS), similar to what we observe in the study area in the front of the section. The amount of shortening in the gently folded strata west of our study area has only about 10% shortening (very rough estimated as the section is partly oblique to some of the fold axes. Furthermore, there are no plane strain conditions in a regional section in a transpression zone). Due to the poor input data, we assume that the actual shortening is in the order of 15% if one would include the non-resolved deformation (wedging/LPS, our sections show 18-20% shortening). We consider that this amount of shortening can be locally accommodated and does not need to propagate to the deformation front – However, with the present data at hand, we cannot define this any better. With 15% of shortening a thick-

skinned solution for the structural elevation west of the Kirthar Escarpment can be justified. A thin-skinned solution can be ruled out.

Changes on the MS:
Section 5.1: Description of the added regional sketch cross-section (Fig. 16g as well as a geological map background in Fig. 2). The regional shortening and how that can be accommodated are discussed (using new Figure 17). See track-changes MS.

3) RC2
Page C2 Paragraph 3 "I am not entirely convinced by the uniqueness of the sequence of thrusting derived in Fig. 9. The advance of a thrust wedge between thrust 1 and backthrust 2 would result in kink band migration and not "progressive limb rotation" as described by the authors (l. 22 in text) and actually suggested by the growth strata geometries. It is also interesting that the kink axis shown to be associated with the tip of the wedge at deeper levels appears offset to the west in the growth strata, but also in the syncline suggested below thrust 1. I could imagine a scenario with no bedding-parallel backthrust and thrust 1 as a late subhorizontal structure displacing the syncline axis towards the east. The implication would be that there must be another thin-skinned thrust further east.

Response:
Indeed, thrust wedge advance of thrust 2 would lead to kink band migration. The observed strata indicates rather limb rotation (although small internal unconformities in the growth strata could mask a higher complexity. The suggested order of deformation by the Referee can be excluded, as there is no additional thin-skinned deformation east of the tip of the wedge (not in the confidential seismic data and there are no indications on surface geology etc.). However, the referee accurately observed the presence of another, deeper kink, offset in respect to the kink in our original Figure 9. We include this to reinvestigate the potential kinematics. Figure 9 has been extended to show a possible evolution of the frontal system. The forelimb of the anticline apparently stays relative stationary due to the stacking of two wedges. Therefore, the growth strata would build two small stacked wedges with kink-band migration that appear similar to limb rotation in the image. This is not necessarily the only explanation and kinematical order, but one in-line with the observations.

Changes on the MS:
Figure 9 has been extended.

In section 4.1 the new Figure 9 and the suggested evolution is described. The caption has been adapted accordingly (see track-changes MS).

4) RC2
Page C3 Paragraph 2 upper part "One thing I am deeply skeptical about is the landslide interpreted in Fig. 6 b. The way this feature is described in the caption I gather that it is supposed to have formed by draping over the topography of the steep forelimb (or did I get that wrong?). I find it hard to believe that you could form the orderly anticline depicted in the satellite image from a rock mass sliding over an irregular land surface."

Response:
The original explanation in the text of Section 3.1 for Fig. 6b is probably too short to reasonably explain this feature. The explanation has been extended. A model is proposed based on similar features known from the Zagros.

Changes on the MS:
We adapted the text and added the reference to similar features in Iran (Harrison and Falcon, 1934, 1936); see track-changes MS. Furthermore, we added a supplementary figure

to illustrate a potential evolution of the slide (into supplement, because we consider this not of key importance for the manuscript and the conclusions).

5) RC2

Page C3 Paragraph 2 lower part: "I think that the paper would strongly benefit from a few additional figures. First, it would help the imagination to have a regional cross-section reaching west to the strike-slip system. Secondly, I strongly recommend to prepare a synthetic figure that combines the new cross-sections with those from published studies whose locations are shown in Fig. 1, preferably redrawn such that comparison is made easy. Nobody wants to look up four other papers to see what the paper they are presently reading is talking about"

Response

Agreed. We prepared an additional figure (Figure 16, note figure numbers will be resorted in the final revised MS), which shows redrafted sections studies mentioned in Section 1. Additionally we added a tentative regional sketch section (Fig. 16g) which includes in the frontal part the simplified version of Fig. 14a, the final section of the northern sector. The original sections (Fig. 12 and Fig. 14) are in a smaller scale, thus showing more details and therefore should remain as they are. The simplified version in Figure 16g should serve the requested purpose to be able to compare scale and style of our results to the published sections.

Changes on the MS:

Added Figure 16 which includes both sections from published studies and a regional section including study results. The background in Fig. 2 has been replaced to show the geological map the regional section is based on. The description of the regional section is now part of the extended Section 5 (as already mentioned above), see track changes MS.

Comments on figure pages in se-2018-137-RC2-supplement.pdf

Referee 2 (Jonas Kley) left some comments and text correction suggestions in two supplementary PDFs. As stated in se-2018-137-RC3.pdf the first supplementary PDF (se-2018-137-RC2-supplement.pdf) contains uncommented mark-ups which are removed or commented in the file se-2018-137-RC3-supplement.pdf. Comments to the figures are only in the file se-2018-137-RC2-supplement.pdf, which will be answered below.

An additional reply will be given for RC3 containing the responses to the comments in the to the manuscript text in file se-2018-137-RC3-supplement.pdf

se-2018-137-RC2-supplement.pdf Page 24, line 4.

"What is actually visible is a strip of emergent land, presumably the Kohistan-Ladakh arc. It would be nice to add to this figure the locations and kinematics of plate boundaries"

Response and Change on MS:

We changed the text in the caption accordingly. Adding locations and kinematics to this figure would indeed be a nice addition but we do not have the database. Researching this seems out-of scope for the purpose of this paper.

se-2018-137-RC2-supplement.pdf Page 25

Explain Kirthar Escarpment

Response and Change on MS:

Added to the caption

se-2018-137-RC2-supplement.pdf Page 31

Several small suggestion to improve Figure 11

Response and Change on MS:

The suggestions have been accepted and are implemented in the reworked Figure 11

se-2018-137-RC2-supplement.pdf Page 32

"Why have you chosen to ignore seismics here?"

Response

The seismic in the background is a combination of a 2D line (the western line) and a section from a 3D seismic (as described in caption to Fig. 8). The 2D line shows on both ends acquisition and processing artefacts especially at greater depth with reflectors curving up. The 3D data shows sub-horizontal reflectors at depth. Therefore, the deepest (dipping) reflectors on the eastern end of the 2D seismic line have been considered unreliable and have been ignored.

se-2018-137-RC2-supplement.pdf Page 34

Mismatch between seismic and dip measurements (Fig. 14)

Response and Change on MS:

The dip measurements in the northern sector of the study area were collected by different campaigns before the acquisition of the seismic. Thus, they are not located on the seismic trace and needed projection between 2.5 and 4 km. Additionally, some locations of the older measurements in the northern sector might not be exact (without GPS).

The projection distance has been added to the caption of Fig. 14

References not listen in the revised MS:

Sibson, R. H., Selective fault reactivation during basin inversion: potential for fluid redistribution through fault-valve action, Geol. Soc. Spec. Publ., 88, 3-19, 1995

Solid Earth

Discussions

Open Access

EGU

Linked thick to thin – skinned inversion in the central Kirthar Fold Belt of Pakistan

Ralph Hinsch[1], Chloé Asmar[1], Muhammad Nasim[2], Muhammad Asif Abbas[2], Shaista Sultan[2]

[1]OMV Upstream, Exploration, Vienna, 1020, Austria
5   [2]OMV (Pakistan) Exploration GmbH (subsidiary of United Energy Group Limited), Islamabad, Pakistan

Abstract

The Kirthar Fold Belt is part of the lateral collision zone in Pakistan linking the Makran accretionary wedge with the Himalaya orogeny. The region is deforming very obliquely, nearly parallel to the regional S-N plate motion vector, indicating strong strain partitioning. In the central Kirthar Fold Belt, folds trend roughly N-S and their structural control is poorly understood.

10   In this study, we use newly acquired 2D seismic data with pre-stack depth migration, published focal mechanisms, surface and subsurface geological data as well as structural modelling with restoration and balancing to constrain the structural architecture and kinematics of the Kirthar Fold Belt.

The central Kirthar Fold Belt is controlled by Pliocene to recent inversion of Mesozoic rift related normal faults. Focal mechanisms indicate dip-slip faulting on roughly N-S trending faults with angles in the order of 45°, which are too steep for

15   newly initiated thrust faults. The hinterland of the study area is primarily dominated by strike slip faulting. The inverting faults do not break straight through the thick sedimentary column of the post-rift and flexural foreland; rather the inversion movements link with a series of detachment horizons in the sedimentary cover, progressively imbricating the former footwall of the normal fault. Due to the presence of a thick incompetent upper unit (Eocene Ghazij shales) these imbricates develop as passive roof duplexes. Finally, the youngest footwall shortcut links with a major detachment and the deformation propagates

20   to the deformation front, forming a large fault-propagation fold. Shortening within the studied sections is calculated to be on the order of 20%.

The central Kirthar fold belt is a genuine example of hybrid thick- and thin-skinned system in which the paleogeography controls the deformation. The locations and sizes of the former rift faults controls the location and orientation of the major folds. The complex tectonostratigraphy (rift, post rift, flexural foreland) alone with the strong E-W gradients defines the

25   mechanical stratigraphy, which in turn controls the complex thin-skinned deformation.

1. Introduction

The external regions of fold-thrust belts are typically interpreted using templates from classical thin-skinned thrust related deformation. However, more and more thrust belts are interpreted as showing a strong influence of linked basement involved deformation (Lacombe and Bellahsen, 2016 and references therein). The inversion of inherited rift faults is one possibility of

thick-skinned contribution in a thrust belt. Furthermore, the direct linkage of inverting basement faults to thin-skinned thrusts in the external parts of orogens (hybrid thick- and thin-skinned system) have received more attention recently (e.g. Giambiagi et al., 2008; Fuentes et al., 2016; Mahoney et al., 2017).

As an outcome of structural investigations for hydrocarbon exploration we are able to report about a well constrained example

5   of linked thin-skinned to thick-skinned deformation at the deformation front of the central Kirthar Fold Belt in Pakistan. This example illustrates the kinematical linkage between inverting deep reaching faults and the associated thin-skinned deformation, and also shows how this hybrid system is strongly controlled by its paleostructural (extension/rift) and paleogeographic (mechanical stratigraphy) inheritance.

The Kirthar fold belt belongs to the western fold belts in Pakistan which is a zone of strike-slip faults and fold belts along the

10   western lateral boundary of the Indian plate linking the Himalaya orogen with the Makran accretionary wedge (Lawrence et al., 1981, Bannert et al., 1992, Fig. 1). The northern Kirthar Fold Belt as well as the Sulaiman Ranges to the North of it, had been traditionally interpreted with classical fold-thrust belt geometries with an implied shortening magnitude of 30-40% (Banks and Warburton, 1986; Humayon et al., 1991; Jadoon et al., 1992, 1993, see location examples in Fig. 1). In contrast, the southern Kirthar Fold Belt had been field investigated (Smewing et al., 2002a) and modeled (Fowler et al., 2004) with the

15   conclusion that the deformation in the belt is dominated by inversion tectonics with an estimated shortening of approximately 17%.

The reported contrasting styles of deformation in the Kirthar fold belt would imply significant and potentially implausible along-strike variation in the shortening magnitudes. In order to understand how deformation is accommodated along this lateral plate boundary, adequate estimations on shortening are essential. Furthermore, constraining the deformation style is

20   fundamentally important for the exploration of resources, as seismic interpreters usually use template structural models to interpret in areas of poor seismic image resolution.

In this study we use observations from surface geology (field work, Google Earth) and subsurface data (recent 2D seismic surveys and well data) to constrain the structural style and kinematics of the central Kirthar Fold Belt. We use seismic interpretation, section analysis techniques and kinematical forward modelling to constrain the balanced cross sections through

25   the area to show that the central Kirthar Fold Belt is driven by thick-skinned inversion which is linked with thin-skinned deformation further toward the foreland. The thin-skinned deformation pattern is dominated by folding with no major thrusts cutting through these structures. The key controlling parameters for the deformation in this area are the pre-existing structures and the mechanical stratigraphy, which is itself a result of the paleo-evolution.

2. Regional setting

30   ## 2.1 Structural setting

The wider Kirthar Range area is situated on the lateral plate boundary of India. The India-Pakistan plate is moving in a northward direction ~~respectively~~ to Eurasia (Mohadjer et al., 2010, Fig. 1), placing the margin in an overall setting of left-

lateral transpression. The Chaman Fault, a large scale strike-slip fault, is considered to represent the lithospheric plate boundary (transform fault) in this lateral collision zone (Lawrence et al., 1981; Bannert et al., 1992). East of the plate boundary, a 150-200 km wide deformation zone is present (Bannert et al., 1992; Szeliga et al., 2009; Fig. 1). Strain partitioning is ongoing (cf. Szeliga et al., 2009 and references therein), documented by the presence of strike-slip faults as well as folds and thrusts (Fig.

5   1). This deformation is also reflected in the distribution of seismic active faults which show strike-slip deformation mainly towards the hinterland and dip-slip reverse faults close to the deformation front (Fig. 2, cf. Reynolds et al., 2015).

Most of the publications on the structural style of the Sulaiman and Kirthar ranges describe these to be thin-skinned fold-thrust belts. Initially, a passive roof duplex style of deformation was attributed to explain the deformation of these fold belts (Banks and Warburton, 1986; Jadoon, 1992). The associated percentage of shortening accommodated by such a thrust and duplex

10   dominated deformation was valued to be in the order of 37%, estimated for a section through the Sulaiman Lobe (Jadoon et al., 1992). These authors propose the same structural style for the northern Kirthar Belt. For the frontal part of the southern Kirthar Fold Belt, thin-skinned fold-thrust styles have been constructed based on field work (Schelling, 1999, see approx. location in Fig. 1). In contrast, Smewing et al. (2002a) infer, based on field work, that the southern Kirthar Fold Belt is dominated by inversion of Jurassic normal faults. Also based on field work and seismic interpretations, Fowler et al. (2004)

15   model the southern Kirthar Fold Belt as inversion deformation. Their sections show shortening on detachment horizons in the sedimentary cover, but the kinematic link between the shortening in the basement and in the cover remains conceptual and partly unclear.

2.2 Tectonostratigraphic evolution

The stratigraphic section in the study area spans from the Triassic to recent (Fig. 3), however older sediments are known along

20   the western margin of the Indian plate. During the Late Precambrian and Early Paleozoic, the Indo-Pakistan plate was part of Gondwana, a situation that persisted until the onset of Triassic to Jurassic rifting (Smith, 2012; Scotese, 2016; cf. Jurassic time step in Fig. 4a). Northern Pakistan was positioned at the northern margin of Gondwana facing the Phantalassic/Paleo-Tethyan Ocean. Salt deposits formed along the Gondwana margin in sub-basins, which are present and observable in the Zagros Hormuz Salt and the Salt Range Formation of Northern Pakistan (Kadri, 1995; Smith 2012). It remains unknown, if deposits (with or

25   without salt) from this period are present in the subsurface of the study area. Further north in Pakistan, Cambrian sediments are overlain unconformably by the Permian stata and it is not certain whether or not the intervening systems were deposited and later eroded (Kadri, 1995). During the Late Permian, the Paleo-Tethys was at its widest, indicating ongoing drifting in the ocean. The passive margin of northern Pakistan was tectonically quiescent with shallow marine to paralic conditions prevailing up to the Late Triassic (Kadri, 1995). The break-up of Gondwana which formed the Indian as well as the Afghanistan-Arabia-

30   Africa plates developed in the Triassic and Jurassic times (see Jurassic time step, Fig. 4a), however, the exact timing for rifting in vicinity of the study area seems uncertain.

Kadri (1995) reports that from the middle Triassic onwards the sedimentation on both sides of the Paleo Tethys suture is different. In general the Triassic mixed successions of shallow marine clastics and carbonates are grouped in the Alozai Group

or Wulgai Formation (Kadri, 1995). Continued rifting is interpreted for the Lower Jurassic deep water Shirinab Formation (which can be separated into three members Springwar, Loralai and Anjira, cf. Fig. 3). Smewing et al. 2002a find evidence for early Jurassic normal faulting due to synkinematical debris flows and slumping in the Lower Jurassic Shirinab Formation. Smewing et al. (2002b) placed the rift in the Kirthar area into Early to Late Jurassic time (Fig. 4a), mainly marked by the

5   successive drowning of the Springwar sandstones and mudstone cycles followed by the pelagic Loralai and Anjira members, as well as the limestones of the Chiltan Formation. The pelagic Anjira limestones are replaced eastward with the thickly bedded limestones of the Chiltan Formation. East of the Kirthar Escarpment, the pelagic Anjira limestones are not known from wells in the study area. We interpret the deep water-shallow water relationship of the Anjira-Chiltan limestones as expression of a hinge zone, related to differential post-rift subsidence. The unconformity on top of the Chiltan limestones is interpreted as

10   break-up unconformity (Smewing et al., 2002b). Wandrey et al. (2004) consider Jurassic or earlier extensional tectonics and failed rifting along the Indus River to contribute to buried horst-and-graben structures and the division of the greater Indus Basin into three sub-basins. The top of the Jurassic strata is marked by a basin wide unconformity (Wandrey et al., 2004; Smewing et al., 2002b). The slightly contradicting reported times for Triassic/Jurassic rifting are likely the result of several pulses of rifting related to the break-up of Gondwana.

15   The Cretaceous sediments are interpreted to be deposited on a westward sloping Indian shield (Kadri, 1995) in the drift phase (cf. Fig. 4b). Large deltas prograded from the emergent Indian continent, depositing the shaly to sandy Sembar and Goru formations in the middle Indus Basin (MIB) and shedding turbidites into the Kirthar Fold Belt area (Fowler et al. 2004). Portions of the Indian shield were uplifted during the Cretaceous which is partly related to the plate passing over an active mantle hot-spot (Eschard et al., 2004) which generated unconformities towards the interior of the continent. The Cretaceous

20   strata thin strongly towards the Jakobad High which is an intrabasinal high in the Indus Basin (Kadri, 1995) northeast of our study area. The internal structuration of the Indus Basin is interpreted as relicts of a failed rift (Zaigham and Mallick, 2000; Wandrey et al., 2004). Mixed clastic and carbonate deposits represent the Upper Cretaceous succession, consisting of the Parh, Mughal Kot and Pab Formations (Fig. 3). Island arc collision and ophiolite obduction occurred on the northwestern margin of the Indian plate during the Paleocene (Khan et al., 2009). The Muslim Bagh and Bela Ophiolites were obducted onto the Indian

25   margin (an island arc is anticipated northwest of the drifting Indian plate in Fig. 4b). Obduction of these ophiolites onto the Indian continental margin in western Pakistan is stratigraphically constrained between the Late Maastrichtian and Early Eocene (between ca. 67 Ma and ca. 50 Ma; Khan et al., 2009 and references herein). Likely as a result of this obduction, the shelf basin deepened and received more clastic influx. Local inversion movements are considered to be responsible for the presence of erosional unconformities. Subsequent quiescent phases are represented by widespread carbonate depositions (e.g. Dungan

30   Formation, Fig. 3). The northwest corner of the Indian plate started to collide with Eurasia during the Eocene (Fig. 4 C). The remaining segment of the Tethys Ocean narrowed further and eventually completely closed. In the study area this phase is represented by, on one side, carbonate deposits on the shelf edge (Laki Formation, Sui Main Limestone Fig. 3) and on the other, a westward rapidly deepening basin sourced partly with shales and siliciclastic deposits shed from the N/NW (Ghazij Formation; Wandrey, 2004; Ahmad et al. 2012). A final and short switch back to slightly more quiet conditions is indicated

by the deposition of the Kirthar Formation (limestones with intercalated shales). During the Oligocene – Lower/Middle Miocene, the Indian Ocean coastline gradually migrated southward in the foreland basin and marine conditions were progressively replaced by continental conditions (Fig. 4D). Marine conditions prevailed in the study area until the Early/Middle Miocene times and are represented by shallow marine carbonates, clastics and shales of the Oligocene Nari Formation and the

5 Mid-Miocene Gaj Formation (Fig. 3). In the late Miocene to Pliocene the collision between India and Eurasia resulted in the uplift of the main Himalaya and enormous quantities of clastic material reached the Lower Indus Basin (i.e. Siwaliks Group, Fig. 3). During this time, transpressive deformation along the western plate margin propagates onto the Lower Indus Basin. Recent ongoing deformation in the study area and regional uplift leads to erosion rather than deposition. Sediments along the Indus are bypassing the foreland into the Indian Ocean.

10 **2.3 Mechanical stratigraphy**

The behaviour of the sedimentary column when deformed is defined by its mechanical stratigraphy, which itself is the result of the tectonostratigraphic evolution. The formations deposited on the shelf margin during the drift phase are located in our study area. The presence of a long lived hinge zone in the study area results in an E-W proximal/distal sedimentological relationship of having successively more incompetent layers present towards the West. Several detachment horizons can be

15 interpreted in the stratigraphic succession (Fig. 3, right column). A colour coding is given to highlight the rationale for interpreting a level as detachment.

3. Remote field work and field work

The core study area is covering the area east of the Kirthar Escarpment, where seismic data is available. In the east of the Kirthar Escarpment, only Cenozoic rocks are outcropping and were partly investigated by field work. The area west of the

20 Kirthar Escarpment, where older rocks crop out, was not accessible due to security reasons. Therefore, the western area was investigated by remote methods: observations in Google Earth and remote assessment of bedding attitude data.

3.1 Remote Fieldwork using Google Earth

Google Earth was utilized in order to investigate structures in the study area on a broad and detailed scale. A quality check of the data quality from Google Earth revealed that images from 2010-2014 fit best to the Digital Elevation Model (DEM) (least

25 draping effects and offset from the DEM).

Fig. 6 shows several examples from the virtual field work with a few important observations on the deformation and mechanical stratigraphy for the study area. The strong mechanical contrast between the Eocene Kirthar limestones and the Eocene Ghazij shales is demonstrated by young gravity book-shelf faulting along an escarpment (Fig. 6a). This young, ongoing deformation is a gravitationally triggered mass movement that is a result of the competency contrast and rapid erosion of the

30 soft shales. Similarly, but a bit more challenging to observe, is the gravity sliding on the large anticline in the northern part of

the study area (Fig. 6b). There, slabs of Kirthar limestones (forming part of the roof of the anticline) slide downwards/eastwards across the already eroded forelimb. As a consequence, sub-horizontal Kirthar limestone beds are superposed over the steep to partly overturned younger beds of the forelimb. Further to the South (towards the background in Fig. 6b) the Kirthar beds are representing the hinge zone of the anticline. There, extensional faults are visible, including relay ramps and other associated

5   features which also demonstrate the young gliding motion on top of the soft Ghazij shales towards the East onto the eroded forelimb.

One example of the deformation style in the west of the Kirthar Escarpment is shown in Fig. 6c. Jurassic limestones and younger strata are partly folded on different wavelengths (disharmonic folding). The large dark, gentle anticline consists of Jurassic basinal limestones. Bright limestones on the ridges of the higher frequency folds are from the Cretaceous Parh Formation. The

10   required decoupling and ductile deformation in-between those layers is located in the Goru Formation, known to consist of soft shales.

Consequently the observations indicate potential decollement horizons in the Ghazij and Goru Formations, as indicated in Fig. 3.

3.2 Remote fieldwork to assess bedding attitude data

15   In addition to the observations done in Google Earth, we used the "Three-Point method" to obtain additional measurements of bedding dip and strike. We used a high resolution DEM and draped satellite images to calculate bedding dip and dip-direction data from three digitized points that are located on a considered geological plane. The quality and level of detail that can be achieved is highly dependent on the quality and resolution of the input data and the outcrop conditions. We used a 30m horizontal resolution SRTM DEM (Jarvis et al., 2008) and Landsat 7 images (Landsat-7 image courtesy of the U.S. Geological

20   Survey). Measurements were only created in areas with univocal identification of large scale bedding planes. QC of generated data and comparison to locally existing field measurements show that bedding strike is general very reliable, whereas the bedding dip results may partly be underestimated.

3.3 Field work

The field work focused on collecting bedding dip data to supplement existing data and to partly QC the remotely assessed data.

25   Furthermore, the style of deformation as observable in field scale was investigated. Sub-recent sediments (Pleistocene to present) are tilted (Fig. 7a), being part of the large scale fold/flexure in the southern sector (Fig. 5, point a). Changes in dip are primarily apparent due to the outcrop conditions where recent outcrop degeneration was present, but small alterations of the dominant dip of the limbs of the large scale structure have been observed, possibly a result of internal thickening within the formation caused by space problems in the inner part of the folds. The necessary flexural slip has been documented even in

30   the very young, likely Pleistocene sediments. Fig. 7b shows striations on bedding planes in sandy beds of a tilted sand/ conglomerate succession (location Fig. 5, point b). It is only in rare cases that small scale (e.g. Fig. 7c) and medium scale (e.g.

Fig. 7d) folds form (locations in Fig. 5, point c and d, respectively). These folds are interpreted to reflect higher order folds caused by local accommodation of space problems in relation to the large scale folding.

4. Seismic interpretation and analysis

The frontal most anticline (Fig. 5) hosts several gas condensate fields and is partly covered by 2D seismic and at least one 3D

5   seismic cube. From 2014-2017 two new 2D seismic surveys were acquired west of this frontal anticline. For confidentiality reasons we are unable to show exact locations of the seismic lines and the well data. However, we subdivided the area into a northern and a southern sector (Fig. 5) and use two representative W-E composed seismic sections to discuss the structural differences of these sectors (Fig. 8). The seismic surveys have up to 6 km horizontal spread and up to 240 fold and utilized dynamite as the source. Processing of the lines in Fig. 8 is up to Pre-Stack Depth Migration (PSDM). These seismic lines have

10   been tied to the vintage seismic data and wells for stratigraphic control.

The seismic quality tends to degrade towards the West and also with depth. Consequently the structural architecture in those parts is less constrained. On both sections, the top of the Eocene Kirthar limestones (cf. Fig. 3) is indicated on locations where well or seismic data unambiguously allow for that interpretation or it is constrained by surface geology (Fig. 8, orange interpretation). In the following section, a brief description of the main structures at Kirthar level is given and structures in

15   areas of good seismic image quality are analysed.

4.1 Northern sector

In the northern sector, the undeformed foreland is marked by relatively horizontal reflectors (Fig. 8a, point a). Sub-horizontal seismic reflectors indicate the presence of sedimentary rocks to at least 8 km depth. A minor anticlinal feature (Fig. 8a, point b) and a more pronounced anticline (Fig. 8a, point d) are separated by a zone of discontinuous reflectors (Fig. 8a, point c), that

20   is interpreted as a fault offsetting the Kirthar limestone. The relative timing of these frontal structures is well depicted in the growth strata imaged on a time-domain seismic section nearby (Fig. 9):

The interpreted growth strata packages GS1 and GS2 show westward thinning and onlap as well as progressive limb rotation related to the triangle deformation at depth (with thrust "1" and roof thrust "2", Fig. 9). The youngest growth strata package, GS3, is only deformed above the projection of fault "3". As a result of the location of this deformation, this fault is younger

25   than faults "1" and "2". Movement on this fault generates a fault-propagation fold in the hanging wall. The good seismic image allows to define the stratigraphic level of the roof thrust (fault "2" in Fig. 9). The thrust has a trend that is parallel to the bedding in the Paleocene shales (upper Ranikot shales, cf. Fig. 3) just below the thick and competent limestones (Sui Main limestones, cf. Fig. 3), characterized by the low-reflectivity seismic character. Tilting of the reflectors below thrust "1" is partly due to a velocity pull-up, but some additional tilting related to layer parallel shortening in deeper levels cannot be excluded. The deeper

30   parts of thrusts "1" and "3" is relatively uncertain based on the seismic profiles. However, the Jurassic Chiltan Formation drilled in the hanging wall of thrust "3", indicating that the thrust cuts below the Jurassic.

A syncline is located west of these frontal structures, though it is not imaged on the seismic due to steeply dipping to overturned beds (Fig. 8a, point e). A large scale anticline with Kirthar limestones on surface level is indicated at point f (Fig. 8a, cf. Fig. 5). The low-reflectivity seismic facies below the Kirthar limestones are Eocene Ghazij Shales (Fig. 8a, point g). These shales thicken dramatically from wells in the East (several tens of meters) towards the West (several hundreds of meters, constrained

5   by outcrop and seismic velocity data). A small scale anticline of higher order is cropping out with Kirthar limestones on the surface (Fig. 8a, point h). A syncline is marking the western end of the seismic (Fig. 8a point i). Kirthar Formation is cropping out also at the Kirthar Escarpment west of the section (Fig. 5 northern sector, at approx. 1150 m above sea level). It is notable that the regional elevation of the Kirthar limestone increases from east to west (approx. 2.5 km in the western syncline, Fig. 8a point i). At the highest outcropping point of Kirthar limestones the difference to the estimated regional level is 5.5 – 6 km

10 with an uncertainty related to the interpreted slope of the regional elevation. A rough depth to detachment analysis conducted with the excess area approach (Epard and Groshong, 1993) on the large scale anticline reveal upper detachment depth of 8-10 km. The spread in the predicted detachment is due to high uncertainty in the deeper stratigraphic picks on the seismic and the fact that the Kirthar Formation is not returning to regional elevation in the syncline to the West.

4.2 Southern sector

15 In the southern section, the undeformed foreland (Fig. 8b, point a) shows sub-horizontal reflectivity to at least 8 km depth. To the West a minor flexure (Fig. 8b, point b) is situated underneath a seismic noise zone hiding a thrust fault (Fig. 8b, point c). This anticline (Fig. 8b, point d) is the southern along-strike continuation of the anticline on the northern section (Fig. 8a, point d). The syncline towards the West (Fig. 8b, point e) is much broader than its northern equivalent. Sub-horizontal reflectors indicate the presence of sedimentary rocks to at least a depth of 10 km. The frontal structures have been analysed and

20 interpreted. Finally the concluded model is illustrated and tested by running a kinematic forward model (Fig. 10). The interpreted fault geometries as well as a stratigraphic template elaborated from wells and outcrop sections are used for the starting configuration of the model (Fig. 10a). Step 1 follows the sequence elaborated in the northern sector (cf. Fig. 9w)ich shows a small fault-bend fold that forms a small triangle structure at the deformation front (Fig. 10b). This triangle structure is cut by a subsequent thrust, forming a fault-propagation fold (figure 10c). This step is modelled using the tri-shear

25 implementation in Move software (Midland Valley, 2016, Fig. 10c). There are several parameters that control the shape of the anticline. In detail, more than one solution (combination of parameters) can generate an approximate fit to the given constraints (seismic, well data (not shown) and surface dips), but differences are not significant. The reasonable fit shown in Fig. 10c supports the fault interpretation and the amount of shortening applied to these frontal structures (about 5000 m of horizontal shortening). To the west of the red stippled line in Fig. 10c, the model does not exactly match the seismic - the interpreted

30 Kirthar Formation is constantly rising until the limestones crop out in a small scale fold (Fig. 8b, point f). West of point f the Kirthar formation continues outcropping at the Kirthar Escarpment (just west of the end of the seismic line) at an elevation of around 1850 m above sea level.

8

Similar to the northern section is the westward thickening of the Eocene Ghazij shale. The shales are thin (several tens of meters) in the frontal anticline (Fig. 8b, below point d) and thicken towards the West (Fig. 8b, point g). This thickening is taking place especially west of the clinoforms (Fig. 8b, point h), which mark the carbonate margin of the Sui/Laki Limestones. On the southern section the regional elevation the West rises constantly from the syncline axis (Fig. 8b, point e) towards the

5 Kirthar Escarpment. The structural elevation gain above regional at the Kirthar Escarpment is more than 6500 m (with uncertainty related to the interpreted regional level, Fig. 8b stippled orange line).

5. Linking thick-skinned and thin-skinned deformation

Despite some structural differences between the sectors, the common observation is the overall increase of the regional elevation level of the Kirthar and other formations from the East to the West. Such an increase in elevation can potentially be

10 explained by several mechanisms: a) a strong wedge shape of the pre-deformational strata below the Kirthar, b) a thrust/fault to a deeper structural level, c) internal structural thickening of formations below the Kirthar Formation or any combination thereof as these proposed mechanisms are not mutually exclusive.

We suggest that the order of structural uplift (larger than 5500 m) is linked to a deeper structural level in the basement. The other mechanisms above might still contribute a smaller part to the regional uplift. This anticipated thick-skinned deformation

15 needs to be linked to the demonstrated thin-skinned deformation close to the deformation front.

In order to generate a most reasonable structural model we briefly review the available nodal plane of earthquakes as well as some indications from the geological map west of the Kirthar Escarpment.

5.1 Focal mechanism from the southern western fold belt

We use ISC bulletin derived nodal planes to constrain potential fault geometries in the subsurface in the wider study area (Fig.

20 2). Given the tectonic setting of a lateral collision zone, it is not surprising that earthquakes towards the current plate boundary at the Chaman Fault document dominantly strike-slip faulting. Some focal mechanisms of earthquakes close to the deformation front show dominant dip-slip shortening (Fig. 2 and Table 1). It is not clear which of the two nodal planes was the moving plane. We could either assume it is the one with the lowest dip or it is westward dipping corresponding to the eastward directed shortening. For the first assumption fault dips are between 15° - 45° and for eastward dipping faults between 15° - 57°. In both

25 cases, the steeper faults are considered to be too steep to represent newly initiated reverse/thrust faults. We interpret these steep faults therefore as reactivated pre-existing faults.

5.2 Deformation pattern west of the Kirthar Escarpment

The outcropping structures west of the seismic coverage/west of the Kirthar Escarpment yield some indications about the structural architecture below the Kirthar and Ghazij Formations (Fig. 5). The area west of the Kirthar Escarpment has a high

30 mean elevation (more than 1000m above sea level). The anticlines with Jurassic outcrops represent the structures with the

highest elevations in the area (labelled with bold numbers 1 in Fig. 5). In-between are areas where Paleocene (and sparsely also Eocene) rocks are preserved, which represent relative structural lows (labelled with bold numbers 2 in Fig. 5). A further characteristic is the presence of long wavelength folds with several km wavelength (labelled with bold numbers 3 in Fig. 5) and anticlines with much smaller wavelengths and higher frequencies (labelled with bold numbers 4 in Fig. 5), indicating a

5   much shallower detachment horizon. The large scale anticlines are usually double plunging and have roughly N-S trending axes, but a variety of additional directions are present as well. A plausible deformation model should be able to explain this complex pattern.

5.3 A simplified thick-skinned - thin-skinned inversion model

We propose that an inversion model is the best solution to explain all the different observations and constraints. Yamada and
10   McClay (2004) demonstrated that the shape of the normal fault with its syn-kinematic fill (Fig. 11a) defines the shape of the inversion anticline (Fig. 11b). Interesting to note is the presence of double plunging anticlines and the possibility of local lows in-between the anticlines and towards the hinterland (Fig. 11b), which can be compared to the structural pattern west of the Kirthar Escarpment in map view. The analogue experiments are limited by the rigid and non-deformable footwall whereas in nature, this is likely not the case. In the study area the shortening of the inverting normal fault is considered to be transferred
15   to detachment in the sediments (Fig. 11c), explaining the presence of short wavelength folds adjacent to the large wavelength folds (cf. Fig. 5). We further suggest that the complex map pattern is likely the result of a much more complex inverted fault pattern as observed in natural rifts. En-echelon pattern and overlaps of faults with intact and broken relay ramps, horses etc. (Fig. 11d) could contribute to a more complex deformation pattern if inverted. Additionally, several stacked detachment horizons allow to accommodate shortening without the necessity of major thrust faults breaking the surface. We consider that
20   the inverting faults are inherited from the original rift phase on the lateral boundary when the Indian plate rifted from northern Godwana (Fig. 4a). The direction of the rift faults thus would also define the N-S direction of the anticlines, which is strongly oblique to the plate kinematic vector.

5.4 Southern section kinematic model and balanced section

The kinematic model of the frontal deformation structures in the southern section (Fig. 10) accommodates approximately
25   5000 m of shortening. However, this amount of shortening is not enough to explain the 6500 m of regional uplift towards the hinterland at the Kirthar Escarpment when taking into consideration reasonable fault dips. A fault with a 45° angle and a displacement of 5000 m would generate a structural uplift of 5000 m from a simple geometric perspective. Either a much steeper fault is necessary, or some additional shortening above/in front the inverting fault are required to explain the 6500 m of regional uplift. From careful seismic interpretation and dip-analysis we have interpreted the presence of small passive roof
30   duplexes underneath the soft Eocene Ghazij shales. Below point g in Fig. 8b some strong but laterally discontinuous reflector packages are present (between points h and i). The reflectors are interpreted to represent the Paleocene limestones. The discontinuous pattern is interpreted to be caused by poor imaging and by structural imbrication. East of point i (Fig. 8b), a

small back-thrust is interpreted. The structural solution is presented in the balanced section (Fig. 12a). By adding the shortening of these small passive roof duplexes to the total displacement on the basement fault, the required regional uplift at the Kirthar Escarpment can be achieved, as is demonstrated in Fig. 13.

The simplified kinematic al model shows the evolution starting from one major normal fault (Fig. 13a). For simplicity we will

5   assume syn-kinematic al growth in the lower Jurassic formations, although the fault might have been active as normal fault earlier and later as well (see Tectonostratigraphic evolution section).

The frontal triangle and the small identified back-thrust are likely formed in an early deformation phase. In the model, this deformation is linked to slight inversion of the displayed normal fault (Fig. 13b), however, the deformation could also be linked to shortening further in the West which is transferred via thin-skinned detachments. The main inversion of the normal

10   fault generates shortcut faults with a slightly smaller dip angle in the sediments of the footwall. The presence of several weak stratigraphic units allows some wedging as well as the passive roof backthrust in the Ghazij shales (Fig. 13b and c). This stage reflects large scale layer parallel shortening of the stratigraphy above/in front of the inverting normal fault. With increasing inversion above the null point, the pressure on the basement in the footwall likely increases and it finally yields. A basement shortcut develops and links with a suitable detachment therefore generating the frontal anticline (Fig. 13d). The

15   features/constraints visible in the seismic and at surface, and especially, the regional elevation uplift at the Kirthar Escarpment can all be explained with one major fault inversion (Fig. 13 D). West of the Kirthar Escarpment the regional elevation remains relatively high and is not dropping as in the simplified model (Fig. 13d hatched area). For that area, additional shortening associated to inverting normal faults is required.

The balanced section in Fig. 12a shows the final interpretation for the seismic displayed in Fig. 8b, with further details than

20   shown in the kinematic section (Fig. 13). This section restores to the pre-contractional situation as shown in Fig. 12b. The balanced section has been constructed by line length restoration onto a carefully constructed stratigraphic template that takes well data and regional thickness trends into account. An overall areal balance has been considered. The amount of shortening is about 10 km, corresponding to 20% between the fixed and the loose line. The Eocene and Oligocene strata have shorter line lengths than the older strata due to roof back-thrusting on the Eocene Ghazij shales and subsequent erosion. The loose line in

25   Fig. 12b is not absolutely straight for Paleocene and older, documenting a small remaining error in the order of 1% which is within the drafting accuracy. The upper part of the section can be considered as well constrained (seismic image, surface geology and well control). The deeper part of the section is constrained by kinematic and balancing considerations. In detail, there could be other solutions fulfilling the constraints (e.g. a more complex pattern of imbrications/duplexes and other structures accommodating layer parallel shortening). In that sense, the presented section is a likely scenario honouring as many

30   constraints as possible and remaining as simple as possible.

5.5 Northern section kinematic model and balanced section

As demonstrated above, the northern sector is dominated by folding and shows a more gradual rise of the regional elevation towards the West. We interpret the shape of the large anticline in Fig. 8a as an uplifted detachment fold (Fig. 14) with plastic

deformation in the fold core. In detail the deformation in the fold core can be accommodated by small scale thrusts (e.g. fishtail wedges etc.). The relative gentler uplift of regional elevation towards the West indicate the presence of several small inverting faults in the basement in comparison to the southern section. A proposed kinematical evolution is displayed in Fig. 15. Several half graben normal faults with thickening strata toward the fault (again in Jurassic for simplicity reasons) are present below

5 some post rift strata (Fig. 15a). The thick-skinned movement is linked with a thin-skinned decollement close to the base of the sedimentary column (Fig. 15b). For simplicity, this step is modelled with one footwall-shortcut on the westernmost fault. The large scale anticline in the northern sector likely starts to grow in this increment. Fig. 14b anticipates a buttressing effect of the easternmost fault causing the folding. Alternatively, early inversion movement on this easternmost fault could generate a perturbation in the sedimentary sequence which is subsequently amplified by shortening which is transferred along the basal

10 décollement. The inversion is modelled with a foreland propagation sequence. The second (middle) fault is also modelled with a small footwall shortcut (Fig. 15c). The associated shortening is amplifying the large scale fold. Some shortening of this increment might cause the observed triangle deformation (Fig. 9). Finally, the easternmost fault is inverting including a footwall shortcut that links to the observed frontal structures (Fig. 15d). The final balanced section honours some more details as constrained by the seismic (Fig. 14a). In total, the northern section is less constrained than the southern section as the seismic

15 is allowing more solutions for the deeper geometry. The main uncertainties are the amount of basement faults, the amount of initial extensional throw, how many faults and shortcuts are present in the sediments and the sequence of deformation propagation. The kinematic model in Fig. 14 as well as the balanced section are thus not unique solutions however they provide a satisfactory explanation for the observed structures that is consistent with the mechanical stratigraphy, the regional observations and the local constraints (seismic and surface geology).

20 The balanced section of the northern sector (Fig. 14a) restores to the pre-contraction geometry as is shown in Fig. 14b. The method of restoration is the same as for the southern sector. The weak formations have been additionally areally balanced. The amount of shortening is approximately 11.2 km, corresponding to 18% between the fixed and the loose line. The loose line in Fig. 14b is not absolutely straight, documenting a small remaining error in the order of the drifting accuracy.

6. Discussion

25 In the following section we discuss implications of the results from the local to regional scale, compare the deformation style to similar fold belts, and finally address some uncertainty issues.

6.1 Local paleogeographic controls on deformation

On a local scale the deformation seen in the geological map (Fig. 5) is partly mimicking the original rift geometry. The large scale folds are most likely representing the former location of the main extensional growth grabens. The dominating N-S

30 orientation of fold trends is thus is directly controlled by the former rift geometry and thus has a strong influence on how strain is partitioned on this lateral margin.

In detail, most local differences in the structural style and orientation seem to be based on slight paleogeographic differences as well. Comparing the northern to the southern sectors of the study area, ~~there is difference of the detachment depth of the trailing thin-skinned deformation.~~ In the South, the large syncline (Fig. 8b) indicates a flat segment of the detachment in lower Jurassic or Triassic rocks. The ~~comparative~~ thrust fault clearly cuts deeper in the North (Figs. 8a, 9, 14). As a consequence the

5   frontal anticline shows a south to north along-strike ~~structural uplift~~. The uplift has been recognized for a long time (wells and the distribution of the existing gas condensate fields), but geometrically they have not been properly investigated. The reason for the along strike change of the basal detachment, however, is not known. It may have geometrical (fault throw, angle, depth) or facies (mechanical stratigraphy) related reasons. Both, however would be inherited from the pre-contractional evolution, with the rifting phase likely having the greatest impact.

10   There is one very clear example on how the long lived hinge zone and the associated facies changes control the young contractional deformation. The tip of the triangle/duplex in the centre of the southern section is localised at the point where the Laki Formation limestones (Sui Main Limestones, stippled orange line) have their paleo-shelf edge and are replaced laterally by Ghazij Formation shales (Fig. 12a, see also Fig. 8b, point h). The limestones have several hundred meters of thickness in the frontal anticline and are overlain by several tens of meters of Ghazij shales only. West of the Kirthar

15   Escarpment, the Laki Formation/Sui Main Limestones are missing, instead several hundred meters of Ghazij shales are present. The clinoforms of the Sui Main Limestones are well imaged (Fig. 8b point h). West of that point most of the Laki Formation is replaced by marls and shales that ~~act a~~ passive roof thrust for the inversion related footwall duplexes underneath. The juxtaposition of carbonate margins that border basinal facies can localize thrust faults as has been demonstrated by centrifuge physical modelling ~~by Dixon, 2004~~

20   **6.2 Kirthar Fold Belt deformation**

Our model of inversion with linked thin skinned deformation for the central Kirthar Fold Belt is in line with the observations and the model proposed by Smewing et al. (2002a) and Fowler et al. (2004) for the southern Kirthar Fold Belt. In our study we demonstrate how thick-skinned inversion and thin-skinned deformation kinematically link to produce the observed deformation pattern. With our model ~~we are~~ to able to explain an observation of Smewing et al. (2002a) where they describe

25   field evidence of a Jurassic normal fault that is still under net extension, despite the assumed inversion and relative high structural elevation. Following our model the upper part of ~~the~~ former normal ~~fault~~ would remain in net extension and be significantly uplifted above their original regional elevation due to footwall imbrication and shortcuts (cf. the former normal faults in Fig. 14). These imbrications however, do not ~~penetrate to the~~ surface but generate structural wedges with a roof thrust in Ghazij shales. They are unlike the passive roof duplexes proposed originally for the northern Kirthar Fold Belt by Banks

30   and Warburton (1986). Those authors use classical thin-skinned fold-trust belt geometries based on the sequential imbrication of the foreland sequence above a pre-Jurassic continuous planar detachment horizon. Their roof thrusts are localized in Ghazij shales and further towards the hinterland in Goru formation shales. Shortening in such a system often approaches 40-50%, a value much higher than the shortening observed in the central (our study) and southern Kirthar Fold Belt (Fowler et al., 2004).

The large scale map pattern does not significantly change from our study area towards the northern Kirthar Fold Belt. We propose that the deformation observed in the northern Kirthar Fold Belt (i.e. Banks and Warburton, 1986) could also be caused by linked thick-skinned and thin-skinned inversion related deformation. Similarly, the thin-skinned deformation observed by Schelling (2000) can be put into this context. The sections investigated by Shelling are relatively short and thus only cover the

5   leading edge margin of the thin-skinned deformation (similar to the frontal structures in Fig. 12). Thus, no major south to north discrepancies in shortening values need to be considered for the Kirthar Fold Belt. The deformation style does not necessarily vary dramatically, however the way the shortening is accommodated is considered to be controlled by local inherited controls.

6.3 Possible lithospheric inheritance of the inversion belt

It is important to briefly discuss some potential reasons why the Kirthar Fold Belt is dominated by inversion with thin-skinned
10   deformation instead of following classical thin-skinned fold-thrust belt model. The importance of a structural inheritance from rifting has already been proposed by Smewing et al. (2002a). However, most pro-wedge thrust belts affect areas which went through rifting and passive margin settings before collision. Whether the continental margin in the collision phase evolves into a dominated system of thin-skinned or thick-skinned deformation depends on several factors.

The presence of a weak (ductile) middle or lower crust seems to be key factor which allows for distributed deformation through
15   most of the crust, which results in forming fold-thrust belts with a dominant/primary thick-skinned character (Lacombe and Bellahsen, 2016). Thermally weakened shear zones might be conserved in little extended proximal continental margins which can also influence the deformation style. Weak crustal levels are often lacking in distal parts of the margins as a result of the rheological evolution of the rifted margin over time (Perez-Gussinye and Reston, 2001; Cloetingh et al. 2005; Reston & Manatschal, 2011). The resulting stronger lithospheric domains are more prone to localized deformation in a continental
20   subduction style (Lacombe and Bellahsen, 2016). Thus, the relative position and the time since rifting apparently play a role in determining in which mode the convergent deformation will reactivate structures.

We therefore speculate, that the inversion dominated Kirthar Fold belt represents the inner part of the continental margin in which a weak continental crust is still present. The long lived hinge line observed in several facies associations is interpreted to reflect approximately the limit of the major post-rift subsidence and the eastern border of the extended lithosphere (assuming
25   pure-shear). The more than 100km wide area from the deformation front to the Ghazaband fault (Fig. 1) is interpreted to be dominated by initial inversion (later partly overprinted by strike-slip deformation). We infer that this large area shares a similar rheology which was inherited from Gondwana and the break up phase. The width of this zone might indicate that the lithosphere rifted in a wide rift mode (Buck, 1991) before continental break-up to the West. Consequently there should be a narrow zone of highly extended crust (external rifted margin) present west of the inversion belt. Today this zone is covered by
30   Flysch sediments, bracketed between the Ghazaband and Chaman Faults (Bannert et al., 1992). How much of the former external rifted margin has been subducted or laterally displaced along the strike-slip faults remains difficult to estimate and is beyond the scope of this paper. Interestingly, further to the North in the Pamir area earthquake tomography data is interpreted to show delamination and rollback of the Indian plate lithosphere (Kufner et al., 2015). India's thinned western continental

margin separates from Cratonic India and subducts beneath Asia while the buoyant northwestern salient of Cratonic India bulldozes into Cratonic Asia (Kufner et al., 2015).

6.4 Hybrid thick- and thin-skinned systems in other areas

Thick-skinned inversion of passive margin or intra-cratonic rifts is considered to be present in 50% of orogens with documented deformation style (Nemčok et al., 2013). There are various possibilities how thick-skinned deformation can contribute to the deformation of a fold-thrust belt (see recent review of Lacombe and Bellahsen, 2016 and references therein). Here, we briefly compare the deformation style elaborated for the central Kirthar Fold Belt with other well constrained examples of linked inversion with thin-skinned deformation.

For the Malargüe Fold-Thrust belt, Giambiagi et al. (2008) revealed that the reactivation of normal faults was coeval with the activation of shallow detachments and low-angle thrusting at the thrust front with several faults moving at the same time in some portions. Also for the Malargüe Fold-Thrust belt Fuentes et al. (2016) work out geometric relationships of the hybrid system with a series of detailed sections based on surface geology, seismic and well data through that thrust belt. Their section "E" show strong similarities with the deformation style in the southern section of our study, especially the imbrication of sediments in the footwall with duplexes and a passive roof thrust on top. Recently, Mahoney et al. (2017) proposed a very similar deformation for the Eastern Muller Ranges in the Papuan Fold Belt in Papua New Guinea. There, the Cenozoic carbonates are shortened to around 13-21% but are partly uplifted up to /km above regional elevation. Mesozoic rift faults, partly inverting and partly linking to thin skinned detachments are considered to reflect the major control on deformation. Triangle structures and back-thrusts are considered transient deformation steps, related to the uplift and erosion history while the deformation accumulates before linking to the frontal deformation structures (Mahoney et al., 2017). The proposed deformation is very similar to the style we consider for the central Kirthar Fold Belt. In our example the presence of a complex mechanical stratigraphy with several detachment horizons in the stratigraphic column seems to produce even more complex geometries than in the example from Papua New Guinea.

6.5 Uncertainty

Basement involvement is very often used in balanced section to account for regional elevation uplift towards the hinterland. However, for a relatively small uplift of regional elevation the thick skinned explanation is often ambiguous, as there are often several alternative possibilities which are not investigated (e.g. strong wedging of the pre-kinematic sedimentary sequence, change in basal detachment depth, change in basement dip etc.).

Recently, Butler et al. (2018) demonstrated that for several reviewed sections that there is a substantially greater range of solutions available for interpreting the geometry and evolution of thrust belt structures than implied by the original idealized models. For a specific section in the Papuan Fold and thrust belt two realisations are available by different authors. One with thin-skinned and one with inversion style tectonics (e.g. Hill, 1997; Buchanan and Warburton 1996; cf. Butler et al. 2018).

Similar, there is a strong discussion on the contribution of thick-skinned deformation below the different segments of the Zagros fold belt (see discussions in Lacombe and Bellahsen, 2016; Hinsch and Bretis, 2015, for the Mountain Front Flexure).

In order to overcome limitations from single deterministic geometries, Butler et al. (2018) propose good documentation, alternative models and to embrace the uncertainties. In this work, we show the original seismic data, review in detail the regional to local context and use these as arguments why we think our presented deformation model is the most plausible for the central Kirthar Fold Belt from the other investigated alternatives. We do not show alternative models, but we highlight our workflow, the considered constraints and indicate uncertainties of the sections. With all the arguments given, the contribution of deep founded faults with associated thin-skinned deformation can be considered as reliable, and the pure thin-skinned deformation style can be considered as obsolete. In detail the interpreted and constructed sections are as good as the constraints allow and thus still have several solutions. The amount of uncertainty in the sections depends also on the level of observation.

7. Conclusions

Large scale strain partitioning along the western Indian plate leads to major left lateral strike-slip faulting close to the plate margin as well as to NW-SE to W-E shortening close to the deformation front of the Kirthar Fold Belt. We analyse regional (focal mechanisms, geological maps) to local (reflection seismic and well data, surface geology) data at the front of the central fold belt to constrain the structural architecture and style. The deformation is controlled by the inversion of inherited rift faults, likely of Jurassic age, which is buried underneath the sediments. The young shortening on the rift faults is coupled with thin-skinned deformation by imbricating and shortcutting into the footwall and transferring some shortening onto a detachment horizon. As a consequence, large scale folds build as a result of the thick-skinned inversion and smaller scale folds and thin skinned related thrust deformation form in front. In the southern sector a structural elevation gain of approximately 6500 m across one large monocline clearly indicates the influence of the deep seated faulting. Towards the North the structural elevation gain is distributed across several folds indirectly related to several inverting faults at depth. The main control on deformation is the presence and orientation of the pre-shortening rift. In addition, the rift and post rift history resulted in some prominent E to W proximal to distal facies trends being reflected in a heterogeneous mechanical stratigraphy which is responsible for the style on how shortening is accommodated in the thin-skinned structures.

The hybrid deformation style of thin-skinned to thick-skinned deformation is also present in other fold-thrust belts around the world with hydrocarbon resources. Combining as many constraints as possible from regional to local scale facilitates the development of plausible structural models and assess uncertainties. The importance of understanding the structural architecture and kinematics is here and there of paramount importance for the successful exploration of these resources.

Manuscript file with coloured track changes

Changes in this colour are referring to changes regarding RC1.

Changes in this colour are done mainly in response to RC2

Linked thick to thin – skinned inversion in the central Kirthar Fold Belt of Pakistan

Ralph Hinsch[1], Chloé Asmar[1], Muhammad Nasim[2], Muhammad Asif Abbas[2], Shaista Sultan[2]

[1]OMV Upstream, Exploration, Vienna, 1020, Austria
[2]OMV (Pakistan) Exploration GmbH (subsidiary of United Energy Group Limited), Islamabad, Pakistan

Abstract

The Kirthar Fold Belt is part of the transpressive transfer zone lateral collision zone in Pakistan linking the Makran accretionary wedge with the Himalaya orogeny. The region is deforming very obliquely, nearly parallel to the regional S-N plate motion vector, indicating strong strain partitioning. In the central Kirthar Fold Belt, folds trend roughly N-S and their structural control is poorly understood. In this study, we use newly acquired 2D seismic data with pre-stack depth migration, published focal mechanisms, surface and subsurface geological data as well as structural modelling with restoration and balancing to constrain the structural architecture and kinematics of the Kirthar Fold Belt.

The central Kirthar Fold Belt is controlled by Pliocene to recent inversion of Mesozoic rift related normal faults. Focal mechanisms indicate dip-slip faulting on roughly N-S trending faults with some dip angles in the order of exceeding 45 40°, which are considered too steep for newly initiated thrust faults. The hinterland of the study area is primarily dominated by strike strike-slip faulting. The inverting faults do not break straight through the thick sedimentary column of the post-rift and flexural foreland; rather the inversion movements link with a series of detachment horizons in the sedimentary cover, progressively imbricating the former footwall of the normal fault. Due to the presence of a thick incompetent upper unit (Eocene Ghazij shales) these imbricates develop as passive roof duplexes. Finally, the youngest footwall shortcut links with a major detachment and the deformation propagates to the deformation front, forming a large fault-propagation fold. Shortening within the studied sections is calculated to be on the order of 20%.

The central Kirthar fold belt is a genuine example of hybrid thick- and thin-skinned system in which the paleogeography controls the deformation. The locations and sizes of the former rift faults controls the location and orientation of the major folds. The complex tectonostratigraphy (rift, post rift, flexural foreland) alone with the strong E-W gradients defines the mechanical stratigraphy, which in turn controls the complex thin-skinned deformation.

1. Introduction

The external regions of fold-thrust belts are typically interpreted using templates from classical thin-skinned thrust related deformation. However, more and more thrust belts are interpreted as showing a strong influence of linked basement involved deformation (Lacombe and Bellahsen, 2016 and references therein). The inversion of inherited rift faults is one possibility of
5 thick-skinned contribution in a thrust belt. Furthermore, the direct linkage of inverting basement faults to thin-skinned thrusts in the external parts of orogens (hybrid thick- and thin-skinned system) have received more attention recently (e.g. Giambiagi et al., 2008; Fuentes et al., 2016; Mahoney et al., 2017).

As an outcome of structural investigations for hydrocarbon exploration we are able to report about a well constrained example of linked thin-skinned to thick-skinned deformation at the deformation front of the central Kirthar Fold Belt in Pakistan. This
10 example illustrates the kinematical linkage between inverting deep reaching faults and the associated thin-skinned deformation, and also shows how this hybrid system is strongly controlled by its paleostructural (extension/rift) and paleogeographic (mechanical stratigraphy) inheritance.

The Kirthar fold belt belongs to the western fold belts in Pakistan which is a zone of strike-slip faults and fold belts along the western lateral boundary of the Indian plate linking the Himalaya orogen with the Makran accretionary wedge (Lawrence et
15 al., 1981, Bannert et al., 1992, Fig. 1). The northern Kirthar Fold Belt as well as the Sulaiman Ranges to the North of it, had been traditionally interpreted with classical fold-thrust belt geometries with an implied shortening magnitude of 30-40% (Banks and Warburton, 1986; Humayon et al., 1991; Jadoon et al., 1992, 1993, Fig. 16a-c, see location examples in Fig. 1). In contrast, the southern Kirthar Fold Belt had been field investigated (Smewing et al., 2002a) and modeled (Fowler et al., 2004) with the conclusion that the deformation in the belt is dominated by inversion tectonics (Fig. 16e) with an estimated shortening
20 of approximately 17%.

The reported contrasting styles of deformation in the Kirthar fold belt would imply significant and potentially implausible along-strike variation in the shortening magnitudes. In order to understand how deformation is accommodated along this lateral plate boundary, adequate estimations on shortening are essential. Furthermore, constraining the deformation style is fundamentally important for the exploration of resources, as seismic interpreters usually use template structural models to
25 interpret in areas of poor seismic image resolution.

In this study we use observations from surface geology (field work, Google Earth) and subsurface data (recent 2D seismic surveys and well data) to constrain the structural style and kinematics of the central Kirthar Fold Belt. We use seismic interpretation, section analysis techniques and kinematical forward modelling to constrain the balanced cross sections through the area to show that the central Kirthar Fold Belt is driven by thick-skinned inversion which is linked with thin-skinned
30 deformation further toward the foreland. The thin-skinned deformation pattern is dominated by folding with no major thrusts cutting through these structures. The key controlling parameters for the deformation in this area are the pre-existing structures and the mechanical stratigraphy, which is itself a result of the paleo-evolution.

2

2. Regional setting

2.1 Structural setting

The wider Kirthar Range area is situated on the lateral plate boundary of India. The India-Pakistan plate is moving in a northward direction ~~respectively~~ relative to Eurasia (Mohadjer et al., 2010, Fig. 1), placing the margin in an overall setting of left-lateral transpression. The Chaman Fault, a large scale strike-slip fault, is considered to represent the lithospheric plate boundary (transform fault) in this lateral collision zone (Lawrence et al., 1981; Bannert et al., 1992). East of the plate boundary, a 150-200 km wide deformation zone is present (Bannert et al., 1992; Szeliga et al., 2009; Figs. 1, 2). Strain partitioning is ~~ongoing~~ active (cf. Szeliga et al., 2009 and references therein), documented by the presence of strike-slip faults as well as folds and thrusts (Fig. 1). This deformation is also reflected in the distribution of ~~seismic~~ seismically active faults which show strike-slip deformation mainly towards the hinterland and dip-slip reverse faults close to the deformation front (Fig. 2, cf. Reynolds et al., 2015).

Most ~~of the~~ publications on the structural style of the Sulaiman and Kirthar ranges describe these to be thin-skinned fold-thrust belts. Initially, a passive roof duplex style of deformation was attributed to explain the deformation of these fold belts (Banks and Warburton, 1986; Jadoon, 1992, Fig. 16a-c). The associated percentage of shortening accommodated by such a thrust and duplex dominated deformation was valued to be in the order of 37%, estimated for a section through the Sulaiman Lobe (Jadoon et al., 1992). These authors propose the same structural style for the northern Kirthar Belt. For the frontal part of the southern Kirthar Fold Belt, thin-skinned fold-thrust styles have been constructed based on field work (Schelling, 1999, Fig. 16f, see approx. location in Fig. 1). In contrast, Smewing et al. (2002a) infer, based on field work, that the southern Kirthar Fold Belt is dominated by inversion of Jurassic normal faults. Also based on field work and seismic interpretations, Fowler et al. (2004) model the southern Kirthar Fold Belt as inversion deformation. Their sections show shortening on detachment horizons in the sedimentary cover, but the kinematic link between the shortening in the basement and in the cover remains conceptual and partly unclear (Fig. 16e).

2.2 Tectonostratigraphic evolution

The known stratigraphic section in the study area spans from the Triassic to recent (from outcrop and wells; Fig. 3), however older sediments are known along the western margin of the Indian plate. During the Late Precambrian and Early Paleozoic, the Indo-Pakistan plate was part of Gondwana, a situation that persisted until the onset of Triassic to Jurassic rifting (Smith, 2012; Scotese, 2016; cf. Jurassic time step in Fig. 4a). Northern Pakistan was positioned at the northern margin of Gondwana facing the Panthalassic~~Phantalassic~~/Paleo-Tethyan Ocean. Salt deposits formed along the Gondwana margin in sub-basins, which are present and observable in the Zagros Hormuz Salt and the Salt Range Formation of Northern Pakistan (Kadri, 1995; Smith 2012). It remains unknown, if deposits (with or without salt) from this period are present in the subsurface of the study area. Further north in Pakistan, Cambrian sediments are overlain unconformably by the Permian stata and it is not certain whether or not the intervening systems were deposited and later eroded (Kadri, 1995). During the Late Permian, the Paleo-

3

Tethys was at its widest, indicating ongoing drifting in the ocean. The passive margin of northern Pakistan was tectonically quiescent with shallow marine to paralic conditions prevailing up to the Late Triassic (Kadri, 1995). The break-up of Gondwana which formed the Indian as well as the Afghanistan-Arabia-Africa plates developed in ~~the~~ Triassic and Jurassic times (see Jurassic time step, Fig. 4a), however, the exact timing for rifting in vicinity of the study area seems uncertain.

5 Kadri (1995) reports that from the middle Triassic onwards the sedimentation on both sides of the Paleo Tethys suture is different. In general the Triassic mixed successions of shallow marine clastics and carbonates are grouped in the Alozai Group or Wulgai Formation (Kadri, 1995). Continued rifting is interpreted for the Lower Jurassic deep water Shirinab Formation (which can be separated into three members Springwar, Loralai and Anjira, cf. Fig. 3). Smewing et al. 2002a find evidence for early Jurassic normal faulting due to synkinematical debris flows and slumping in the Lower Jurassic Shirinab Formation.

10 Smewing et al. (2002b) placed the rift in the Kirthar area into Early to Late Jurassic time (Fig. 4a), mainly marked by the successive drowning of the Springwar sandstones and mudstone cycles followed by the pelagic Loralai and Anjira members, as well as the limestones of the Chiltan Formation. The pelagic Anjira limestones are replaced eastward with the thickly bedded limestones of the Chiltan Formation. East of the Kirthar Escarpment, the pelagic Anjira limestones are not known from wells in the study area. We interpret the deep water-shallow water relationship of the Anjira-Chiltan limestones as expression of a

15 hinge zone, related to differential post-rift subsidence. The unconformity on top of the Chiltan limestones is interpreted as break-up unconformity (Smewing et al., 2002b). Wandrey et al. (2004) consider Jurassic or earlier extensional tectonics and failed rifting along the Indus River to contribute to buried horst-and-graben structures and the division of the greater Indus Basin into three sub-basins. The top of the Jurassic strata is marked by a basin wide unconformity (Wandrey et al., 2004; Smewing et al., 2002b). The slightly contradicting reported times for Triassic/Jurassic rifting could be either ~~are likely~~ the

20 result of several pulses of rifting related to the break-up of Gondwana or interpretational uncertainty.

The Cretaceous sediments are interpreted to ~~be~~ have been deposited on a westward sloping Indian shield (Kadri, 1995) in the drift phase (cf. Fig. 4b). Large deltas prograded from the emergent Indian continent, depositing the shaly to sandy Sembar and Goru formations in the middle Indus Basin (MIB) and shedding turbidites into the Kirthar Fold Belt area (Fowler et al. 2004). Portions of the Indian shield were uplifted during the Cretaceous which is partly related to the plate passing over an active

25 mantle hot-spot (Eschard et al., 2004) which generated unconformities towards the interior of the continent. The Cretaceous strata thin strongly towards the Jakobad High which is an intrabasinal high in the Indus Basin (Kadri, 1995) northeast of our study area. The internal structuration of the Indus Basin is interpreted as relics of a failed rift (Zaigham and Mallick, 2000; Wandrey et al., 2004). Mixed clastic and carbonate deposits represent the Upper Cretaceous succession, consisting of the Parh, Mughal Kot and Pab Formations (Fig. 3). Island arc collision and ophiolite obduction occurred on the northwestern margin of

30 the Indian plate during the Paleocene (Khan et al., 2009). The Muslim Bagh and Bela Ophiolites were obducted onto the Indian margin (an island arc is anticipated northwest of the drifting Indian plate in Fig. 4b). Obduction of these ophiolites onto the Indian continental margin in western Pakistan is stratigraphically constrained between the Late Maastrichtian and Early Eocene (between ca. 67 Ma and ca. 50 Ma; Khan et al., 2009 and references herein). Likely as a result of this obduction, the shelf basin deepened and received more clastic influx. Local inversion movements are considered to be responsible for the presence of

4

erosional unconformities. Subsequent quiescent phases are represented by widespread carbonate depositions (e.g. Dungan Formation, Fig. 3). The northwest corner of the Indian plate started to collide with Eurasia during the Eocene (Fig. 4 C). The remaining segment of the Tethys Ocean narrowed further and eventually completely closed. In the study area this phase is represented by, on one side, carbonate deposits on the shelf edge (Laki Formation, Sui Main Limestone Fig. 3) and on the other, a westward rapidly deepening basin ~~sourced~~ filled partly with shales and siliciclastic deposits shed from the N/NW (Ghazij Formation; Wandrey, 2004; Ahmad et al. 2012). For the study area Ahmad et al. (2012) observe a dramatic east to west thickness increase of the Ghazij formation from thin layers of shale (in the Mazerani 1 well on the frontal anticline) to about 1000 m thickness (outcrop section) in the area west of the Kirthar escarpment in less than 40km distance. A final and short switch back to slightly more quiet conditions is indicated by the deposition of the Kirthar Formation (limestones with intercalated shales). During the Oligocene – Lower/Middle Miocene, the Indian Ocean coastline gradually migrated southward in the foreland basin and marine conditions were progressively replaced by continental conditions (Fig. 4D). Marine conditions prevailed in the study area until ~~the~~ Early/Middle Miocene times and are represented by shallow marine carbonates, clastics and shales of the Oligocene Nari Formation and the Mid-Miocene Gaj Formation (Fig. 3). In the late Miocene to Pliocene the collision between India and Eurasia resulted in the uplift of the main Himalaya and enormous quantities of clastic material reached the Lower Indus Basin (i.e. Siwaliks Group, Fig. 3). During this time, transpressive deformation along the western plate margin propagates onto the Lower Indus Basin. Recent ongoing deformation in the study area and regional uplift leads to erosion rather than deposition. Sediments along the Indus are bypassing the foreland into the Indian Ocean.

2.3 Mechanical stratigraphy

The behaviour of the sedimentary column when deformed is defined by its mechanical stratigraphy, which itself is the result of the tectonostratigraphic evolution. The formations deposited on the shelf margin during the drift phase are located in our study area. The presence of a long lived hinge zone in the study area results in an E-W proximal/distal sedimentological relationship of having successively more incompetent layers present towards the West. Several detachment horizons can be interpreted in the stratigraphic succession (Fig. 3, right column). A colour cod~~eing~~ indicates if a certain level is interpreted as detachment based on field or seismic observations, or modelling.~~is given to highlight the rationale for interpreting a level as detachment.~~

3. Remote field work and field work

The core study area is covering the area east of the Kirthar Escarpment, where seismic data is available. ~~In the east of the Kirthar Escarpment~~There, only Cenozoic rocks are outcropping and were partly investigated by field work. The area west of the Kirthar Escarpment, where older rocks crop out, was not accessible due to security reasons. Therefore, the western area was investigated by remote methods: observations in Google Earth and remote assessment of bedding attitude data.

3.1 Remote Fieldwork using Google Earth

Google Earth was utilized in order to investigate structures in the study area on a broad and detailed scale. A quality check of the data quality from Google Earth revealed that images from 2010-2014 fit best to the Digital Elevation Model (DEM) (least draping effects and offset from the DEM).

Fig. 6 shows several examples from the virtual field work with a few important observations on the deformation and mechanical stratigraphy for the study area. The strong mechanical contrast between the Eocene Kirthar limestones and the Eocene Ghazij shales is demonstrated by young gravity book-shelf faulting along an escarpment (Fig. 6a). This young, ongoing deformation is a gravitationally triggered mass movement that is a result of the competency contrast and rapid erosion of the soft shales. These shales reach several hundred meters of thickness east of the Kirthar Escarpment. Similarly, but a bit more challenging to observe, is the gravity sliding on the large anticline in the northern part of the study area (Fig. 6b). There, slabs of Kirthar limestones (forming part of the roof of the anticline) slide have collapsed downwards/eastwards and slid across parts of the already eroded forelimb. As a consequence, sub-horizontal Kirthar limestone beds are superposed over the steep to partly overturned younger beds of the forelimb. Similar features have been observed in numerous examples in the Zagros in Iran (Harrison and Falcon 1934, 1936). A potential sequence of the landslide evolution after the mechanism suggested by Harrison and Falcon (1934, 1936) is shown in Supplement Figure 1 along with an alternative solution. The main requirements for the landslide solution is the presence of a thick weak layer underneath the Kithar limestone that can act as a decollement. Further to the South (towards the background in Fig. 6b) the Kirthar beds are representing represent the hinge zone of the anticline. There, extensional faults are visible, including relay ramps and other associated features which also demonstrate the young gliding motion on top of the soft Ghazij shales towards the East onto the eroded forelimb.

One example of the deformation style in the west of the Kirthar Escarpment is shown in Fig. 6c. Jurassic limestones and younger strata are partly folded on different wavelengths (disharmonic folding). The large dark, gentle anticline consists of Jurassic basinal limestones. Bright limestones on the ridges of the higher frequency folds are from the Cretaceous Parh Formation. The required decoupling and ductile deformation in-between those layers is located in the Goru Formation, known to consist of soft shales.

Consequently the observations indicate potential decollement horizons in the Ghazij and Goru Formations, as indicated in Fig. 3.

3.2 Remote fieldwork to assess bedding attitude data

In addition to the observations done in Google Earth, we used the "Three-Point method" to obtain additional measurements of bedding dip and strike. We used a high resolution DEM and draped satellite images to calculate bedding dip and dip-direction data from three digitized points that are located on a considered geological plane. The quality and level of detail that can be achieved is highly dependent on the quality and resolution of the input data and the outcrop conditions. We used a 30m horizontal resolution SRTM DEM (Jarvis et al., 2008) and Landsat 7 images (Landsat-7 image courtesy of the U.S. Geological

Survey). Measurements were only created in areas with univocal identification of large scale bedding planes. QC of generated data and comparison to locally existing field measurements show that bedding strike is general very reliable, whereas the bedding dip results may partly be underestimated.

3.3 Field work

The field work focused on collecting bedding dip data to supplement existing data and to partly ~~QC~~ quality-check the remotely assessed data. Furthermore, the style of deformation as observable ~~in~~ at the field scale was investigated. Sub-recent sediments (Pleistocene to present) are tilted (Fig. 7a), being part of the large scale fold/flexure in the southern sector (Fig. 5, point a). Changes in dip are primarily apparent due to the outcrop conditions where recent outcrop degeneration was present, but small alterations of the dominant dip of the limbs of the large scale structure have been observed, possibly a result of internal thickening within the formation caused by space problems in the inner part of the folds. The necessary flexural slip has been documented even in the very young, likely Pleistocene sediments. Fig. 7b shows striations on bedding planes in sandy beds of a tilted sand~~stone~~-conglomerate succession (location Fig. 5, point b). ~~It is only i~~In rare cases ~~that small~~ small-scale (e.g. Fig. 7c) and medium scale (e.g. Fig. 7d) folds ~~form~~ were observed (locations in Fig. 5, point c and d, respectively). These folds are interpreted to reflect higher order folds caused by local accommodation of space problems in relation to the large scale folding.

4. Seismic interpretation and analysis

The frontal~~-~~most anticline (Fig. 5) hosts several gas condensate fields and is partly covered by 2D seismic and at least one 3D seismic cube. From 2014-2017 two new 2D seismic surveys were acquired west of this frontal anticline. For confidentiality reasons we are unable to show exact locations of the seismic lines and the well data. However, we subdivided the area into a northern and a southern sector (Fig. 5) and use two representative W-E composed seismic sections to discuss the structural differences of these sectors (Fig. 8). ~~-~~The seismic surveys have up to 6 km horizontal spread and up to 240 fold and utilized dynamite as the source. Processing of the lines in Fig. 8 is ~~up~~ to Pre-Stack Depth Migration (PSDM). These seismic lines have been tied to the vintage seismic data and wells for stratigraphic control. Stratigraphic control on the lines is given by wells on the frontal anticline or in the foreland via a grid of vintage 2D lines or the 3D seismic cube. Based on this data robust grids of Oligocene to Cretaceous (Jurassic partly) horizons exist along the frontal anticline and the un-deformed foreland. Horizons are indicated in the un-deformed foreland in Figure 8 as well as in the stratigraphic column (Fig. 3).

The seismic quality tends to degrade towards the West and also with depth. Consequently the structural architecture in those parts is less constrained. On both sections, the top of the Eocene Kirthar limestones (cf. Fig. 3) is indicated on locations where well or seismic data unambiguously allow for that interpretation or where it is constrained by surface geology (Fig. 8, orange interpretation). The top of the Kirthar limestones is one of the most characteristic features in the seismic data. It is represented by a strong, continuous reflector on top of a package of weaker reflectors with good continuity. In the following section, a

brief description of the main structures at ~~the level of the Kirthar limestones~~ ~~Kirthar level~~ is given and structures in areas of good seismic image quality are analysed.

4.1 Northern sector

In the northern sector, the undeformed foreland is marked by ~~relatively~~ approximately horizontal reflectors (Fig. 8a, point a).

5 Sub-horizontal seismic reflectors indicate the presence of sedimentary rocks to at least 8 km ~~in~~ depth. A minor anticlinal feature (Fig. 8a, point b) and a more pronounced anticline (Fig. 8a, point d) are separated by a zone of discontinuous reflectors (Fig. 8a, point c), that is interpreted as a fault offsetting the Kirthar limestone. ~~The relative timing~~ Some more details of these frontal structures is ~~well~~ depicted in the growth strata imaged on a time-domain seismic section nearby (Fig. 9): The interpreted growth strata packages "a" and "b" show westward thinning and onlap, thus a pattern of apparent progressive

10 limb rotation. The seismic interpretation at depth indicate a thrust fault (thrust "1" in Fig. 9 a). There is no additional thin-skinned deformation east of the tip of the wedge documented in confidential seismic data east of the section or on the surface. Therefore, this thrust is interpreted as part of a structural wedge, roofed by a bedding parallel thrust (thrust "2" in Fig. 9 a). Tilted strata below thrust "1" with a slightly westward offset kink axis (white stippled line in Fig. 9a) indicate a potential deeper wedge. Fig. 9 b-d show a possible sequence of deformation events that honours the growth strata pattern and structures

15 identified on the seismic. By stacking two wedges the deformation front can stay relatively stationary and develop a growth strata package similar to the imaged one. Migrating kink bands likely are not resolved due to low sedimentation rates and potential intervals of erosion. Unlike shown the wedges might also be partial active at the same time, complexly accommodating large scale layer parallel shortening. The youngest thrust short-cuts the wedges (Fig. 9d, fault "3" in Fig. 9a) and deforms the youngest growth strata package ("c" in Fig. 9a). ~~The interpreted growth strata packages GS1 and GS2 show~~

20 ~~westward thinning and onlap as well as progressive limb rotation related to the triangle deformation at depth (with thrust "1"~~ ~~and roof thrust "2", Fig. 9). The youngest growth strata package, GS3, is only deformed above the projection of fault "3". As~~ ~~a result of the location of this deformation, this fault is younger than faults "1" and "2". Movement on this fault generates a~~ ~~fault propagation fold in the hanging wall.~~ The relatively good seismic image and nearby well control allows to define the stratigraphic level of the roof thrust (fault "2" in Fig. 9). The thrust has a trend that is parallel to the bedding in the Paleocene

25 shales (upper Ranikot shales, cf. Fig. 3) just below the thick and competent limestones (Sui Main limestones, cf. Fig. 3), characterized by the low-reflectivity seismic character. ~~Tilting of the reflectors below thrust "1" is partly due to a velocity pull-~~ ~~up, but some additional tilting related to layer parallel shortening in deeper levels cannot be excluded.~~ The deeper ~~parts~~ segments of thrusts "1" and "3" ~~is~~ are relatively uncertain based on the seismic profiles. However, the Jurassic Chiltan Formation ~~is~~ has been drilled in the hanging wall of thrust "3", indicating that the thrust cuts below the Jurassic.

30 A syncline is located west of these frontal structures, though it is not imaged on the seismic data due to steeply dipping to overturned beds (Fig. 8a, point e). A large scale anticline with Kirthar limestones on surface level is indicated at point f (Fig. 8a, cf. Fig. 5). The low-reflectivity seismic facies below the Kirthar limestones ~~are~~ is the Eocene Ghazij (Shales) Formation ~~Shales~~ (Fig. 8a, point g). These shales thicken dramatically from the well~~s~~ on the frontal anticline ~~s~~ in the East (several tens of

8

meters) towards the West (several hundreds of meters, constrained by seismic velocities and outcrop information just west of the Kirthar Escarpment, cf. Fig. 5 and seismic velocity dataAhmad et al. 2012). A small scale anticline of higher order is cropping out with exposes Kirthar limestones on the surface (Fig. 8a, point h). A syncline is markingmarks the western end of the seismic line (Fig. 8a point i). The Kirthar Formation is croppingcrops out also at the Kirthar Escarpment west of the section

5 (Fig. 5 northern sector, at approx. 1150 m above sea level). It is notable that the regional elevationstructural elevation of the Kirthar limestone increases from east to west (approx. 2.5 km in the western syncline, Fig. 8a point i). At the highest outcropping point of Kirthar limestones the difference to the estimated regional level is 5.5 – 6 km with an uncertainty related to the interpreted slope of the regional elevation. A rough depth depth-to-to-detachment analysis conducted with the excess area approach (Epard and Groshong, 1993) on the large scale anticline reveals suggests an upper detachment depth of 8-10

10 km. The spread in the predicted detachment is due to high uncertainty in the deeper stratigraphic picks on the seismic and the fact that the Kirthar Formation is not returning to regional elevation in the syncline to the West.

4.2 Southern sector

In the southern section, the undeformed foreland (Fig. 8b, point a) shows sub-horizontal reflectivity to at least 8 km in depth. To the West a minor flexure (Fig. 8b, point b) is situated underneath a seismic noise zone hiding a thrust fault (Fig. 8b, point

15 c). This The anticline above the thrust (Fig. 8b, point d) is the southern along-strike continuation of the anticline on the northern section (Fig. 8a, point d). The syncline towards the West (Fig. 8b, point e) is much broader than its northern equivalent. Sub-horizontal reflectors indicate the presence of sedimentary rocks to at least a depth of 10 km. The frontal structures have been analysed and interpreted. Finally the concluded model is illustrated and tested by running a kinematic forward model (Fig. 10). The interpreted fault geometries as well as a stratigraphic template elaborated from wells and outcrop sections are used for the

20 starting configuration of the model (Fig. 10a). Step 1 follows the sequence elaborated in the northern sector (i.e. wedging before fault-propagation folding cf. Fig. 9) which shows a small fault-bend fold that forms a small triangle structure at the deformation front (Fig. 10b). This triangle structure is cut by a subsequent thrust, forming a fault-propagation fold (figure Fig. 10c). This step is modelled using the tri-shear implementation in Move software (Midland Valley, 2016, Fig. 10c). There are several parameters that control the shape of the anticline. In detail, more than one solution (combination of parameters) can

25 generate an approximate fit to the given constraints (seismic, well data (not shown) and surface dips), but differences are not significant. The reasonable fit shown in Fig. 10c supports the fault interpretation and the amount of shortening applied to these frontal structures (about 5000 m of horizontal shortening). To the west of the red stippled line in Fig. 10c, the model does not exactly match the seismic image- the interpreted Kirthar Formation is constantly rising until the limestones crop out in a small scale fold (Fig. 8b, point f). West of point f the Kirthar formation continues outcroppingis continuously exposed to the Kirthar

30 Escarpment (just west of the end of the seismic line) at an elevation of around 1850 m above sea level.
Similar to the northern section is the westward thickening of the Eocene Ghazij shales thicken westward

9

. The shales are thin (several tens of meters) in the frontal anticline (Fig. 8b, below point d) and thicken towards the West (Fig. 8b, point g). This thickening is ~~taking place~~ especially pronounced west of the clinoforms (Fig. 8b, point h), which ~~mark~~ are interpreted as the carbonate margin of the Sui/Laki Limestones.

On the southern section the ~~regional elevation~~structural elevation of the Kirthar limestones ~~to the West~~ rises constantly from the syncline axis (Fig. 8b, point e) towards the Kirthar Escarpment in the West. The structural elevation gain above regional at the Kirthar Escarpment is more than 6500 m (with uncertainty related to the interpreted regional level, Fig. 8b stippled orange line).

5. Linking thick-skinned and thin-skinned deformation

Despite some structural differences between the northern and southern sectors, the common observation is the overall increase of the ~~regional elevation~~elevation ~~level~~ of the Kirthar and other formations above the regional from the East to the West. Such an increase in elevation can ~~potentially~~ be explained by several mechanisms: a) a strong wedge shape of the pre-deformational strata below the Kirthar, b) a thrust/fault to a deeper structural level, c) internal structural thickening of formations below the Kirthar Formation or any combination thereof as these proposed mechanisms are not mutually exclusive.

~~We suggest that the order of structural uplift (larger than 5500 m) is linked to a deeper structural level in the basement. The other mechanisms above might still contribute a smaller part to the regional uplift. This anticipated thick-skinned deformation needs to be linked to the demonstrated thin-skinned deformation close to the deformation front.~~

~~In order to generate a most reasonable structural model we briefly review the available nodal planes of earthquakes as well as some indications from the geological map west of the Kirthar Escarpment.~~

For several reasons discussed throughout this chapter, we propose that the most likely scenario for driving the structural uplift is a thick-skinned contribution that is probably caused by partial inversion of existing structures linking upwards with suitable detachments in the sedimentary column. The balanced sections of the southern and the northern zone are displayed in Fig. 12 and 14, respectively. The sections honour the seismic interpretation and constraints from the structural modelling and fit the regional context and constraints. Before discussing the sections individually in detail we need to elaborate these constraints and arguments. This includes addressing the following main questions: a) Could a pure thin-skinned (duplex) solution explain the same (regional) pattern? b) Which are the indications for inversion in contrast to a (non-inversion) basement involved model?

5.1. Constraints from regional structures (thin- vs. thick-skinned)

West of the area covered in Figure 5 the topographic and structural elevation remains high (more than 6000m), as indicated by the outcropping of the Jurassic in various folds (Figs. 2, 5). A conceptual regional cross section is displayed in Figure 16g. West of the area covered in Figure 5 the section is mainly based on a low resolution geological map (scale, Bannert et al., 1992). The section tentatively shows some relatively steep thick-skinned faults and gently folded strata above. Due to the

limited data and the problems of cross-section orientation and non-plane strain conditions balancing of this regional section is problematic. However, the folds shown in the section accommodate approximately 10% of line length shortening. Based on the balancing results from our own sections where higher resolution data is present, we argue that the actual shortening can be somewhat higher (in the order of 15-20%) and that the difference is due to scale problems as well as unresolved shortening in

5 wedges and other distributed shortening. A conceptual section compares a thick-skinned to a thin-skinned solution (Fig. 17). In both cases the deformation is pinned at the deformation front. The thick-skinned model envisages that the total amount of shortening is accommodated in the contractional structures above the approximately equally shortened basement (Fig. 17a). The thin-skinned model assumes that the basement remains undeformed beneath the duplex structures (Fig. 17b) and has to be shortened towards the hinterland. The thin-skinned duplex solution shown (assuming reasonable stratigraphic thicknesses)

10 does not reach the structural uplift observed (more than 6000m) and has serious balancing problems. Increasing the magnitude of shortening would allow to attain higher structural elevation(s), but increases the balancing issue at the same time. The shortening of the strata above the duplexes would likely require a set of back-thrusts as the plane of the roof-thrust is severely folded and thus not likely a viable slip-plane. No such back-thrusts or other structures that would accommodate the excess shortening are observable on the geological maps. Furthermore, the basement would require to shorten somewhere as well

15 with the same magnitude, which would usually happen by a staircase thrust system towards the hinterland – with the consequence that deeper stratigraphic rocks or basement are uplifted (tentatively shown in Fig. 17b). However, towards the hinterland no such root zone is present (cf. Figs. 2, 16 g). Furthermore, the fold belt as such does not show a prominent surface slope (only 0.5° -1°, Fig. 16h). This could indicated that the transpressive fold belt likely does not represent a critical tapered accretionary wedge (cf. Dahlen et al. 1984, Suppe 2007), although, we do not have good control on the basal angle of a potential

20 wedge. A governing wedge shape is probably necessary to allow sustained basal accretion of duplexes.
Steeper faults, also affecting the basement, do require much less shortening to uplift overlying strata to a high structural elevation (Fig. 17 a) and are consistent with the missing root zone towards the plate boundary (Figs. 2, 16 g).
In our study area, Tthe outcropping structures west of the seismic coverage/west of the Kirthar Escarpment yield some indications about the structural architecture below the Kirthar and Ghazij Formations (Fig. 5). The area west of the Kirthar

25 Escarpment has a high mean elevation (more than 1000 m above sea level, cf Fig. 16h). The anticlines with Jurassic outcrops represent the structures with the highest elevations in the area (labelled with bold numbers 1 in Fig. 5). In-between are areas where Paleocene (and sparsely also Eocene) rocks are preserved, which represent relative structural lows (labelled with bold numbers 2 in Fig. 5). A further characteristic is the presence of long wavelength folds with several km wavelength (labelled with bold numbers 3 in Fig. 5) and anticlines folds with much smaller wavelengths and higher frequencies (labelled with bold

30 numbers 4 in Fig. 5), indicating a much shallower detachment horizon. The large scale anticlines are usually double plunging and have roughly NNW-SSE to N-S trending axes, but a variety of additional subordinate directions are present as well. A plausible deformation model should be able to explain this complex pattern.
As lined out above, a thick-skinned contribution to the structural elevation is necessary. In a transpressional system we would expect a zone of shortening in which the shortening features are striking 45° to parallel to the dominant strike-slip features

11

(Sanderson and Marchini, 1984, Fossen et al., 1994, Schreurs and Colleta, 1998). The Chaman and Ghazeraband faults are in an N-S to NNE to SSW orientation (Fig. 1), thus, shortening structures should have a strike orientation of NE-SW to NNE-SSW. The NNW-SSE to N-S trending axes west of the Kirthar Escarpment in the central Kirthar fold belt (Fig. 5) seem rather unusual in respect to the orientation of the transpressive margin. Thus, it seems reasonable to assume, that the NNW-SSE to N-S orientation is not linked to newly initiated faults at depth but is associated to localized deformation controlled by inherited zones of weaknesses.

5.1 2 Focal mechanism from theConstraints from seismicity southern western fold belt

We use ISC bulletin database derived nodal planes to constrain potential fault geometries in the subsurface in the wider study area (Fig. 2). Given the tectonic setting of a lateral collision zone, it is not surprising that earthquakes towards the current plate boundary at the Chaman Fault document dominantly strike-slip faulting. Some focal mechanisms of earthquakes close to the deformation front show dominant dip-slip shortening (Fig. 2 and Table 1). All these events are in depth ranges of 10-15 km, with the exception of F4 (Fig. 2 and Table 1), which is at greater depth (33 km). Interestingly is that this event is the only one with a slight oblique character. Given the potential error ranges on the depth of the events the shallow events could be located in the crystalline basement or in the lower part of the sedimentary column.

It is not clear which of the two nodal planes was the moving plane. We could either assume it is the one with the lowest dip or it is westward dipping corresponding to the South-east or eastward directed shortening. For the first assumption fault dips are between 15° - 45° and for eastward dipping faults between 15° - 57°. In both cases, the steeper faults are considered to be too steep to represent newly initiated reverse/thrust faults. We interpret these steep faults therefore as parts of reactivated pre-existing faults that are in a suitable angle for reactivation. The shallower dipping events could represent newly initiated faults, of which those in depth above 12 km could be located in the sedimentary column.

Based on levelling data surface deformation associated with the 1931 Mach Earthquake in front of the northern Kirthar ranges has been investigated by Ambraseys and Bilham (2003) as well as by Szeliga et al. (2009). The authors model different fault slip solutions to match the seismic and post seismic elevation gain at the deformation front. In a geological section Szeliga et al. (2009) consider listric thrust faults with angles exceeding 45° linking shortening on a deep flat decollement (likely in the basement) to higher levels in the sediments (Fig. 16d). In order to match the surface deformation after the 1931 Mach earthquake with elastic models a fault geometry comprising deep detachment, a ramp section (part of a steep listric fault) and a branching gently dipping thrust towards the deformation front are needed. The fault shape considered responsible for the event by Szeliga et al. (2009) is tentatively shown in Figure 16d as red line. Such a geometry supports our proposed model close to the deformation front, where basement faults link with shallower detachments and thrusts in the sediments.

5.3 A simplified thick-skinned - thin-skinned inversion model

We propose that an inversion model is the best solution to explain all the different observations and constraints. Yamada and McClay (2004) demonstrated that the shape of the normal fault and associated (half-) graben with its syn-kinematic fill (Fig.

5   11a) defines the shape of the inversion anticline (Fig. 11b). Interesting to note is the presence of double plunging anticlines and the possibility of local lows in-between the anticlines and towards the hinterland (Fig. 11b), which can be compared toresembles the structural pattern west of the Kirthar Escarpment in map view. The analogue experiments are limited by the rigid boundary conditions (rigid and non-deformable footwall, constant length of the hanging-wall fault-) whereas in nature, this is likely not the case. Inversion likely does affect only those parts of the faults that are suitable for frictional reactivation.

10   In listric fault systems these would be dominantly the lower/deeper segments located in the ridged basement (depending on the post-rift strain history). Other inversion related deformation like hanging wall shortcut faults, reverse faults, buttressing effects (cf. Cooper et al., 1989; Hayward and Graham, 1989) are likely to be present as well and can be considered as indirect inversion. In the study area the shortening of the inverting normal fault is considered to be transferred to a detachment in the sediments (Fig. 11c), explaining the presence of short wavelength folds adjacent to the large wavelength folds (cf. Fig. 5). The

15   linking from the deeper inverting fault to the detachment in the sediments might be associated with the above mentioned complex deformation, e.g. a footwall short-cut fault (Fig. 11c).

We further suggest that the complex map pattern is likely the result of a much more complex inverted fault pattern as observed in natural rifts. En-echelon pattern and overlaps of faults with intact and broken relay ramps, horses etc. (Fig. 11d) could contribute to a more complex deformation pattern if directly or indirectly inverted. Additionally, several stacked detachment

20   horizons allow to accommodate shortening by linking stacked wedges and distributed ductile strain. As a consequence the amount of shortening introduced by basement faults is partly disseminated and thrusts, if they reach the surface have relatively small displacements (relative to the amount introduced by the basement faults) without the necessity of major thrust faults breaking the surface. We consider that the inverting faults are inherited from the original rift phase on the lateral boundary when the Indian plate rifted from northern Gondwana (Fig. 4a). The direction of the rift faults thus would also define the N-S

25   direction of the anticlines, which is strongly oblique to the plate kinematic vector.

5.4 Southern section kinematic model and balanced section

The kinematical model of the frontal deformation structures in the southern section (Fig. 10) accommodates approximately 5000 m of shortening. However, this amount of shortening is not enough to explain the 6500 m of regional uplift towards the hinterland at the Kirthar Escarpment when taking into consideration reasonable fault dips. A fault with a 45° angle and a

30   displacement of 5000 m would generate a structural uplift of 5000 m from a simple geometric perspective. Either a much steeper fault is necessary (i.e. >52°), or some additional shortening above/in frontassociated to the inverting fault are is required to explain the 6500 m of regional uplift. From careful seismic interpretation and dip-analysis we have interpreted the presence

13

of small passive roof duplexes underneath the soft Eocene Ghazij shales. Below point g in (Fig. 8b) some strong but laterally discontinuous reflector packages are present (between points h and i). The reflectors are interpreted to represent the Paleocene limestones. The discontinuous pattern is interpreted to be caused by poor imaging and by structural imbrication. East of point i (Fig. 8b), a small back-thrust is interpreted. The structural solution is presented in the balanced section (Fig. 12a). By adding the shortening of these small passive roof duplexes to the total displacement on the basement fault, the required regional uplift at the Kirthar Escarpment can be achieved, as is demonstrated in Fig. 13.

To test our model, we generated a The simplified kinematical forward model that shows the evolution from the restored section (Fig. 12b) to the present stage (Fig. 12a). The initial configuration of the model has starting from one major normal fault (Fig. 13a) as in the restoration. For simplicity we will assume syn-kinematical growth in the lower Jurassic formations, although the fault might have been active as normal fault earlier and later as well (see Section 2.2 Tectonostratigraphic evolution section). The frontal triangle and the small identified interpreted back-thrust (corresponding to the wedge modelled in Fig. 10 and the back-thrust east of point i (Fig. 8b) are likely formedis suggested to have formed in an early deformation phase of dominant wedging and layer parallel shortening in the section. In the model, this deformation is linked to slight inversion of the displayed normal fault (Fig. 13b), however, the deformation could also be linked to shortening further in the West which is transferred via thin-skinned detachments. The generation of the interpreted small passive roof thrusts is considered to be the result The of the main inversion of the normal fault generatesgenerating shortcut faults with a slightly smaller dip angle in the sediments of the footwall. The presence of several weak stratigraphic units allows some wedging as well as the passive roof backthrust in the Ghazij shales (Fig. 13b and c). This stage reflects large scale layer parallel shortening of the stratigraphy above/in front of the inverting normal fault. The youngest deformation is occurring on the thrust in the frontal anticline. In order to explain this we suppose Withthat with increasing inversion above the null point, the pressure stress on the basement in the footwall likely increases and it finally yields. A basement shortcut develops and links with a suitable detachment generating the frontal anticline (Fig. 13d). With such a kinematical model all The the features/constraints visible in the seismic and at surface, and especially, the regional elevationstructural elevation uplift at the Kirthar Escarpment can all be explained with one major fault inversion (Fig. 13 D). West of the Kirthar Escarpment the regional structural elevation remains relatively high and is not dropping as in the simplified model (Fig. 13d hatched area). For that area, additional shortening is required to maintain the high structural elevation, which could be related to associated toadditional (partly) inverting normal faults is required, similar to the sketch section in Fig. 16 g.

The balanced section in Fig. 12a shows the final interpretation for the seismic line displayed in Fig. 8b, with further details than shown in the kinematic section (Fig. 13). This section restores to the pre-contractional situation as shown in Fig. 12b. The balanced section has been constructed by line length restoration onto a carefully constructed stratigraphic template that takes well data and regional thickness trends into account. An overall areal balance has been considered. The amount of shortening is about 10 km, corresponding to 20% between the fixed pin and the loose line. The Eocene and Oligocene strata has have shorter line lengths than the older strata due to roof back-thrusting on the Eocene Ghazij shales and subsequent erosion. The loose line in Fig. 12b is not absolutely straight for Paleocene and older, documenting a small remaining error in the order of

14

1% which is within the ~~drafting~~ accuracy <u>which is meaningful in respect to all uncertainties</u>. The upper part of the section can be considered as well constrained (seismic image, surface geology and well control). The deeper part of the section is constrained by kinematic and balancing considerations <u>(interpretation and kinematic modelling go hand in hand in an iterative process)</u>. In detail, there could be other solutions fulfilling the constraints (e.g. a more complex pattern of imbrications/duplexes and other structures accommodating layer parallel shortening). In that sense, the presented section is a likely scenario honouring as many constraints as possible and remaining as simple as possible.

5.5 Northern section kinematic model and balanced section

As demonstrated above, the northern sector is dominated by folding and shows a more gradual rise of the ~~regional elevation~~<u>structural elevation</u> towards the West. We interpret the shape of the large anticline in Fig. 8a as a <u>partly</u>~~n~~ uplifted detachment fold (Fig. 14) with plastic deformation in the fold core. In detail the deformation in the fold core can be accommodated by small scale thrusts (e.g. fishtail wedges etc.). The relative gentler uplift of ~~regional elevation~~<u>structural elevation</u> towards the West indicate<u>s</u> the presence of several small inverting faults in the basement in comparison to the southern section. <u>The balanced section of the northern sector (Fig. 14a) restores to the pre-contraction geometry</u> ~~as is~~ shown in Fig. 14b. <u>The method of restoration is the same as for the southern sector. The weak formations have been additionally areally balanced. The amount of shortening is approximately 11.2 km, corresponding to 18% between the fixed and the loose line. The loose line in Fig. 14b is not absolutely straight, documenting a small remaining error in the order of the (reasonably) achievable accuracy. We</u> ~~A~~ propose<u>d a</u> kinematic~~al~~ evolution <u>that takes a simplified version of the restored section as starting configuration</u> ~~is displayed in~~ (Fig. 15<u>)</u>. Several half graben normal faults with thickening strata toward the fault (again in Jurassic for simplicity reasons) are <u>interpreted to be</u> present below some post rift strata (Fig. 15a). The thick-skinned movement is linked with a thin-skinned decollement close to the base of the sedimentary column (Fig. 15b)<u>, a requirement from restoration and balancing (Fig. 14).</u> For simplicity, this step is modelled with one footwall-shortcut on the westernmost fault. The large scale anticline in the northern sector likely starts to grow in this increment. Fig. 14b anticipates a buttressing effect of the easternmost fault causing the folding. Alternatively, early inversion movement on this easternmost fault could generate a perturbation in the sedimentary sequence which is subsequently amplified by shortening which is transferred along the basal décollement. The inversion is modelled with a foreland propagation sequence<u>, although a more complex kinematic cannot be ruled out</u>. The second (middle) fault is also modelled with a small footwall shortcut (Fig. 15c). The associated shortening is amplifying the large scale fold. Some shortening of this increment might cause the observed ~~triangle~~ deformation <u>of stacked wedges</u> (Fig. 9). Finally, the easternmost fault is inverting including a footwall shortcut that links to the observed frontal structures (Fig. 15d). The final balanced section honours some more details as constrained by the seismic <u>data</u> (Fig. 14a). In total, the northern section is less constrained than the southern section as the seismic is allowing ~~more~~<u>a wider range of</u> solutions for the deeper geometry. The main uncertainties are the ~~amount~~<u>number</u> of basement faults, the amount of initial extensional throw, how many faults and shortcuts are present in the sediments and the sequence of deformation propagation. The kinematic model in Fig. 14 as well as the balanced section are thus not unique solutions ~~however they~~<u>but</u> provide a satisfactory

15

explanation for the observed structures that is consistent with the mechanical stratigraphy, the regional observations and the local constraints (seismic and surface geology).

~~The balanced section of the northern sector (Fig. 14a) restores to the pre-contraction geometry as is shown in Fig. 14b. The method of restoration is the same as for the southern sector. The weak formations have been additionally areally balanced. The~~

5 ~~amount of shortening is approximately 11.2 km, corresponding to 18% between the fixed and the loose line. The loose line in Fig. 14b is not absolutely straight, documenting a small remaining error in the order of the drafting accuracy.~~

6. Discussion

In the following section we discuss implications of the results from the local to regional scale, compare the deformation style to similar fold belts, and finally address some uncertainty issues.

10 ### 6.1 Local paleogeographic controls on deformation

On a local scale the deformation seen in the geological map (Fig. 5) is partly mimicking the original rift geometry. The large scale folds are most likely representing the former location of the main extensional growth grabens. The dominating N-S orientation of fold trends ~~is thus is directly~~seems to be controlled by the former rift geometry ~~and thus~~which apparently has a strong influence on how strain is partitioned on this lateral margin.

15 In detail, most local differences in the structural style and orientation seem to be based on slight paleogeographic differences as well. Comparing the northern to the southern sectors of the study area, the detachment depth at the trailing edge of thin-skinned deformation is different.~~there is difference of the detachment depth of the trailing thin-skinned deformation~~. In the South, the large syncline (Fig. 8b) indicates a flat segment of the detachment in lower Jurassic or Triassic rocks. The ~~comparative~~ correlative thrust fault clearly cuts deeper in the North (Figs. 8a, 9, 14). As a consequence the frontal anticline

20 shows a south to north along-strike ~~structural~~ increase in structural relief~~uplift~~. The uplift has been recognized for a long time (wells and the distribution of the existing gas condensate fields), but geometrically ~~they~~ it has~~have~~ not been properly investigated. The reason for the along strike change in depth of the basal detachment, however, is not known. It may have geometrical (fault throw, angle, depth) or facies (mechanical stratigraphy) related reasons. Both, however would be inherited from the pre-contractional evolution, with the rifting phase likely having the greatest impact.

25 There is one very clear example on how the long-lived hinge zone and the associated facies changes control the young contractional deformation. The tip of the triangle/duplex in the centre of the southern section is localised at the point where the Laki Formation limestones (Sui Main Limestones, stippled orange line) have their paleo-shelf edge and are replaced laterally by Ghazij Formation shales (Fig. 12a, see also Fig. 8b, point h). The limestones have several hundred meters of thickness in the frontal anticline and are overlain by several tens of meters of Ghazij shales only. West of the Kirthar

30 Escarpment, the Laki Formation/Sui Main Limestones are missing, instead several hundred meters of Ghazij shales are present. The clinoforms of the Sui Main Limestones are well imaged (Fig. 8b point h). West of that point most of the Laki Formation

16

is replaced by marls and shales that ~~act as~~host the passive roof thrust for the inversion related footwall duplexes underneath. The juxtaposition of carbonate margins that border basinal facies can localize thrust faults as has been demonstrated by centrifuge physical modelling ~~by~~ (Dixon, 2004).

6.2 Kirthar Fold Belt deformation

5 Our model of inversion with linked thin-skinned deformation for the central Kirthar Fold Belt is in line with the observations and the model proposed by Smewing et al. (2002a) and Fowler et al. (2004) for the southern Kirthar Fold Belt. In our study we ~~demonstrate~~propose how thick-skinned inversion and thin-skinned deformation kinematically link to produce the observed deformation pattern. ~~With O~~our model ~~we are~~is also able to explain an observation of Smewing et al. (2002a) ~~where~~in which they describe field evidence of a Jurassic normal fault that is still under net extension, despite the assumed inversion and

10 relative high structural elevation. Following our model the upper part of ~~the~~former normal fault s could remain in net extension and be significantly uplifted above their original regional elevation due to footwall imbrication and shortcuts (cf. the former normal faults in Fig. 14). These imbrications however, do not ~~penetrate to~~reach the surface but generate structural wedges with a roof thrust in Ghazij shales. They are unlike the passive roof duplexes proposed originally for the northern Kirthar Fold Belt by Banks and Warburton (1986). Those authors use classical thin-skinned fold-trust belt geometries based on the sequential

15 imbrication of the foreland sequence above a pre-Jurassic continuous planar detachment horizon. Their roof thrusts are localized in Ghazij shales and further towards the hinterland in Goru formation shales. Shortening in such a system often approaches 40-50%, a value much higher than the shortening observed in the central (our study) and southern Kirthar Fold Belt (Fowler et al., 2004). The large scale map pattern does not significantly change from our study area towards the northern Kirthar Fold Belt. We propose~~,~~ that the deformation observed in the northern Kirthar Fold Belt (i.e. Banks and Warburton,

20 1986) could also be caused by linked thick-skinned and thin-skinned ~~inversion~~related deformation, as the thin-skinned solution has significant regional balance problems.~~.~~ The modelled fault shape responsible for the 1931 Mach Earthquake by Szeliga et al. 2009 comprises a thrust fault up-dip of a steep thrust ramp section that links to a deeper decollement, either in thick sediments or in the basement (cf. Fig. 16 d). The general structure is similar to what we interpret at the deformation front in the central Kirthar Fold belt. The linkage between a relatively steep, deep-reaching fault and a more shallow dipping frontal

25 thrust can be interpreted as the potential transition from a thick-skinned (inverted?) fault a the frontal thin-skinned system. Similarly, the thin-skinned deformation observed by Schelling (2000, cf. Fig. 16f) can be put into this context. The sections investigated by Shelling are relatively short and thus only cover the leading edge margin of the thin-skinned deformation ~~(similar to the frontal structures in Fig. 12)~~. Thus, no major south to north discrepancies in shortening values need to be considered for the Kirthar Fold Belt. The deformation style does not necessarily vary dramatically, however the way the

30 shortening is accommodated is considered to be controlled by local inherited ~~controls~~structures.

17

6.3 Possible lithospheric inheritance of the inversion belt

It is important to briefly discuss some potential reasons why ~~the~~ the central Kirthar Fold Belt is dominated by inversion with thin-skinned deformation instead of following classical thin-skinned fold-thrust belt model. The importance of a structural inheritance from rifting has already been proposed by Smewing et al. (2002a). However, most pro-wedge thrust belts affect

5 areas which went through rifting and passive margin settings before collision. Whether the continental margin in the collision phase evolves into a dominated system of thin-skinned or thick-skinned deformation depends on several factors.

The presence of a weak (ductile) middle or lower crust seems to be key factor which allows for distributed deformation through most of the crust, which results in forming fold-thrust belts with a dominant/primary thick-skinned character (Lacombe and Bellahsen, 2016). Thermally weakened shear zones might be conserved in little extended proximal continental margins which

10 can also influence the deformation style. Weak crustal levels are often lacking in distal parts of the margins as a result of the rheological evolution of the rifted margin over time (Perez-Gussinye and Reston, 2001; Cloetingh et al. 2005; Reston & Manatschal, 2011). The resulting stronger lithospheric domains are more prone to localized deformation in a continental subduction style (Lacombe and Bellahsen, 2016). Thus, the relative position and the time since rifting apparently play a role in determining in which mode the convergent deformation will reactivate structures.

15 We therefore speculate, that the inversion dominated central Kirthar Fold belt represents the inner part of the continental margin in which a weak continental crust is still present. The long lived hinge line observed in several facies associations is interpreted to reflect approximately the limit of ~~the~~ major post-rift subsidence and the eastern border of the extended lithosphere (assuming pure-shear). The more than 100 km wide area ~~from~~ east of the dominating strike slip faults (Chaman and Ghazaband Faults, Fig. 1) could be considered to have initially accommodated the shortening component of transpression, hence show

20 inversion where suitable faults are located. Sustained deformation should have rotated faults and folds closer to the margin~~deformation front to the Ghazaband fault (Fig. 1) is interpreted to be dominated by initial inversion (later partly overprinted by strike slip deformation)~~. We infer that this large area shares a similar rheology which was inherited from Gondwana and the ~~break~~ break-up phase. The width of this zone might indicate that the lithosphere rifted in a wide rift mode (Buck, 1991) before continental break-up to the West. Consequently there should be a narrow zone of highly extended crust

25 (external rifted margin) present west of the inversion belt. Today this zone is covered by ~~Flysch~~ flysch sediments, bracketed between the Ghazaband and Chaman Faults (Bannert et al., 1992, Fig. 2). How much of the former external rifted margin has been subducted or laterally displaced along the strike-slip faults remains difficult to estimate and is beyond the scope of this paper. Interestingly, further to the North in the Pamir area earthquake tomography data is interpreted to show delamination and rollback of the Indian plate lithosphere (Kufner et al., 2015). India's thinned western continental margin separates from

30 ~~Cratonic~~ cratonic India and subducts beneath Asia while the buoyant northwestern salient of ~~Cratonic~~ cratonic India bulldozes into ~~Cratonic~~ cratonic Asia (Kufner et al., 2015).

18

6.4 Hybrid thick- and thin-skinned systems in other areas

Thick-skinned inversion of passive margin or intra-cratonic rifts is considered to be present in 50% of orogens with documented deformation style (Nemčok et al., 2013). There are various possibilities how thick-skinned deformation can contribute to the deformation of a fold-thrust belt (see recent review of Lacombe and Bellahsen, 2016 and references therein).

5   Here, we briefly compare the deformation style elaborated for the central Kirthar Fold Belt with other well constrained examples of linked inversion with thin-skinned deformation.

For the Malargüe Fold-Thrust belt, Giambiagi et al. (2008) revealed that the reactivation of normal faults was coeval with the activation of shallow detachments and low-angle thrusting at the thrust front with several faults moving at the same time in some portions. Also for the Malargüe Fold-Thrust belt Fuentes et al. (2016) work out geometric relationships of the hybrid

10   system with a series of detailed sections based on surface geology, seismic and well data through that thrust belt. Their section "E" shows strong similarities with the deformation style in the southern section of our study, especially the imbrication of sediments in the footwall with duplexes and a passive roof thrust on top. Recently, Mahoney et al. (2017) proposed a very similar deformation for the Eastern Muller Ranges in the Papuan Fold Belt in Papua New Guinea. There, the Cenozoic carbonates are shortened to around 13-21% but are partly uplifted up to 7 km above regional elevation. Mesozoic rift faults,

15   partly inverting and partly linking to thin skinned detachments are considered to ~~reflect~~ exert the major control on deformation. Triangle structures and back-thrusts are considered transient deformation steps, related to the uplift and erosion history while the deformation accumulates before linking to the frontal deformation structures (Mahoney et al., 2017). The proposed deformation is very similar to the style we consider for the central Kirthar Fold Belt. In our example the presence of a complex mechanical stratigraphy with several detachment horizons in the stratigraphic column seems to produce even more complex

20   geometries than in the example from Papua New Guinea.

6.5 Uncertainty

Basement involvement is very often used in balanced section to account for a high ~~regional elevation~~structural elevation ~~uplift~~ towards the hinterland. However, for a relatively small uplift of ~~regional elevation~~structural elevation the thick skinned explanation is often ambiguous, as there are often several alternative possibilities which are not investigated (e.g. strong

25   wedging of the pre-kinematic sedimentary sequence, change in basal detachment depth, change in basement dip etc.).

Recently, Butler et al. (2018) demonstrated ~~that~~ for several reviewed sections that there is a substantially greater range of solutions available for interpreting the geometry and evolution of thrust belt structures than implied by the original idealized models. For a specific section in the Papuan Fold and thrust belt two realisations are available by different authors. One with thin-skinned and one with inversion style tectonics (e.g. Hill, 1997; Buchanan and Warburton 1996; cf. Butler et al. 2018).

30   Similarly there is a strong discussion on the contribution of thick-skinned deformation below the different segments of the Zagros fold belt (see discussions in Lacombe and Bellahsen, 2016; Hinsch and Bretis, 2015, for the Mountain Front Flexure).

19

In order to overcome limitations from single deterministic geometries, Butler et al. (2018) propose good documentation, alternative models and to embrace the uncertainties. In this work, we show the original seismic data, review in detail the regional to local context and use these as arguments why we think our presented deformation model is the most plausible for the central Kirthar Fold Belt from the other investigated alternatives. We do not show alternative models, but we highlight our workflow, the considered constraints and indicate uncertainties of the sections. ~~With all the arguments given, t~~The contribution of deep founded faults with associated thin-skinned deformation can be considered as reliable, and the pure thin-skinned deformation style can be considered as obsolete.

Based on several observations (folding pattern, fold orientation, focal mechanism) this thick-skinned deformation is interpreted to invert inherited zones of weakness from the rift phase that generated the lateral margin of India. This model is very likely, but remains a conclusion, rather than a direct observation.

In detail the interpreted and constructed sections are as good as the constraints allow and thus still have several solutions. The amount of uncertainty in the sections depends also on the level of observation. How much change on our model is a new solution or just a modification is a matter of definition and also scale dependent.

7. Conclusions

Large scale strain partitioning along the western Indian plate leads to major left lateral strike-slip faulting close to the plate margin as well as to NW-SE to W-E shortening close to the deformation front of the Kirthar Fold Belt. We analyse regional (geological maps, focal mechanisms, ~~geological maps~~) to local (reflection seismic and well data, surface geology) data at the front of the central fold belt to constrain the structural architecture and style. The deformation is most probable controlled by the inversion of inherited rift faults, likely of Jurassic age, which is buried underneath the sediments. The young shortening on the rift faults is coupled with thin-skinned deformation by imbricating and shortcutting into the footwall and transferring some shortening onto a detachment horizon. As a consequence, large scale folds build as a result of the thick-skinned inversion and smaller scale folds and thin skinned related thrust deformation form in front. In the southern sector a structural elevation gain of approximately 6500 m across one large monocline clearly indicates the influence of the deep seated faulting. Towards the North the structural elevation gain is distributed across several folds indirectly related to several inverting faults at depth. The main control on deformation is considered the presence and orientation of the pre-shortening rift. In addition, the rift and post rift history resulted in some prominent E to W proximal to distal facies trends being reflected in a heterogeneous mechanical stratigraphy which is responsible for the style on how shortening is accommodated in the thin-skinned structures.

The hybrid deformation style of thin-skinned to thick-skinned deformation is also present in other fold-thrust belts around the world with hydrocarbon resources. Combining as many constraints as possible from regional to local scale facilitates the development of plausible structural models and assess uncertainties. The importance of understanding the structural architecture and kinematics is here and there of paramount importance for the successful exploration of these resources.

References

Ahmad, A., Ali, Baitu, A.H. and Sardar, N.: Tectono-Stratigraphic Model for Ghazij Formation and its Implication on Hydrocarbon Exploration in Kirthar Foldbelt, Pakistan, AAPG Search and Discovery Article #90155, AAPG International Conference & Exhibition, Singapore, 16-19 September 2012, 20pp., 2012

Ambraseys, N., and R. Bilham, Earthquakes and associated deformation in northern Baluchistan, Bull. Seismol. Soc. Am., 93, 1573 – 1605, 2003

Banks, C. J., and Warburton, J.: 'Passive-roof' duplex geometry in the frontal structures of the Kirthar and Sulaiman mountain belt, Pakistan: J. Struct. Geol., 8, 229–237, 1986

Bannert, D., Cheema, A., Ahmed. A. and Schafer, U.: The structural development of the western fold belt. Pakistan. Geologisches Jahrbuch Reihe B., 80, 3-60, 1992

Buchanan, P.G. and Warburton, J.: The influence of pre-existing basin architecture in the development of the Papuan fold and thrust belt: implications for petroleum prospectivity. In: Buchanan, P.G. (Ed.), Petroleum Exploration, Development and Production in Papua New Guinea. Proceedings of the Third PNG Petroleum Convention, Port Moresby, pp. 89–109, 1996

Buck, W.R.: Modes of continental lithospheric extension, J. Geophys. Res., 96, 20161–20178, doi:10.1029/91JB01485, 1991

Butler, R.W.H, Bond, C. E., Cooper, M.A. and Watkins, H.: Interpreting structural geometry in fold-thrust belts: Why style matters, J. Struct. Geol., 114, 251-273, doi.org/10.1016/j.jsg.2018.06.019, 2018

Cloetingh, S., Ziegler, P., Beekman, F., Andriessen, P., Matenco, L., Bada, G., Garcia-Castellanos, D.,Hardebol, N.,Dezes, P. and Sokoutis, D.: Lithospheric memory, state of stress and rheology: neotectonic controls on Europe's intraplate continental topography. Quaternary Sci. Rev., 24, 241–304, 2005

Cooper, M. A.,Williams, G. D., de Graciansky, P. C., Murphy, R. W., Needham, T., de Paor, D., Stoneley, R., Todd, S. P., Turner, J. P. and Ziegler, P.A., In: Inversion Tectonics, edited by Cooper, M. A. and Williams, G. D., Geol. Soc. Spec. Publ., 44, 335–347, 1989

Dahlen, F.A., Suppe, J., Davis, D.M., Mechanics of fold-and-thrust belts and accretionary wedges (continued): Cohesive Coulomb Theory, J. Geophs. Res., 89, 10,087-10,101, 1984

21

Dixon, J. M.: Physical (centrifuge) modeling of fold-thrust shortening across carbonate bank margins—timing, vergence, and style of deformation, in: Thrust tectonics and hydrocarbon systems, edited by: K. R. McClay, AAPG Memoir, 82, 223 – 238, 2004

Epard, J.-L. and Groshong, J.H.: Excess Area and Depth to Detachment. AAPG Bull, 77, 1291-1302, 1993

5 Eschard, R., E. Albouy, F. Gaumet, and A. Ayub: Comparing the depositional architecture of basin floor fans and slope fans in the Pab Sandstone, Maastrichtian, Pakistan, in: Continued turbidite systems, edited by: S. A. Lomas and Joseph, P., Geol. Soc. Spec. Publ., 222, 159–185, 2004

Fowler, J. N., Graham, R., Sassi, W., Smewing, J. D. and Warburton, J.: Two-dimensional kinematic modeling of the southern Kirthar fold belt, Pakistan, in: Deformation, fluid flow, and reservoir appraisal in foreland fold and thrust belts, edited by:

10 Swennen, R., Roure, F. and Granath, J. W., AAPG Hedberg Series, no. 1, 117–131, 2004

Fossen, H., Tikoff, T. B. and Teyssier, C. T., Strain modeling of transpressional and transtensional deformation. Norsk Geologisk Tidsskrift, 74, 134–145, 1994

Fuentes, F., Horton, B., Starck, D., and Boll, A.: Structure and tectonic evolution of hybrid thick- and thin-skinned systems in the Malargüe fold–thrust belt, Neuquén basin, Argentina. Geol. Mag., 153, 1066-1084. doi:10.1017/S0016756816000583,

15 2016

Giambiagi, L., Bechis, F., García, V. and Clark, A.H.: Temporal and spatial relationships of thick- and thinskinned deformation: A case study from the Malargüe fold-and-thrust belt, southern Central Andes, Tectonophysics, 459, 123–139, doi:10.1016/j.tecto.2007.11.069, 2008

Hinsch, R. and Bretis., B.: A semi-balanced section in the northwestern Zagros region: Constraining the structural architecture

20 of the Mountain Front Flexure in the Kirkuk Embayment, Iraq, GeoArabia, 20, 41-62, 2015

Hill, K.C.: Structure of the Papuan fold belt, Papua New Guinea, AAPG Bull., 75, 857–872, 1991

Harrison, J.V., Falcon, N.L., Collapse Structures. Geological Magazine 71, 529-539. doi:10.1017/S0016756800095005, 1934

Harrison, J.V., Falcon, N.L., Gravity collapse structures in mountain ranges, as exemplified in south-western Persia. Quarterly Journal Geological Society of London 92, 91-102, 1936

25 Hayward, A. B. & Graham, R. H., Some geometrical characteristics of inversion. In: Inversion Tectonics, edited by Cooper, M. A. and Williams, G. D., Geol. Soc. Spec. Publ., 44 335–347, 1989

Humayon, M., Lillie, R.J. and Lawrence, R.D.: Structural interpretation of eastern Sulaiman foldbelt and foredeep, Pakistan, Tectonics, 10, 299-324, 1991

International Seismological Centre, Internatl. Seismol. Cent., Thatcham, United Kingdom, On-line Bulletin,

30 http://www.isc.ac.uk, 2015

Jadoon, I. A. K., Lawrence, R. D., and Lillie, R. J.: Balanced and retrodeformed geological cross-section from the frontal Sulaiman Lobe, Pakistan: Duplex development in thick strata along the western margin of the Indian plate, in: Thrust tectonics and hydrocarbon systems, edited by: K. R. McClay, AAPG Memoir, 82, 343-356, 1992

Jackson, J.A., Reactivation of basement faults and crustal shortening in orogenic belts, Nature, 283, 343–346, 1980

22

Jadoon, I.A.K.; Lawrence, R.D.; Lillie, R.J.: Evolution of foreland structures: an example from the Sulaiman thrust lobe of Pakistan, southwest of the Himalayas, Geol. Soc. Spec. Publ., 74, 589-602, 1993

Jarvis A., Reuter, H. I., Nelson, A., and Guevara, E.: Hole-filled seamless SRTM data V4, International Centre for Tropical Agriculture (CIAT), http://srtm.csi.cgiar.org, 2008

5   Kadri, I.B.: Petroleum Geology of Pakistan. Pakistan Petroleum Limited, Karachi, Pakistan, 275 pp., 1995

Khan, S. D.. Walker, D. J., Hall, S. A., Burke. K. C. Shah, M. T. and Stockli, L.: Did the Kohistan-Ladakh island arc collide first with India?, GSA Bulletin, 121, 366–384, 2009

Kufner, S-K., Schurr,, B., Sippl, C., Yuan, X., Ratschbacher, L., Akbar, M., Ischuk, A., Murodkulov, S., Schneider, F., Mechie, J., and F. Tilmann, F.: Deep India meets deep Asia: Lithospheric indentation, delamination and break-off under Pamir and
10   Hindu Kush (Central Asia). Earth Planet. Sc. Lett., 435, 171–184, doi.org/10.1016/j.epsl.2015.11.046, 2016.

Lacombe, O. and Bellahsen, N.: Thick-skinned tectonics and basement-involved fold–thrust belts: insights from selected Cenozoic orogens, Geol. Mag., doi:10.1017/S0016756816000078, 2016.

Lawrence, R.D., Yeats, R.S., Khan, S.H., Farah, A., and DeJong, K.A.: Thrust and strike slip fault interaction along the Chaman transform zone, Pakistan, Geol. Soc. Spec. Publ., 9, 363-370, 1981.

15 Lentas, K., Di Giacomo, D., Harris, J., and Storchak, D.: The ISC Bulletin as a comprehensive source of earthquake source mechanisms, Earth Syst. Sci. Data Discuss., https://doi.org/10.5194/essd-2018-143, in review, 2018

Mahoney, L., Hill, K., McLaren, S., and Hanani, A.: Complex fold and thrust belt structural styles: Examples from the Greater Juha area of the Papuan Fold and Thrust Belt, Papua New Guinea, J. Struct. Geol., 100, 98-119, DOI: 10.1016/j.jsg.2017.05.010, 2017.

20 Midland Valley 2016, Move Software, Midland Valley Exploration Ltd, Glasgow, UK, 2016.

Mohadjer, S., Bendick, R., Ischuk, A., Kuzikov, S., Kostuk, A., Saydullaev, U., Lodi, S., Kakar, D.M.,Wasy, A., Khan, M.A., Molnar, P., Bilham, R., and Zubovich, A.V.: Partitioning of India–Eurasia convergence in the Pamir-Hindu Kush from GPS measurements, Geophys. Res. Lett., 37, http://dx.doi.org/10.1029/2009GL041737, 2010

Nemčok, M., Mora, A. and Cosgrove, J.: Thick-skin-dominated orogens; from initial inversion to full accretion: an
25   introduction. In: Thick-Skin-Dominated Orogens: From Initial Inversion to Full Accretion, edited by Nemčok, M., Mora A. and Cosgrove j.), Geol. Soc. Spec. Publ., 377, 1-17, 2013.

Pérez-Gussinyé M., Reston T. J.: Rheological evolution during extension at passive non-volcanic margins: onset of serpentinization and development of detachments to continental break-up, J. Geophys. Res., 106, 3691–3975, 2001.

Reston, T. and Manatschal, G.: Rifted margins: building blocks of later collision. In Arc-Continent Collision: Frontiers in
30   Earth Sciences, edited by: Brown, D. and Ryan, P.D., Springer-Verlag, Berlin: 3–21, 2011.

Reynolds, K., Copley, A., and Hussain, E.: Evolution and dynamics of a fold-thrust belt: the Sulaiman Range of Pakistan, Geophys. J. Int., 201, 683–710, 2015.

Sanderson, D. and Marchini, R.D., Transpression. J. Struct. Geol., 6: 449–458, 1984

Schelling, D. D.: Frontal structural geometries and detachment tectonics of the northeastern Karachi arc, southern Kirthar Range, Pakistan, in Himalaya and Tibet: Mountain Roots to Mountain Tops, edited by Macfarlane, A., Sorkhabi, R. B. and Quade, J., Geol. S. Am. S., 328, 287-302, DOI: 10.1130/0-8137-2328-0.287, 1999.

5 Schreurs, G., Colleta, B., Analogue modelling of faulting in zones of continental transpression and transtension. In: Continental Transpressional and Transtensional Tectonics, edited by: Holdsworth, R.E., Strachan, R.A. and Dewey, J.F., Geol. Soc. Spec. Publ., 195. 59-79, 1998

Scotese, C.R.: The PALEOMAP Project PaleoAtlas for ArcGIS, version 1, Volume 3, Triassic and Jurassic Paleogeographic and Plate Tectonic Reconstructions, Maps 32 – 48, PALEOMAP Project, Evanston, IL, DOI:10.13140/RG.2.1.4108.5685, 2014a.

10 Scotese, C.R.: The PALEOMAP Project PaleoAtlas for ArcGIS, version 1, Volume 2, Cretaceous Paleogeographic and Plate Tectonic Reconstructions, Maps 16 – 31, PALEOMAP Project, Evanston, IL, DOI:10.13140/RG.2.1.2011.4162, 2014b.

Scotese, C.R.: The PALEOMAP Project PaleoAtlas for ArcGIS, version 1, Volume 1, Cenozoic Paleogeographic and Plate Tectonic Reconstructions, Maps 1 – 15. PALEOMAP Project, Evanston, IL, DOI:10.13140/RG.2.1.2535.7041, 2014c.

Scotese, C.R.: PALEOMAP PaleoAtlas for GPlates and the PaleoData Plotter Program, PALEOMAP Project,
15 http://www.earthbyte.org/paleomap-paleoatlas-for-gplates, 2016.

Smewing, J. D., Warburton, J., Cernuschi, A., and Ul-Haq, N.: Structural inheritance in the southern Kirthar fold belt: Soc. Petrol. Eng.- Pakistan Association of Petroleum Geologists, 26–34, 2002a.

Smewing, J.D., Warburton, J., Daley, T., Copestake. P., and Ul-Haq, N.: Sequence stratigraphy of the southern Kirthar Fold Belt and Middle Indus Basin, Pakistan, in The Tectonic and Climatic Evolution of the Arabian Sea Region, edited by: Clift,
20 P.D., Kroon, D., Gaedicke, C. and Craik, J., Geol. Soc. Spec. Publ., 195, 273–299, 2002b.

Smith A. G.: A review of the Ediacaran to Early Cambrian ('Infra-Cambrian') evaporites and associated sediments of the Middle East, Geol. Soc. Spec. Publ., 366, 28, 2012.

Suppe, J., Absolute fault and crustal strength from wedge tapers. Geology, v. 35; no. 12; p. 1127–1130, 2007

Szeliga, W., Bilham, R., Schelling, D., Kakar, D.M., and Lodi, S.: Fold and thrust partitioning in a contracting fold belt:
25 insights from the 1931 Mach earthquake in Baluchistan. Tectonics, 28, http://dx.doi.org/10.1029/2008TC002265, 2009.

Tectostrat: Mehar Block Study 2000/2001, International Tectostrat Geoconsultants B.V.: un-published report, 2001.

Wandrey, C. J., Law, B.E., and Shah, H.A.: Sembar-Goru/Ghazij Composite Total Petroleum System, Indus and Sulaiman-Kirthar Geologic Provinces, Pakistan and India, in: Petroleum Systems and Related Geologic Studies in Region 8, South Asia, edited by: Wandrey, C. J., U.S. Geological Survey Bulletin, 2208-C, 23 pp., 2004.

30 Yamada, Y., and McClay, K.: 3-D Analog modeling of inversion thrust structures, in: Thrust tectonics and hydrocarbon systems, edited by: K. R. McClay, AAPG Memoir, 82, 276-301, 2004.

Zaigham, N.A., and Mallick, K.A.: Prospect of Hydrocarbon Associated with Fossil-Rift Structures of the Southern Indus Basin, Pakistan, AAPG Bull., 84, 1833-1848, 2000.
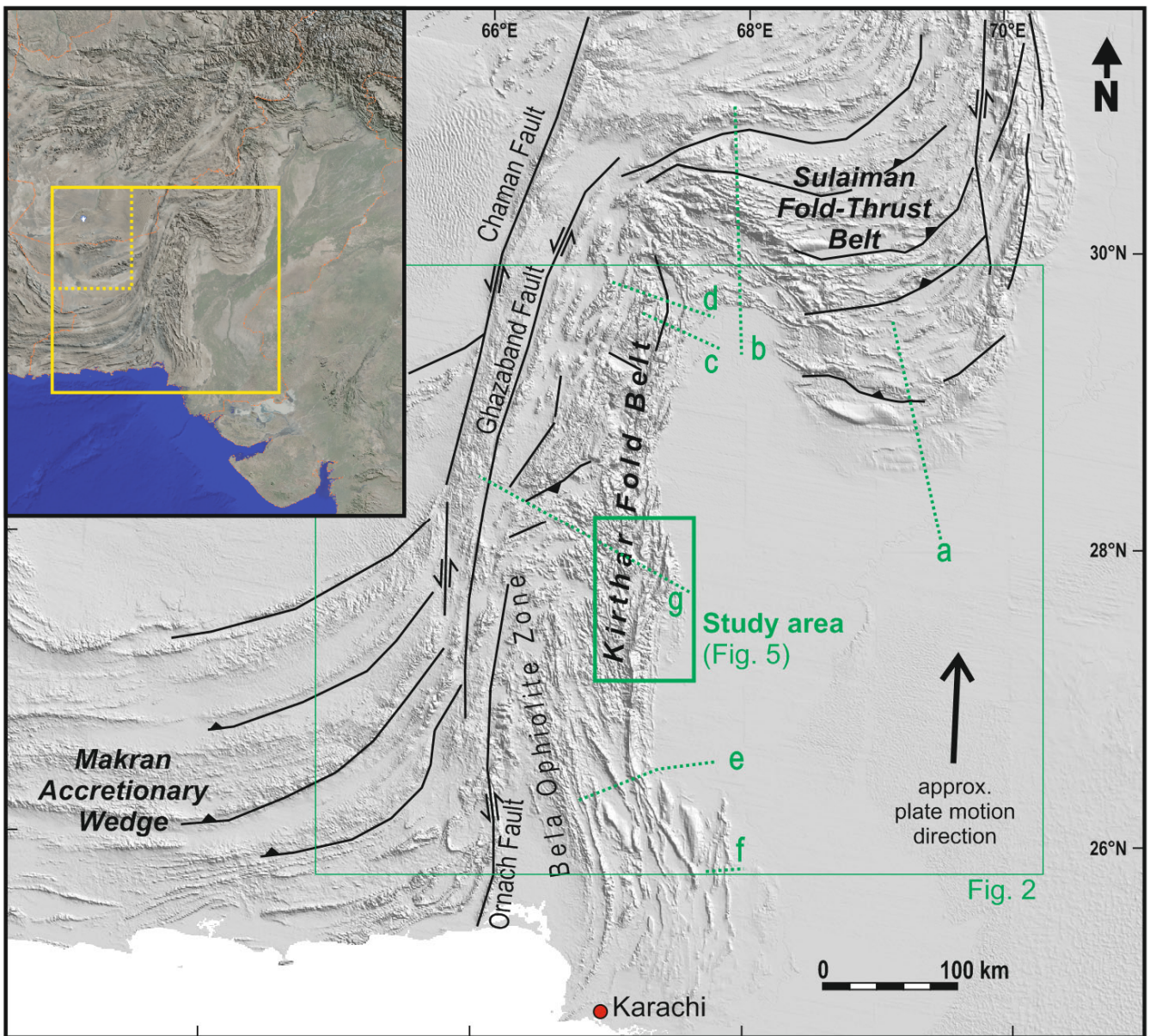
Figures and captions

Figure 1: Simplified structural sketch of the wider Kirthar fold-belt area on a shaded relief map. Location is indicated in in the inset map. The approximate plate motion is from Mohadjer et al. (2010); Locations of sSections in Fig. 16 from other studies are indicated: a: Jadoon et al. (1992), a+bb+c: Banks and Warburton (1986), c: Jadoon et al. (1992), d:Szeliga et al. (2009), e: Fowler et al. (2004), ef: Schelling (1999), g: this study..
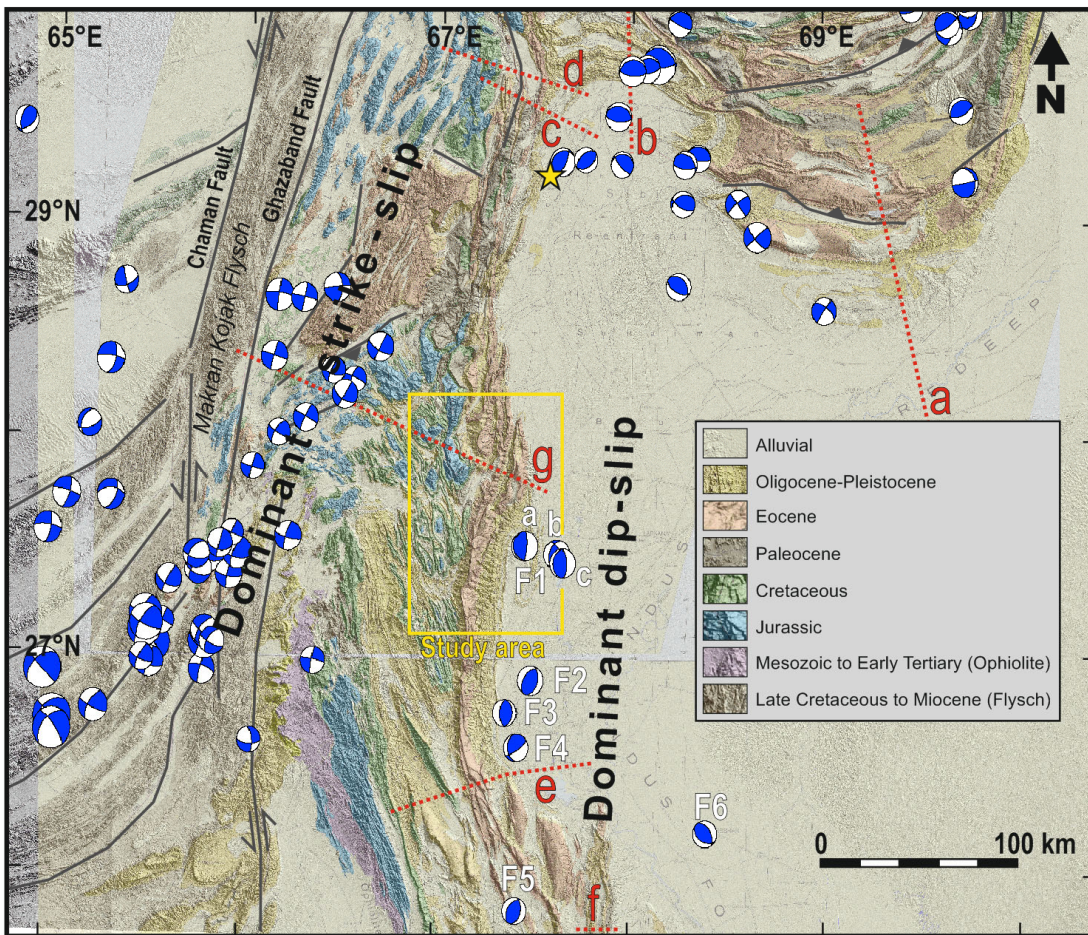
Figure 2: Nodal planes from International Seismological Centre (2015) database~~, plotted on satellite image~~DEM with draped geological map after Bannert et al. (1992) and selected structural elements. **Location of the figure is indicated in Fig. 1.** Dotted red lines are locations of sections in Fig. 16. **Labelled events are listed in Table 1.** Yellow star marks the 1931 Mach event after Szeliga et al. (2009).
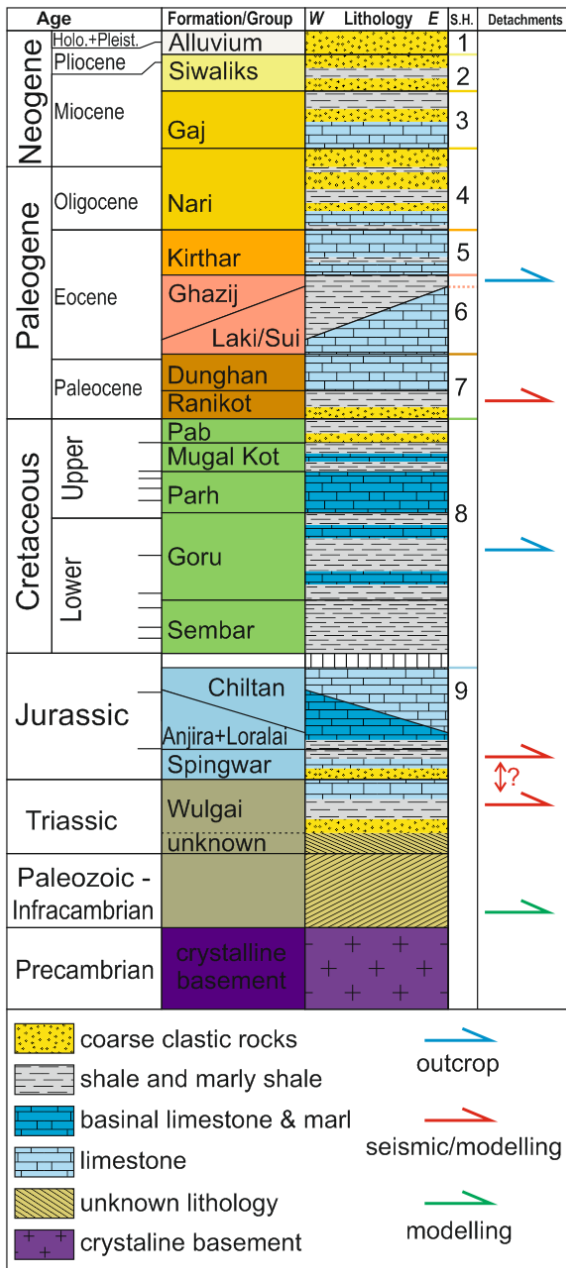
Figure 3: Litostratigraphic overview with hydrocarbon play elements and mechanical stratigraphic interpretations (after Kadri, 1995; Tectostrat 2001; Smewing et al. 2002b and author observations). S.H. = seismic horizons used in this study

5
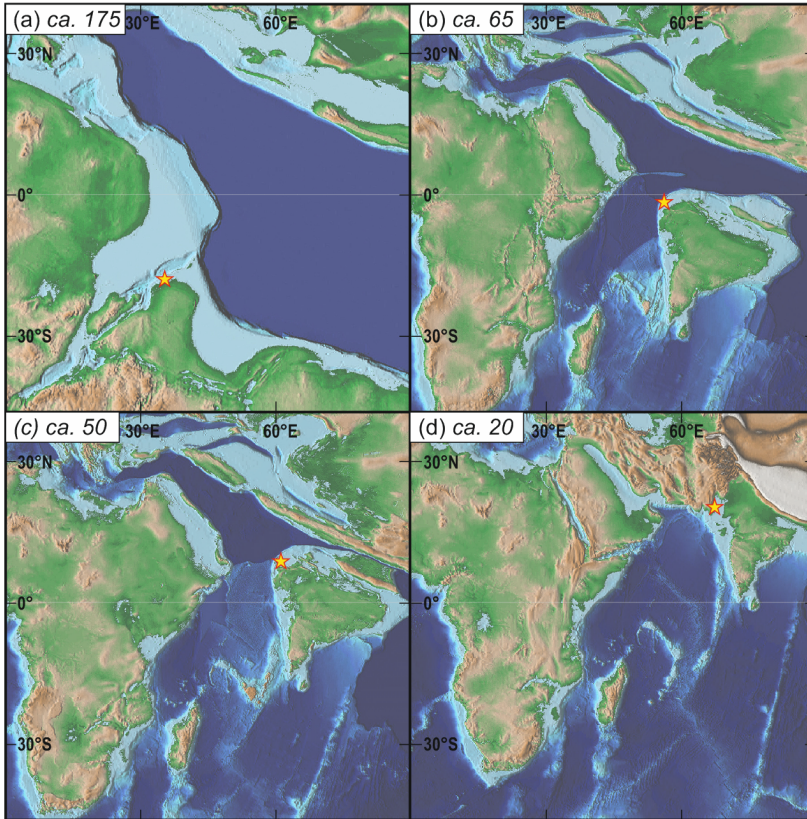
Figure 4: Paleogeographic evolution of the study area as part of the Indian plate since the Jurassic. (a) Jurassic, ca. 175 million years, a rift evolves northwest of the approximate study area location (star; map from Scotese, 2014a), (b) ca. 65 million years, Cretaceous/Paleocene, drifting northward. An strip of emergent land ~~Island arc~~ (likely an intra oceanic arc) is visible north of the approx. study area location (map from Scotese, 2014b). (c) ca. 50 Eocene, post ophiolite obduction, but pre-collision with Eurasia (map from Scotese, 2014c). (d) ca. 20 Miocene, early collision stage with flexural foreland stage (map from Scotese, 2014c).
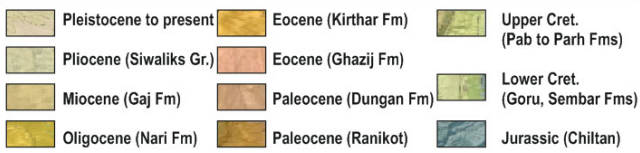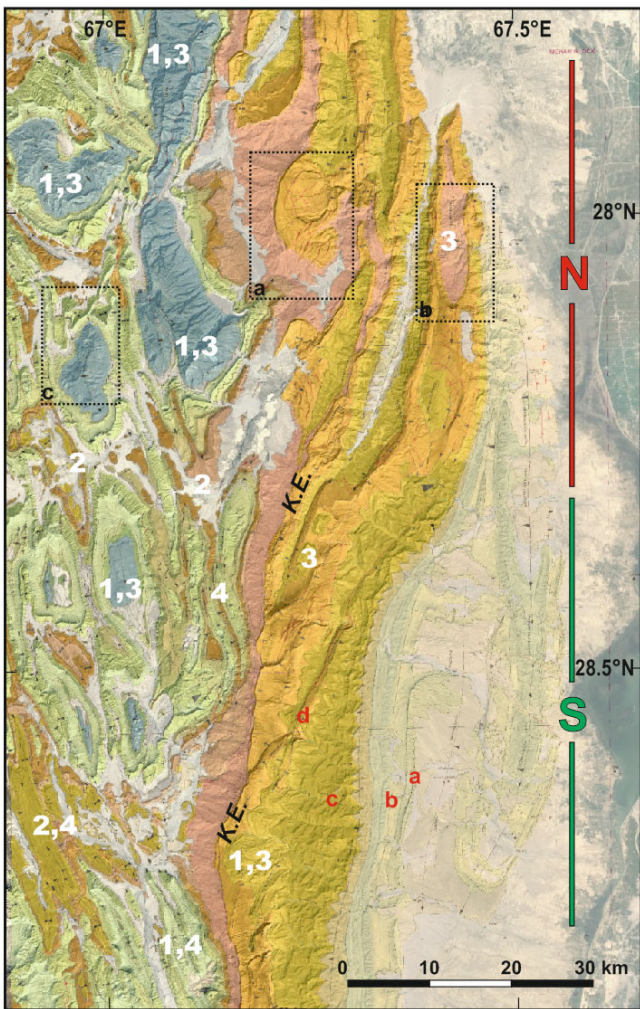
Figure 5: Semi-transparent lithostratigraphic map (modified after Tectostrat, 2001) of the study area draped in Google Earth. Dotted rectangles with labels a, b, c indicate approx. areas seen in slanted view in Fig. 6a-c. Red labels a-d indicate locations of field photographs in Fig. 7. Northern and southern sectors of the fold belt are indicated by bold red and green lines, respectively. Bold white numbers indicate examples for 1: structural highs, 2: structural lows, 3: long wavelength anticline, 4: short wavelength folding.
K.E:= Kirthar Escarpment
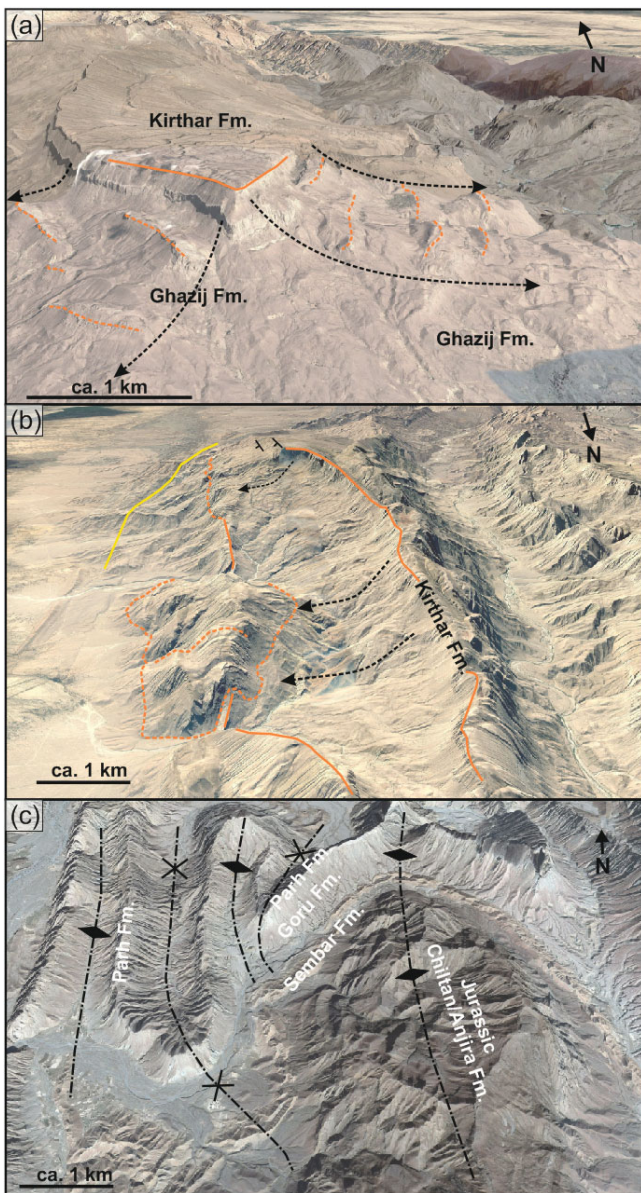
Figure 6: Example for remote field work with Google Earth. Locations of the views are indicated in Fig. 5. (a) Recent mass wasting: Blocks of Kirthar Limestones glide down the eroded flanks of soft Ghazij Formation; (b) Sub-recent to recent mass wasting: a large slab of Kirthar Limestones from the anticline roof is now folded over the ~~previously eroded~~ forelimb of the anticline (cf. Supplementary Figure I). In the background extensional faults are visible in the Kirthar limestones ~~on~~ representing the roof of the ~~boy fold~~ anticline ~~in the Kirthar limestones~~. The limestones partly glide/collapse over the vertical beds of the forelimb. (c) Disharmonic folding: Jurassic rocks show large wavelength folding, while the hard limestones of the Cretaceous Parh formation are folded in smaller wavelength and higher frequency. A weak decollement zone is located in the Goru Shales.

30
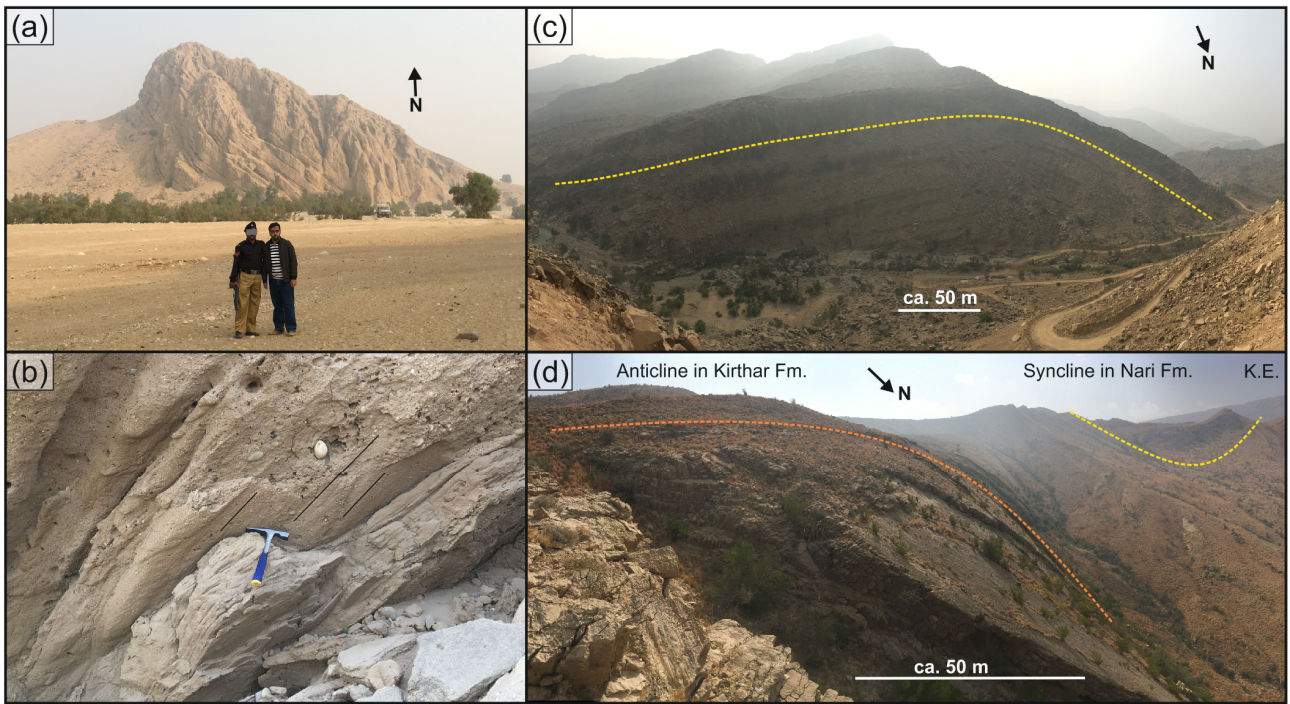
Figure 7: Examples for observations from fieldwork. (a) Sub-recent conglomeratic sediments are folded and eroded. **(b)** Striations on a bedding plane in (Pleistocene?) conglomerates indicating flexural slip folding. **(c)** small scale anticline in Nari Formation rocks. The amplitude and wavelength of the fold suggest, that the lower detachment horizon is likely in lower Nari Formation. **(d)** small to medium scale folding in Kirthar and Nari Formations. The fold is a mappable feature (cf. Fig. 5) and indicates to a detachment horizon below the Kirthar limestones.

5

31
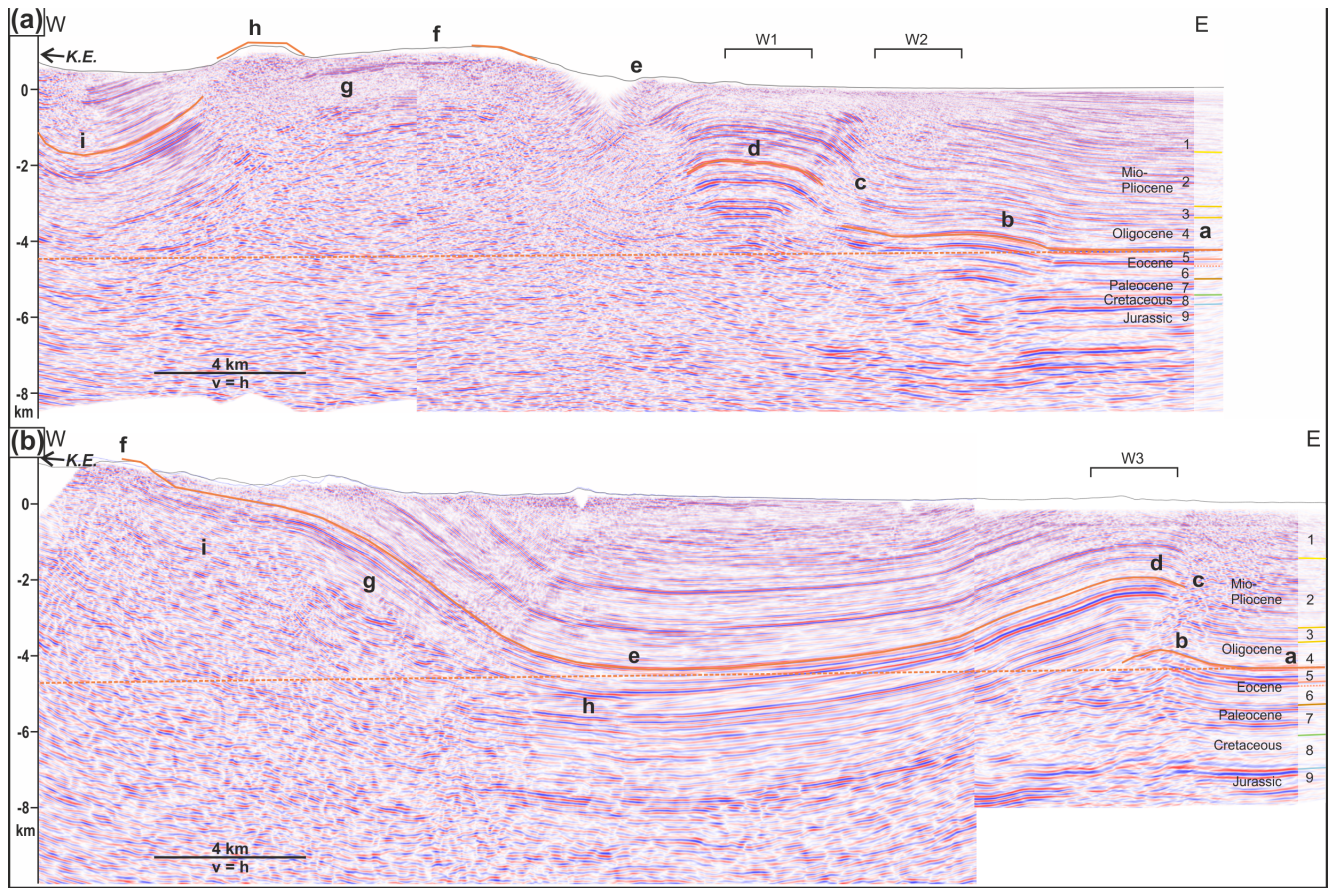
Figure 8: Two W-E composed seismic sections of pre-stack depth migrated seismic. Orange interpretations indicate clearly constrained Top Kirthar Formation from seismic, wells and outcrop. Stippled orange line is anticipated pre-contractional regional elevation of the Kirthar Formation. K.E.: Kirthar Escarpment. A high resolution image without interpretation is available as supplementary figure. The final interpreted seismic lines are part of Figs. 12a and 14a; (a) Seismic section composed from two overlapping 2D seismic lines in the northern Sector (exact position not shown for confidentiality reasons). W1: well control within 4 km to Jurassic level. W2: well control within 5 km to Paleogene level. Labels a-i are used to indicated features discussed in the text. Numbered horizons in the East refer to horizons as in Fig. 3 (b) section composed from 2D and 3D seismic data. W3: well control within 1 km to Upper Cretaceous level. Labels a-i are used to indicated features discussed in the text. Numbered horizons in the East refer to horizons as in Fig. 3
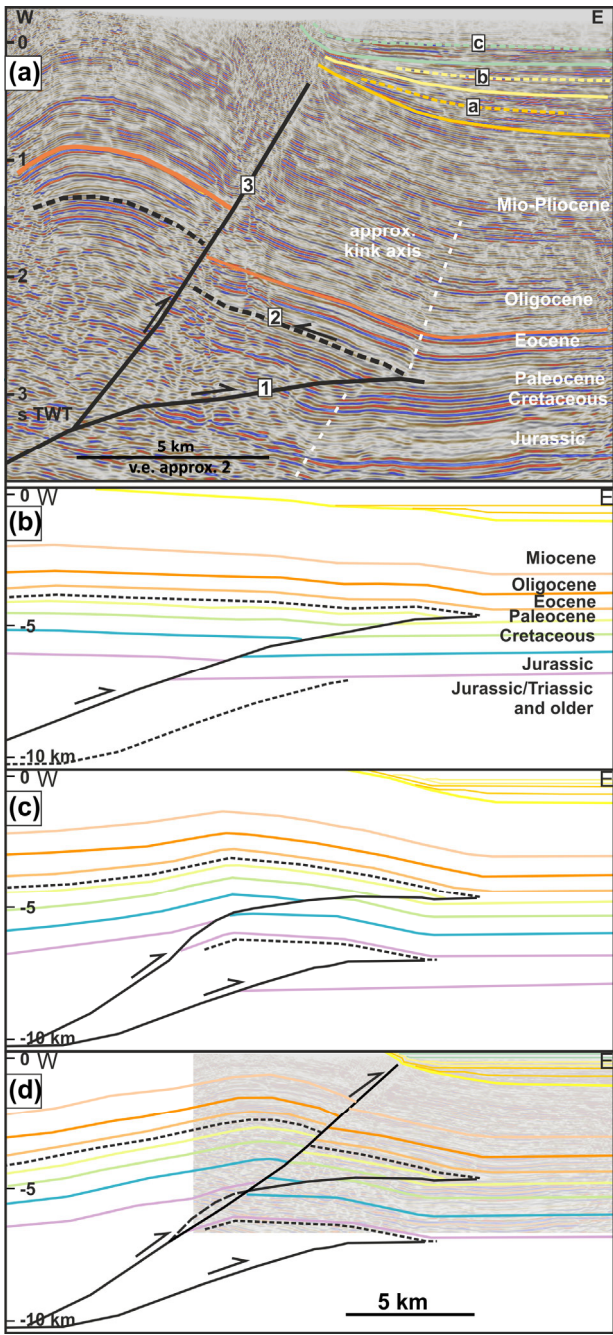
Figure replaced

Figure 9: (a) 2D seismic section in time domain in the northern sector (exact position not shown for confidentiality reasons) with fault and growth strata interpretation. ~~Faults 1-3 and growth strata packages GS1-GS3 are discussed in the text.~~ (b-d) show a possible solution for the growth strata pattern as discussed in the text. Seismic in the background of (d) is roughly depth converted version of (a).
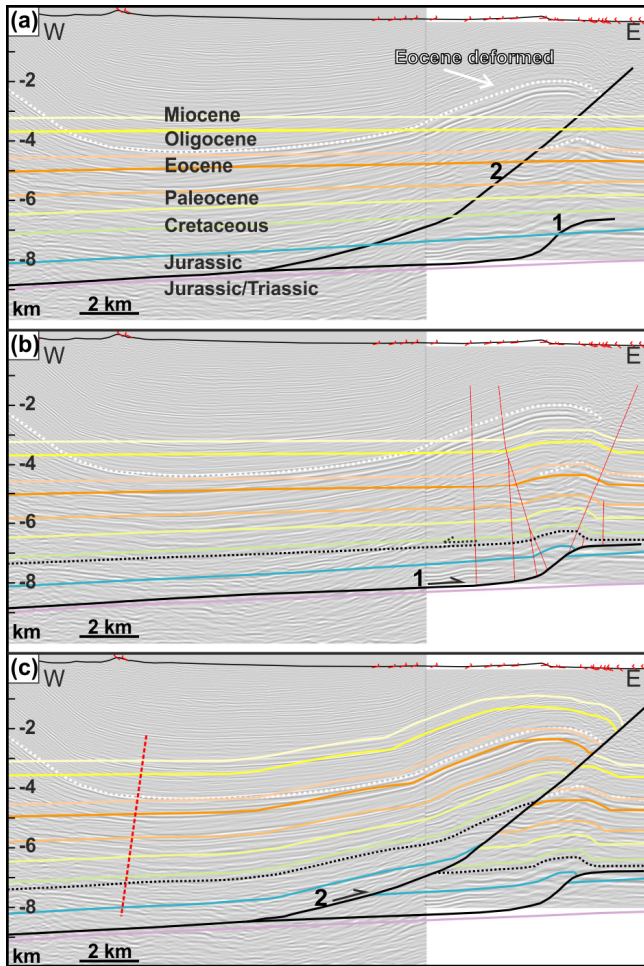
Figure 10: Forward modelling of the frontal structures in the southern sector (a) The seismic image, surface geometry including dips, the present day deformed state of the Top Eocene limestones (constrained by nearby well control) as well as the interpreted and constructed faults are given as reference frame for the forward model. The model uses a stratigraphic wedge with thicknesses which are constrained by well and outcrop observations. (b) A small triangle structure at the deformation front is modelled with fault-bend folding. The lower detachment (1) is in lower Jurassic or Triassic succession, the upper one is interpreted in the soft Cretaceous Goru shales (dotted line). (c) A fault-propagation fold forms hinterland-ward of the triangle structure by a thrust ramp (2) modelling done with tri-shear. The model mimics the structure imaged in the seismic approximately from the deformation front (east) to the red stippled line.
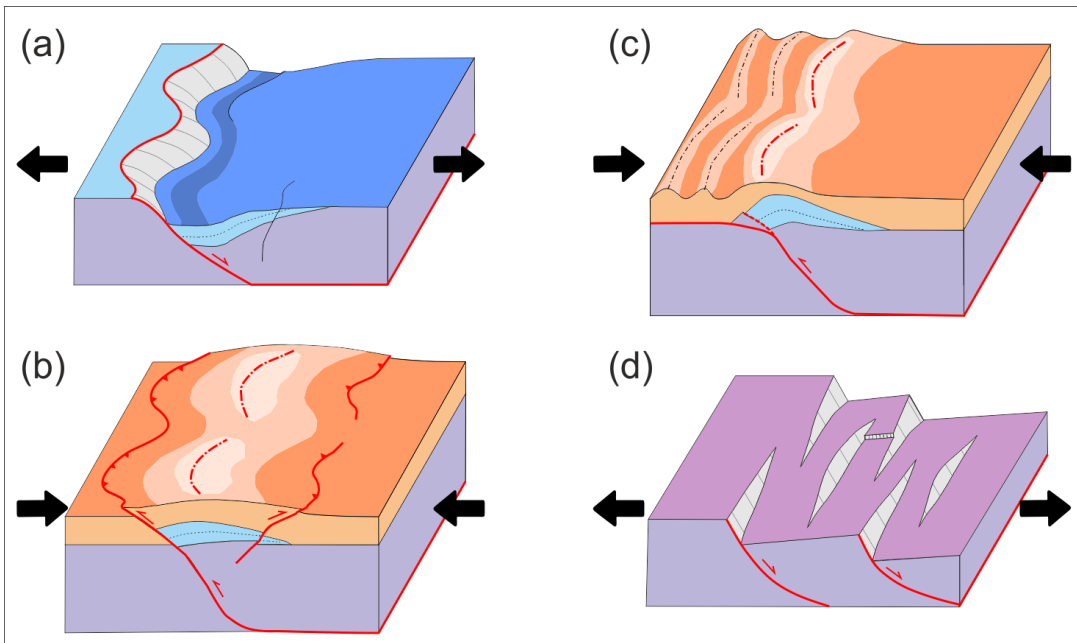
34

Figure 11: (a) and (b) Model of extension with subsequent inversion on curved linked faults (modified after Yamada and McClay, 2004). (c) Adding ~~a~~leading ~~-~~thin-skinned deformation and short-cut ~~element~~ fault to the sketch of inverted curved linked fault system (d) Sketch of half graben systems with overlapping faults for anticipation of more complex subsurface geometries before inversion.
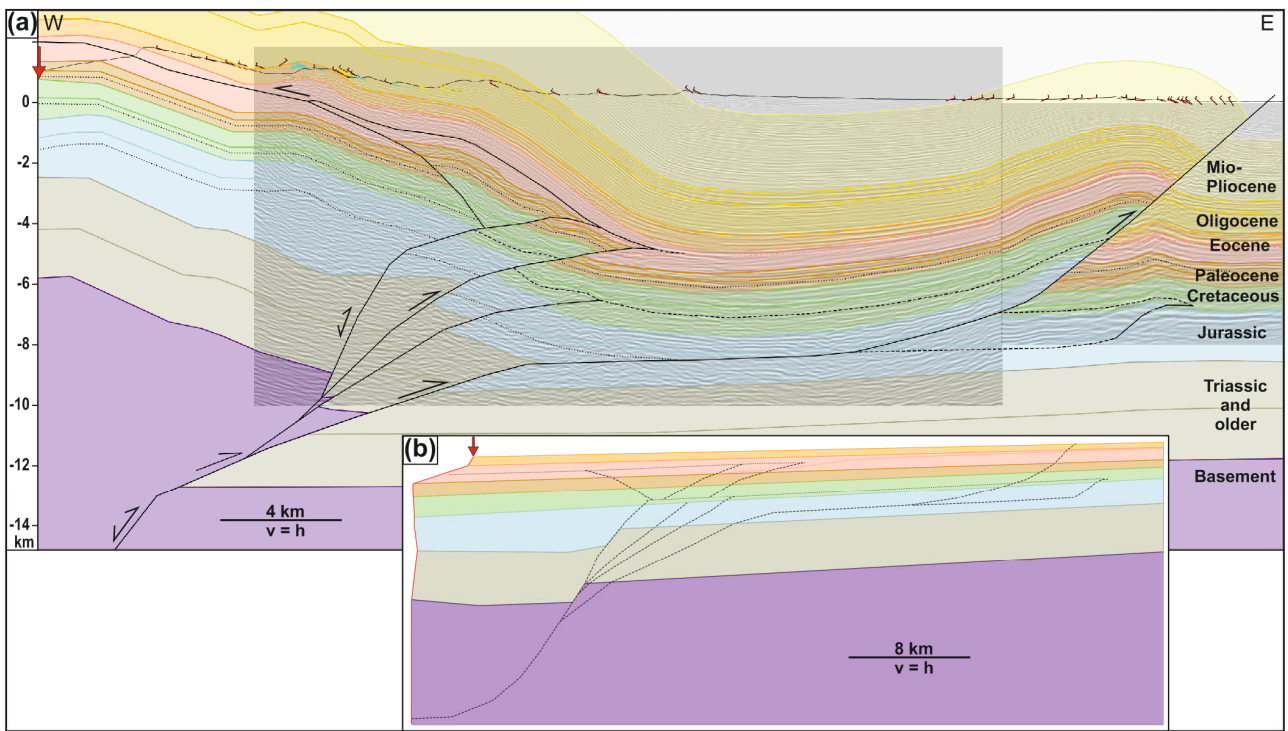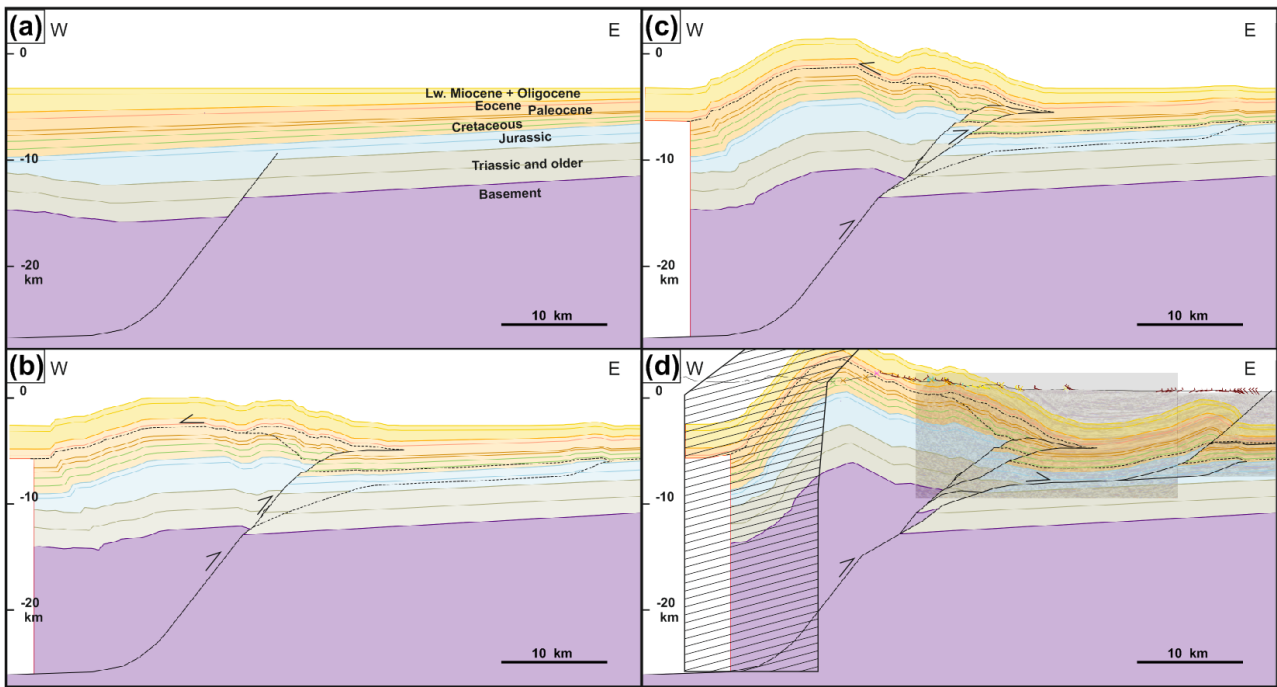
5

Figure 12: (a) Constructed W-E section in the southern sector of the study area with PSDM seismic in the background (i.e. Figure 8b). The section is balanced between the red lose line and the eastern end of the section (fixed line), KE: Kirthar Escarpment; (b) restored section (50% scale of (a)). Calculated shortening is approx. 10 km or 20%.

5

Figure 13: Simplified kinematical evolution of the southern sector. (a) Pre-contractional situation with Jurassic normal fault. Thin stippled lines indicate faults of dominant layer parallel shortening, (c) and (b) Incremental deformation of imbrication and passive roof thrusting above the inverting normal fault. (d) Final geometry of the kinematical forward model compared to seismic and surface geology. The geometry in the hatched area in the western part of the section does not fit the surface geology and would require additional deformation by inverting faults and cover sediments not regarded in this model.
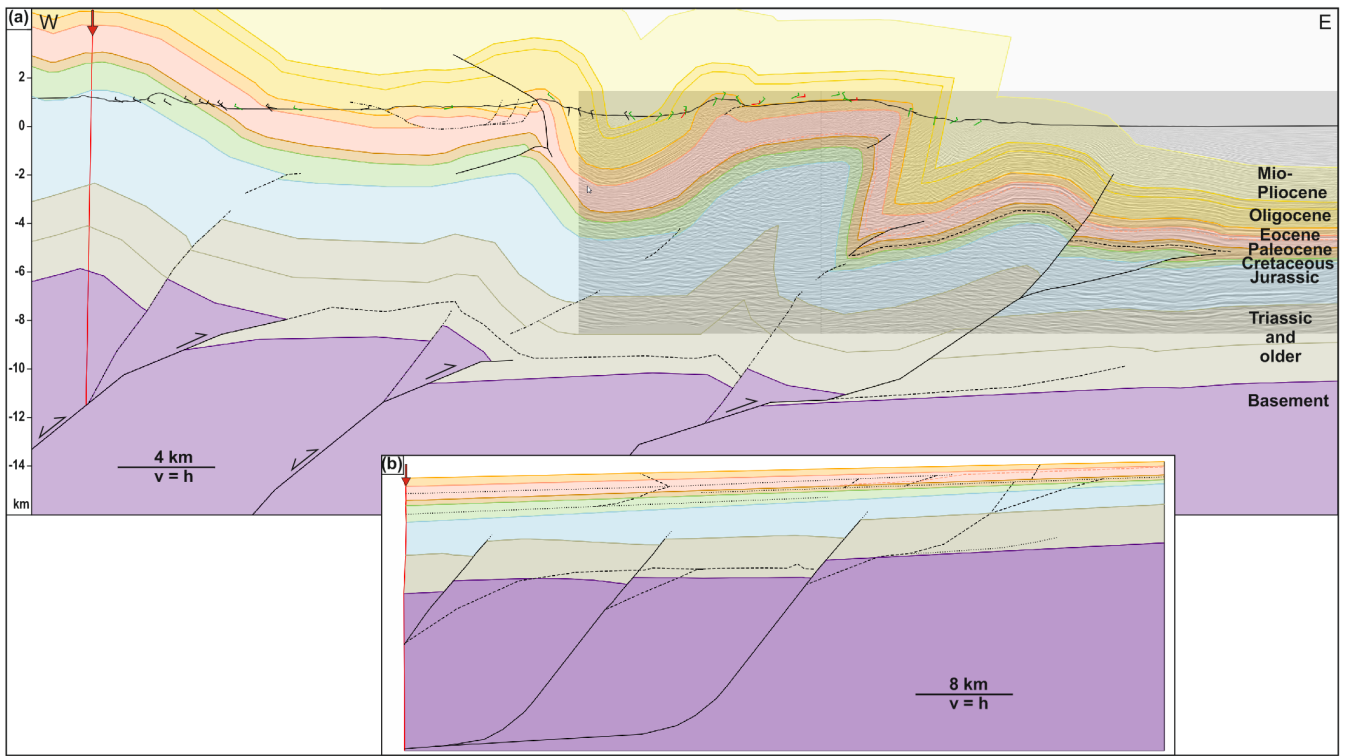
Figure 14: (a) Constructed W-E section in the northern sector of the study area with PSDM seismic in the background (i.e. Fig. 8a). Dip-measurements projected between 2.5 and 4km. The section is balanced between the red lose line and the eastern end of the section (fixed line). (b) Restored section (at 50% scale of (a)) by using line length and area balancing methods. Calculated shortening is approx. 11.2 km or 18%
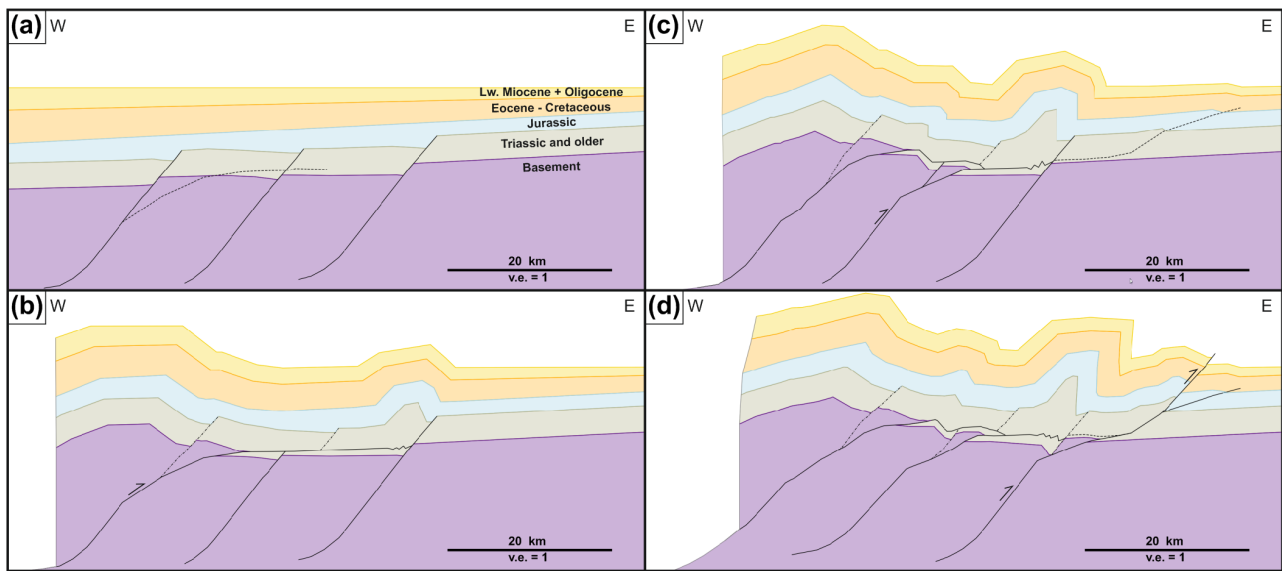
Figure 15: Simplified kinematical evolution of the southern sector, shown for Eocene to Basement rocks. (a) pre-contractional situation with Jurassic normal faults. Stippled line indicated future shortcut fault. (b) and (c) Increments of inversion with shortcut faulting and detachment folding related to buttressing. (d) Final geometry of the kinematical forward model.
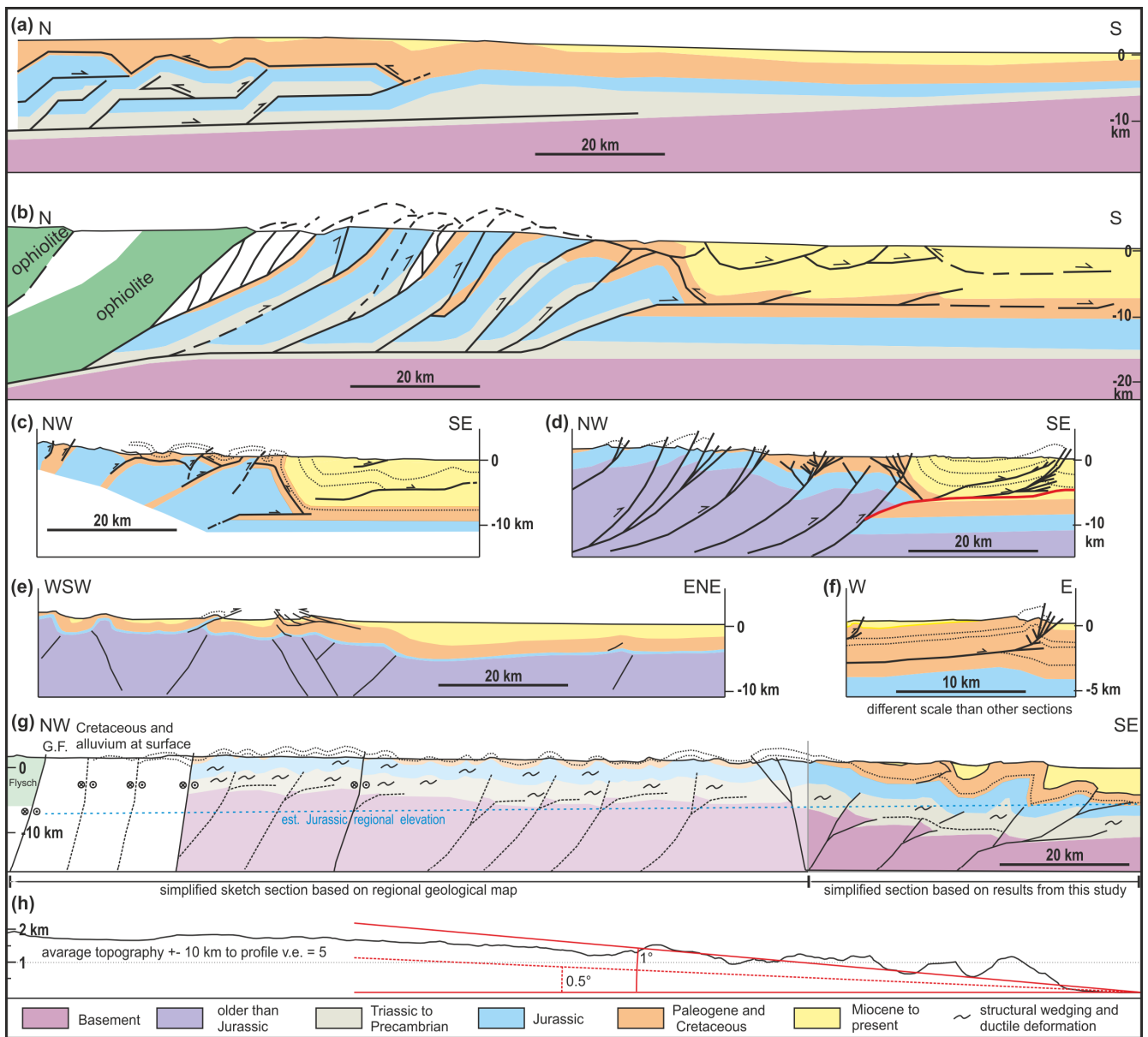
Figure 16 Selected sections in southern western fold belt of Pakistan (for section locations see Figs.1 and 2). a: after Jadoon et al. (1992), b+c: after Banks and Warburton (1986), d:after Szeliga et al. (2009), red fault indicate approx. shape of fault considered responsible for Mach 1931 event, e: after Fowler et al. (2004), f: after Schelling (1999), g: this study, the frontal part (strong colours) is a slightly projected section elaborated for the northern sector of this study area. The western part is a tentative regional sketch section based on the geological map of Bannert et al. 1992, as shown in Fig. 2, G.F. = Ghazeraband fault, h:average topography of a 20 km wide section centred on the trace of (g). 5 times vertical exaggeration.
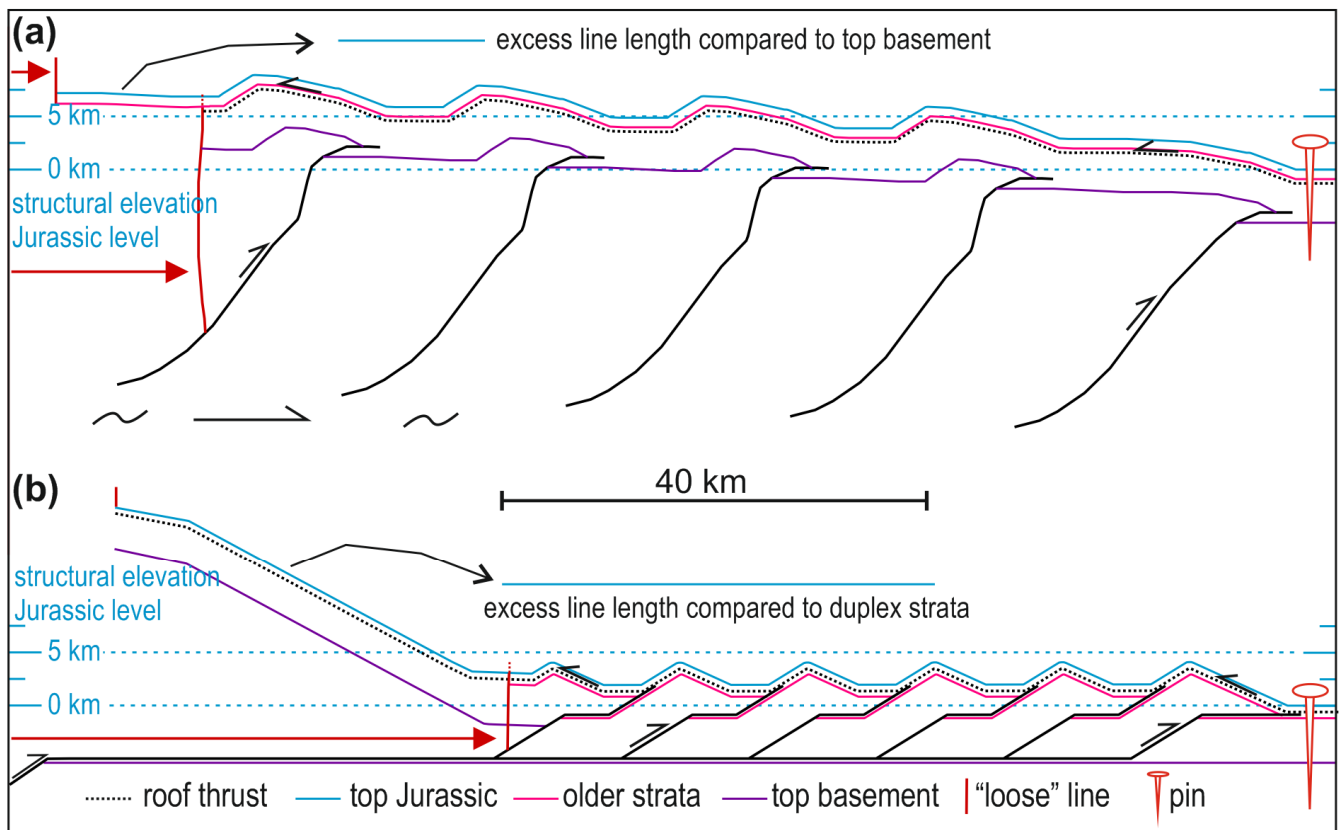
Figure 17 simplified sketch comparing thick- vs. thin skinned solutions for the structural elevation uplift of the Jurassic level. Elevations are in respect to the regional elevation of the Jurassic (0 km); a) A series of thick skinned faults with a total of 20 km shortening (16%). Due to the pinning at the deformation front a roof thrust under the horizons need to be present. The excess line length of the sediments above the roof thrust needs to be accommodated in the section as well, which could happen in internal shortening and amplification of the folds. The solution explains a structural uplift towards the hinterland of 5-7 km. b) One example of a duplex solution with total 48 km of shortening (38%). Due to the pinning at the deformation front a roof thrust under the horizons need to be present. The excess line length of the sediments above the roof thrust (about 40km) needs to be accommodated in the section as well. The example solution stays below 5 km structural uplift. In order to increase the uplift, more shortening in the duplexes would be required, which would increase the balancing issues. A tentative thrust cutting into the basement behind the duplexes would uplift basement rocks towards the hinterland.

Figure Label	Event Id	Mw	Z	Date	Author	Dip-azimuth	Dip	Strike	Rake	Dip-azimuth	Dip	Strike	Rake
F1a	603867342	5.4	-10100	19.12.2013	NEIC	253.8	14.7	163.8	70.9	93.5	76.2	3.5	94.9
F1b	603867342	5.4	-12000	19.12.2013	GCMT	291.0	39.0	201.0	133.0	61.0	63.0	331.0	61.0
F1c	603867342	5.4	-12000	19.12.2013	NEIC	277.0	26.0	187.0	99.0	87.0	64.0	357.0	85.0
F2	308027	5.4	-15000	21.01.1992	HRVD	306.0	48.0	216.0	104.0	105.0	44.0	15.0	75.0
F3	301671	4.9	-15000	28.03.1992	HRVD	272.0	57.0	182.0	89.0	93.0	33.0	3.0	91.0
F4	259589	5.1	-33000	28.12.1992	HRVD	263.0	33.0	173.0	32.0	146.0	73.0	56.0	119.0
F5	13436558	5.0	-12000	17.03.2009	GCMT	304.0	45.0	214.0	106.0	102.0	47.0	12.0	75.0
F6	604543379	5.0	-12000	08.05.2014	GCMT	212.0	42.0	122.0	69.0	59.0	52.0	329.0	108.0

Table 1: Nodal planes from International Seismological Centre (2015) database, reviewed events only. In addition to the dip the dip-azimuth of the planes is calculated. The strike and rake values from the database are given for completeness and assessment of obliquity. Event F1 has 3 different solutions in the database. The differences are a rough indication of the uncertainty of the data. Green/red dip values indicate the lower and higher dip surfaces of the pair. The author column refers to the original provider in the database (cf. Lentas et al.; 2018 and references therein).

5

Supplementary figures on the following pages/extra PDF